MITOCHONDRIAL ENERGY FAILURE IN THE EYE INDUCES LOSS OF VISUAL ACUITY IN EARLY METABOLIC SYNDROME: A NOVEL THERAPEUTIC TARGET

A Dissertation

Presented to the Faculty of the Weill Cornell Graduate School

of Medical Sciences

in Partial Fulfillment of the Requirements for the Degree of

Doctor of Philosophy

by

William Campbell Mills IV

May 2015

MITOCHONDRIAL ENERGY FAILURE IN THE RPE INDUCES LOSS OF VISUAL ACUITY IN EARLY METABOLIC SYNDROME: A NOVEL THERAPEUTIC TARGET

William C. Mills IV, Ph.D.

Cornell University 2015

Subtle changes in the neural retina can be detected much earlier than retinal vasculopathy in diabetic retinopathy. In mice fed a high fat diet, we have found early and progressive decline in visual acuity, as measured by optokinetic tracking, even before significant weight gain and hyperglycemia. Fundus examination was normal and fluorescein angiography showed normal retinal vasculature. The only major histologic findings were swollen mitochondria, edema and degenerative changes in the retinal pigment epithelium (RPE). Outer retinal ischemia and inflammation are supported by elevated VEGF, TNFa, MCP-1, and choroidal neovascular tufts. Treatment with a mitochondria-targeted tetrapeptide (SS-31/MTP-131) reversed visual decline without reducing blood glucose, body weight or insulin resistance. SS-31 is known to target cardiolipin and promote electron transfer and ATP synthesis. SS-31 preserved mitochondrial morphology and integrity of the RPE, reduced inflammatory markers, and prevented choroidal neovascularization. These results demonstrate a causal relationship between RPE mitochondrial energy failure and loss of visual acuity in early metabolic syndrome, and support a bioenergetics-based approach for preventing diabetic complications. A topical formulation of SS-31 (Ocuvia^{TM}) is in Phase 2 clinical trial for diabetic macula edema and non-proliferative age-related macular degeneration.

BIOGRAPHICAL SKETCH

William Mills was born in Concord, Massachusetts in the United States of America and was raised in Carlisle, Massachusetts where his family still lives. He attended Cornell University to study Biology with a concentration in Neurobiology, and graduated *cum laude* with a Bachelors of Arts in May 2011. As an undergraduate, he worked in the laboratory of Thomas Cleland, Ph.D., where he received a Howard Hughes Medical Institute Student Scholar Grant and wrote a thesis titled "Elucidation of an olfactory deficit in the transgenic APP/PS1 Alzheimer's mouse model through behavioral paradigms and complementary imaging methodologies."

After matriculating at the Weill Cornell Graduate School of Medical Sciences in the Pharmacology Ph.D. program, he joined the laboratory of Hazel H. Szeto, M.D., Ph.D, where his thesis work was conducted. Following graduation, he will return to Cornell University on the Lee Family Scholarship to pursue a Masters in Business Administration

To my parents

ACKNOWLEDGMENTS

I would like to formally thank a number of people who have been integral to the completion of this undertaking. First and foremost, I want to thank my mentor, Hazel H. Szeto, M.D., Ph.D., who has been instrumental in my intellectual and scientific growth over my years at Weill Cornell. Her patience, encouragement and rigor went far beyond the norm, and for that I will be eternally thankful.

I'm thankful for the support my of lab members, Yi M. Soong and Shaoyi Liu, who have spent months of their time training me and supporting my various scientific pursuits. I want to especially thank Alex V. Birk, who devoted countless hours as I struggled through a seemingly endless course of troubleshooting and development of new ideas. Without his help, my time at Weill Cornell would have been significantly longer and more difficult.

Furthermore, I want to thank Nazia Alam of the Weill Cornell Graduate School of Medical Sciences and Burke Research Institute, without whom none of this work would have been possible. Her tireless support and animal care founded the basis on which this thesis was built, and for that I am forever grateful.

I appreciate the wholehearted support I have received from my advisory committee, especially Enrique Rodriguez-Boulan, M.D., who has provided help and encouragement since the beginning of my research. His RO1 (EY08538) and Tri-Institutional Training Program in Vision Research through the National Eye Institute

of the National Institutes of Health (T32EY007138) funded my time here and made this thesis possible. His lab welcomed me as one of their own; especially Ryan P. Schreiner and Guillermo Lehmann Mantaras who were integral to the completion of this work.

Finally, I would like to extend my gratitude to my family, William, Susan and Katie Mills. Their unwavering support and encouragement allowed me to pursue this dream, and without them it would not have been possible. I would also like to thank Victoria Kushelev for her optimism, reassurance and care throughout the last two years. I love you all.

TABLE OF CONTENTS

LIST OF FIGURES

Chapter 2

Chapter 3

LIST OF TABLES

LIST OF ABBREVIATIONS

AGE: Advanced Glycation End Products

AICAR: AMPK-activating compound 5- aminoimidazole-4-carboxamide riboside

AMPK: AMP-activated protein kinase

ATP: Adenosine Triphosphate

ADP: Adenosine Diphosphate

AMP: Adenosine Monophosphate

DNA: Deoxyribonucleic Acid

DR: Diabetic Retinopathy

eNOS: Endothelial Nitric Oxide Synthase

ET-1: Endothelin

ETC: Electron Transport Chain 1

FADH2: Flavin Adenine Dinucleotide

FDA: Food and Drug Administration

FFA: Free Fatty Acid

GLP-1: Glucagon-Like Peptide-1

GSH: Glutathione

IMM: Inner Mitochondrial Membrane

NADH: Nicotinamide Adenine Dinucleotide

NF-κB: Nuclear Factor Kappa-light-chain-enhancer of activated B cells

NO: Nitric Oxide

OKT: Optokinetic Tracking

OMM: Outer Mitochondrial Membrane

PPARγ: Peroxisome Proliferator-Activated Receptor gamma

ROS: Reactive Oxygen Species

RPE: Retinal Pigment Epithelium

STZ: Streptozotocin

T1DM: Type 1 Diabetes Mellitus

T2DM: Type 2 Diabetes Mellitus

TCA: Tricarboxylic Acid (Cycle)

TGF-β: Transforming growth factor beta

TPP: Triphenylphosphonium

TZD: Thiazolidinedione

USD: United States Dollars ($)

VEGF: Vascular Endothelial Growth Factor

VEGFR: Vascular Endothelial Growth Factor Receptor

INTRODUCTION

Diabetes

First described 3000 years ago by the Egyptians, it would take another millennium before the Ancient Greek physician Araetus of Cappodocia (81-133AD) named the disease "diabetes" (Ahmed 2002). In 1776, English physician and experimental physiologist Matthew Dobson first identified the sugar found in the urine of diabetic patients, yet was unsuccessful in finding a dietary remedy for the disease (Luderitz 1993). The first real therapeutic was realized in 1921, with Frederick Banting and Charles Best's administration of insulin to diabetic patients, yet close to a century later diabetes still threatens the lives of those afflicted (Luderitz 1993).

As of 2013, 382 million people worldwide were living with diabetes, with 46% of these people remaining undiagnosed (Aguiree et al. 2013). This number is expected to increase drastically in the coming decades, with current estimates placing the global total at 592 million by 2035. Currently, 80% of people with diabetes live in low- and middle-income countries, and the rising population in the developing world accounts for the majority of the expected increase in diabetes diagnoses. The predicted surge in diabetes prevalence in Africa (109%), the Middle East and North Africa (96%) and South-East Asia (71%) from 2013 to 2035 is particularly worrying, as the associated mortality under the age of 60 in these areas is 76%, 50% and 55% respectively (Aguiree et al. 2013).

Each year, diabetes is directly accountable for 5.1 million deaths, a loss of one human life every six seconds. The long-term, progressive nature of the disease results in a massive burden for healthcare systems worldwide; diabetes is the foremost cause of end-stage renal disease, non-traumatic loss of limb, and blindness in working adults (Shulman 2014). It generates a current 11% (548 billion USD) of total healthcare spending worldwide with 263 billion from the US alone, a total further expected to reach a global level of 627 billion USD by 2035 (Aguiree et al. 2013).

Diabetes is a multifaceted and heterogeneous disorder. It can broadly be divided into two separate diseases, commonly referred to as Juvenile or Type 1 Diabetes and Adult Onset or Type 2 Diabetes. Type 1 diabetes (T1DM) occurs predominantly in patients under 18 years of age and is caused by an autoimmune destruction of the insulin-producing pancreatic beta cells, resulting in a deficiency in insulin secretion. Without insulin, patients fail to remove glucose from their blood, leading to a drastically elevated blood glucose level known as hyperglycemia. Patients with T1DM require daily insulin administration to control blood glucose levels, without which they will die.

Type 2 diabetes (T2DM) is far more prevalent, and is typically seen in overweight adults, although it is becoming more common in adolescents and children. Unlike in T1DM, Type 2 diabetics can still produce insulin, but the production is either insufficient or the body cannot properly respond to its release (Polonsky 2012). The most important factors associated with T2DM are obesity, high-fat and high-calorie “Western” diets and sedentary lifestyle. The increase of these factors

throughout the world have led to the drastic increase in type 2 diabetes over the past half century.

Insulin signaling is required to maintain a proper blood glucose level. Release of insulin when blood sugar levels rise promotes glucose uptake in the muscle and fat while inhibiting glucose production in the liver. A dysregulation of this signaling pathway leads to a breakdown in blood glucose control, ultimately resulting in hyperglycemia (Saltiel & Kahn 2001). Insulin resistance represents a lack of adequate response to insulin signaling, and while not yet fully understood, multiple causes have been implicated including phosphorylation insufficiencies of the insulin receptor protein and IRS and PiP-3 kinase substrates, ectopic lipid accumulation, endoplasmic reticulum stress and activation of the unfolded protein response, as well as a complex interplay of inflammatory pathways (Wilcox 2005; Samuel & Shulman 2012). Compensatory increases in insulin secretion can initially curtail some of the early loss of signaling, but ultimately pancreatic beta cell failure results in a loss of glucose-dependent insulin secretion, further exacerbating the dysfunction of blood glucose homeostasis (Ashcroft & Rorsman 2012).

Diabetic Retinopathy – History and Therapy

Retinopathy and visual dysfunction have always been linked to diabetes, with 20% of diabetic patients developing proliferative retinopathy after 30 years despite intensive glycemic control (Nathan et al. 2009). In low- and middle-income countries,

where monitoring and treatment options are limited, this poses an even greater problem.

The clinical features of diabetic retinopathy, detectable by early ophthalmoscopy, were first described in the 19th century. Early microaneurysms lead to abnormal exudation, including the leakage of both hard lipoprotein and blood, resulting in macular edema. Ischemia, intraretinal microvascular abnormalities and dilatation of venules precede proliferative changes in the retina and vitreous hemorrhage. These changes manifest in the early non-proliferative stage as impaired contrast sensitivity, dark adaptation and disturbances to the visual field that cause particular trouble with reading and driving at night (Antonetti et al. 2012). Further visual loss is experienced in the proliferative stage as improperly formed new vessels disrupt retinal function.

Treatment by pituitary ablation fell out of favor in the 1960s due to a wide array of potential risks and was replaced with the development of panretinal photocoagulation. This technique uses hundreds of pinpoint laser burns with the intention of reducing retinal oxygen demand and destroying dead tissue to prevent further neovascularization within the eye. While effective in preventing additional vision loss in some patients, it cannot reverse current degeneration.

In the early 1990s it was discovered that vascular endothelial growth factor (VEGF) drove neovascularization in hypoxia (Miller et al. 1994; Shweiki et al. 1992). Based on these findings, a seminal study concluded that patients with diabetic retinopathy had elevated VEGF levels in vitreous samples, thus implicating VEGF as a driving cause of retinal neovascularization in proliferative diabetic retinopathy

(Aiello et al. 1994). With this result, VEGF became a therapeutic target, resulting in the development of Ranibizumab (Lucentis) for the treatment of diabetic-related ocular dysfunction (NLM Identifier: NCT00445003). Approved for the treatment of diabetic macular edema in 2012, this anti-VEGF monoclonal antibody fragment was derived from the angiogenesis inhibitor Bevacizumab and functions to inhibit angiogenesis by removal of the VEGF signaling molecule (Gupta et al. 2013). Results were positive, with reduction of edema and visual degeneration. Many patients unfortunately fail to see benefit from Ranibizumab, and the side effect profile of this monthly intervitrial injection leaves something to be desired as well as its cost at a price of $2000 USD per monthly dose. Furthermore, increased VEGF presence in the eye is indicative of hypoxia and retinal dysfunction, and the removal of this signaling protein fails to treat the underlying cause of vision loss.

Diabetic Retinopathy – A Deeper Understanding

The metabolic abnormalities of the pre-diabetic and diabetic state cause damage to the surrounding tissue through various and complicated mechanisms. Most research into the etiology of this damage has focused on circulating high blood glucose, yet elevated levels of free fatty acids (FFA), insulin resistance and hyperinsulinemia are all known to play different yet related roles. Together, these alterations drive vasculopathy and cause changes to endothelial function throughout the body (Zhang et al. 2011). The effects vary by the tissue affected, but often include

attenuation of endothelium-mediated vasomotor function, increased endothelial apoptosis, promotion of endothelium activation/endothelium–monocyte adhesion, upregulation of an atherogenic response and the decrease of proper barrier function (Zhang et al. 2011). A multitude of signaling pathways underlie these detrimental modifications driven by glucotoxicity and abnormal insulin signaling. Furthermore, FFA level increases are known to further promote insulin resistance and increase inflammation and oxidative stress. These factors act not only individually, but also synergistically, hastening the feed-forward cycle of endothelial damage to the ultimate demise of the surrounding tissue nourished by this blood flow.

Michael Brownlee pioneered early research into the damaging effects of hyperglycemia-driven microvascular pathology in the diabetic eye. Hyperglycemia creates abnormalities in blood flow and disrupts proper vascular permeability by altering vasoregulatory elements. Permanent increases in permeability drive cell death which results in improper perfusion (Brownlee 2001). Such alterations result in edema, ischemia and hypoxia, and ultimately a compensatory neovascularization and visual degeneration. This endothelial disruption, caused by hyperglycemia and insulin resistance, is driven by four unique pathways that some believe underlie diabetes-induced damage to the eye. Increased polyol pathway flux coupled with an activation of protein kinase C can lead to a plethora of destructive changes including blood flow abnormalities mediated by eNOS and ET-1, vascular permeability changes via VEGF secretion, capillary occlusion through TGF-β, pro-inflammatory gene expression by NF-κB and an increase in ROS generation (Brownlee 2001; Giacco & Brownlee 2010). Separate from the above, Brownlee further demonstrates hyperglycemia-driven

increases in advanced glycation end products (AGEs) which damage cells in three important ways: altered protein function, abnormal modifications to the extracellular matrix and AGE receptor activation, all leading to pathological damage which is partially preventable by AGE inhibition (Soulis-liparota et al. 1991; Nakamura et al. 1997). Finally, an increased flux through the hexosamine pathway results in detrimental changes to gene and protein expression, which, along with the other three hyperglycemia-induced alterations, contributes to the pathology of diabetic retinopathy. More recent research has brought doubt to this hypothesis, as blocking a number of these pathways fails to reverse endothelial damage and end-organ dysfunction, as well as the fact that degeneration can occur earlier than pronounced blood sugar levels.

Renu Kowluru has furthered the understanding the diabetes-driven oxidative and inflammatory damage in the eye, focusing on impairment of the retinal microvasculature and the subsequent increases in reactive oxygen species (ROS) (Madsen-Bouterse et al. 2010). Noting that an imbalance in the production and removal of ROS damages DNA, lipids, proteins, and carbohydrates, disrupts cellular homeostasis and induces permeability of mitochiondria, all of which leads to cellular failure underlying diabetic retinopathy (Kowluru & Chan 2007). This inflammation and oxidative stress causes damage to the mitochondria, reducing the ability of cells to generate an adequate level of ATP needed to maintain primary cellular functions (Kowluru 2005). The increased flux of glucose through the mitochondria leads to an overproduction of superoxide, commencing a cascade of damage from the production of more superoxide, hydrogen peroxide, hydroxyl radicals, and peroxynitrite which

further damage macromolecules either at or near the site of their formation (Bergamini et al. 2004).

Further insight into the development of early diabetic retinopathy has focused on the microvasculature of the eye, specifically the choroidal vasculature of the outer retina. The retina is extremely metabolically active, with 90% of the oxygen provided by the choroidal vasculature and only 10% by the inner retina's vascular supply (Nickla & Wallman 2011). For the requisite oxygen concentrations to reach the photoreceptors, a very steep oxygen gradient is required. For this to occur, the blood flow in the delicate choroidal capillaries is most likely the highest of any tissue in the body per unit tissue weight, with a rate approximately an order of magnitude higher than the brain (Nickla & Wallman 2011). The choroidal vasculature is especially affected by metabolic syndrome and high-fructose diet, where fructose-fed rats exhibited choroidal damage and neovascularization to a significantly increased degree (Thierry et al. 2014). Even before hyperglycemia, insulin resistance damage causes disruption and endothelial dysfunction, and the choroid may be particularly susceptible (Mather et al. 2013; Zhang et al. 2012).

The disruption of insulin signaling, either through insulin resistance or altered insulin levels, has been implicated in endothelial dysfunction through perturbations of sensitive vasoregulatory systems (Zhang et al. 2012). These alterations occur very early in the progression of diabetes, even before hyperglycemia. Insulin induces the release of counteracting factors including endothelin-1 (ET-1), leading to vasoconstriction, and nitric oxide (NO), leading to vasodilation (Potenza et al. 2009). Disruption of NO signaling in particular, as evidenced by depleted levels of

endothelial nitric oxide synthase (eNOS), prevents proper vasodilation leading to occlusion and a reduction in the blood flow necessary to sustain RPE and photoreceptor function (Potenza et al. 2009; Vicent et al. 2003). Furthermore, alterations to insulin signaling can produce structural changes to the vasculature, including increased basal membrane thickness and improper matrix crosslinking, resulting in a loss of permeability and barrier function (Bakker et al. 2009). Reduction of the vasoregulatory capability of the microvasculature leads to a failure to adequately respond to stimuli, limiting the delivery of oxygen, nutrients and hormones critical for visual function. Insulin signaling disruption additionally creates an increase in inflammation, resulting in oxidative stress and the subsequent damage of tissues and apoptosis of both endothelial, pericyte and retinal cells (Kowluru & Chan 2007; Bakker et al. 2009). Premature vascular senescence resulting in reduced endothelial vasoregulatory capability and susceptibility to inflammation and oxidative stress, has also been linked to insulin resistance and high fat diets in rats (Chen et al. 2007). Thus, the insulin resistance-induced disruption of the critical choroidal blood supply creates an ischemic and hypoxic outer retina, ultimately resulting in degeneration of the retina and corresponding visual dysfunction.

The Mitochondria in Diabetic Retinopathy

Mitochondria are cellular organelles primarily responsible for the generation of adenosine triphosphate (ATP), the energy currency of the cell. An outer mitochondrial

membrane (OMM) surrounds an intricately folded inner mitochondrial membrane (IMM), which houses the protein complexes of the electron transport chain (ETC). To generate energy from glucose, the sugar follows a complex metabolic pathway involving its conversion to pyruvate (via glycolysis), acetyl CoA (via pyruvate dehydrogenase) and finally CO_2 (via the TCA or citric acid cycle), which generates the electron-carrying products NADH and $FADH_2$. These products donate their electrons to drive the ETC, where four complexes couple redox reactions with the pumping of protons (H^+ ions) into the intermembrane space between the OMM and IMM. The energy obtained from this proton gradient, the proton motive force, is used by the fifth and final complex, ATP synthase, to generate ATP from ADP and an inorganic phosphate. Known as oxidative phosphorylation, this process produces the majority of cellular energy in aerobic conditions and can utilize not only sugars, but products from fatty acid oxidation and amino acid oxidation as well.

This implication of the mitochondria as a critical underlying focus in the etiology of diabetes is not new, as mitochondrial dysfunction is a hallmark of multiple diabetic complications. Recent studies have implicated a mitochondrial role in the etiology of diabetes even before hyperglycemia (Du et al. 2003; Kowluru et al. 2011). Brownlee's hypothesis of mitochondrial overproduction of ROS is based on an increased concentration of glucose-derived pyruvate feeding unsustainable amounts of electron donors into the ETC. Electrons fail to flow through the complexes properly, backing up at coenzyme Q where they're donated to O_2, thus generating superoxide (Giacco & Brownlee 2010). Superoxide can be converted to H_2O_2 by superoxide dismutase, and both these radical oxygen molecules can cause cellular damage to the

surrounding mitochondria. Uncoupling proteins, which allow H^+ ions to cross the IMM and thereby destroy the proton gradient, can prevent the increase in ROS generation (Du et al. 2001). This has recently been contested, however, where reduced superoxide generation is seen in diabetic tissue due to suppressed mitochondrial activity via reduced AMP-activated protein kinase (AMPK) activity (Dugan et al. 2013). Furthermore, pharmacological activation of AMPK led to an increase in superoxide production and a beneficial reduction of pathophysiological characteristics (Dugan et al. 2013). This newer line of reasoning is supported in separate studies that found decreased, not increased mitochondrial oxidative phosphorylation in diabetic tissues (Mootha et al. 2003).

Mitochondrial hormesis is the theory of increased ROS within the mitochondria initiating a compensatory cellular response that improves stress resistance (Ristow & Zarse 2010). Built from theories of caloric restriction and reduced glucose metabolism, hormesis has been demonstrated as a novel therapeutic route, whereby AMPK activation and thus the restoration of superoxide and mitochondrial function has been associated with improvement in diabetic dysfunction (Sharma 2015). ROS serve a multitude of roles as critical endogenous messengers, and it appears that early work implicating elevated ROS levels for diabetic dysfunction was oversimplified, and in some cases, completely incorrect.

Insulin resistance has been shown to produce detrimental effects to mitochondrial function in both skeletal muscle and the heart (Sleigh et al. 2011; Szendroedi et al. 2011). Furthermore, cardiac mitochondrial deficiencies persist irrespective of elevated HbA1c or blood glucose levels (Croston et al. 2014).

Morphological changes to pancreatic β-cell mitochondria before and after the onset of hyperglycemia correspond with altered membrane potential and respiratory capacity with a decrease in cellular ATP content (Lu & Koshkin 2010). The remodeling of cardiolipin, a mitochondrial phospholipid essential for the control of membrane dynamics and the organization of respiratory complexes, has been documented in diabetic cardiomyopathy (Houtkooper & Vaz 2008; He & Han 2014). Peroxidation of this crucial phospholipid in diabetic models leads to a decrease in oxidative phosphorylation and the facilitation of cytochrome c detachment, an initiating event of the apoptotic pathway (Ferreira et al. 2013).

Recently, a new understanding of mitochondrial failure termed "metabolic inflexibility" has been elucidated. Mitochondria must change energy sources depending on a variety of stimuli and alternative fuel availability. In models of metabolic syndrome, however, nutrient overload and heightened substrate competition can overwhelm the delicate network of crosstalk responsible for proper regulation of mitochondrial energy generation (Muoio 2014). Diabetic patient's mitochondria fail to satisfactorily alter substrate consumption, whereas healthy patient's mitochondria properly shift from fatty acid oxygenation to glucose oxidation after a high-carbohydrate meal (Kelley et al. 1999). Drastic substrate excess overwhelms signaling pathways regulating optimal substrate use, resulting in inflexibility and a suboptimal utilization of fuels, ultimately leading to functional changes in the cell and tissue including alterations of insulin action, glucose disposal, lipolysis, lipid storage, immune function, and inflammatory responses (Muoio 2014). This inflexibility has been linked to alterations to insulin action, glucose disposal, lipolysis, lipid storage,

immune function, and inflammatory response, all of which hasten the development of end organ dysfunction.

Mitochondrial abnormalities are notable in diabetic retinopathy as well. In the early stages of the disease, mitochondrial dysfunction is evident even before histopathological abnormalities arise (Kowluru et al. 2011). Alterations to mitochondrial structure, including swelling and loss of cristae are seen in animal models and human patients, as well as an accumulation of defects in mitochondrial DNA (mtDNA) and a deficit in transport protein levels, with cessation of hyperglycemia failing to reverse these changes (Zhong & Kowluru 2011; Madsen-Bouterse et al. 2010; Santos & Kowluru 2013). Similar swollen mitochondria are seen in hyperglycemic retinal ganglion cells before apoptosis, while impaired mitochondria within the retinal pigment epithelium (RPE) are associated with an increased sensitivity to oxidative stress, lowered ATP levels and impaired autophagic and phagocytic capacities of shed photoreceptor outer segments (Xie et al. 2008; He et al. 2011; Schütt et al. 2012). Mitochondrial swelling and a loss of cristae are commonly seen in hypoxic conditions (Zhao et al. 2004; Liu et al. 2014). The enlarged, cristae-deficient mitochondria found in the RPE indicate the presence of a similar hypoxic environment, potentially caused by reduced blood flow following damage to the choroidal microvasculature. Impaired mitochondria drive the feed-forward cycle of oxidative damage and inadequate ATP production, which robs the cell's endogenous antioxidant defense capabilities of the requisite energy to preform adequately, thereby creating even more damage. This bioenergetic failure is a critical component of diabetic retinopathy, due to the specialized nature of the retina.

The RPE's critical role within the eye

There is one cellular layer in particular that has become the target of interest in degenerative vision disorders: the retinal pigment epithelium (RPE). The RPE is a highly metabolically active single cell layer separating the outer retina from the blood supply of the choroid. It performs a number of interrelated jobs, each crucial to visual function (Strauss 2005). Beyond the adsorption of light passed though the retina, the RPE plays a critical role in the caretaking of overlaying photoreceptors, of which each RPE cell is responsible for 15-50 photoreceptors (Kennedy et al. 1995; Snodderly et al. 2002). Each day, 10-15% of the photoreceptor outer segment is shed, with the RPE responsible for its phagocytization, digestion and the recycling of essential components (Snodderly et al. 2002). This recycling capacity further extends to the reisomerization of all-trans-retinal to 11-cis-retinal, without which the visual cycle ceases (Strauss 2005). The RPE additionally serves to ensure photoreceptor action by stabilizing the ionic composition of the subretinal space, allowing for adequate photoreceptor excitability. Maintenance of proper choriocapillary endothelium and photoreceptor integrity is dependent on the secretion of neurotrophic, adhesion, and vascular regulatory factors from the RPE, a disruption of which is implicated in visual dysfunction (Ambati & Fowler 2012). VEGF secretion in particular is critical to proper maintenance of the choroidal endothelium, and an upregulation of this signaling is the driving cause of neovascularization in DR via VEGFR activation (Costa & Soares 2013; Kurihara et al. 2012). The RPE acts as an active barrier to the

outer retina, controlling and supporting the flow of essential nutrients from the choroidal blood supply to the photoreceptors (glucose, retinal), and from the subretinal space to the blood (ions and water). This process is supported by the intricate basolateral infoldings, creating a large surface area for proper transport to occur. The removal of water, a byproduct of metabolism from the photoreceptors and neurons, is critical, as a failure of this action leads to macular edema, the hallmark of early diabetic retinopathy (Strauss 2005; Kovach & Schwartz 2009). Mitochondrial failure within the RPE thus results in a bioenergetic failure. This failure impairs the cell layer's tight-junction formation and therefore the integrity of the blood/retina barrier, prevents the epithelial transport necessary for the uptake of retinal and ω-3 fatty acids required for photoreceptor function, and impedes the removal of metabolic end products. Furthermore, such bioenergetic failure reduces the phagocytic capability required for sustaining the visual cycle and the secretory capabilities required to preserve the microvasculature and immune privilege of the eye (Strauss 2005; Duh 2008)

Current approaches for the treatment of diabetes

There are multiple pharmacological therapies intended to restore proper blood glucose levels and prevent the end-organ complications associated with diabetes. The first such therapeutic is insulin itself, which began human trials in 1922. Administered either via injection or insulin pump, insulin is effective in controlling hyperglycemia

and has no upper limit in dosage for therapeutic effect (Skugor 2014). Daily injection, however, is complicated for some patients and is usually considered as a "last resort" by physicians (Funnell 2007).

Additional pharmacologic therapies have been developed in order to provide alternative or additional support with blood glucose regulation. The Thiazolidinediones (TZDs) are peroxisome proliferator-activated receptor gamma (PPARγ) agonists that function to partially restore insulin sensitivity to muscle and fat. Activating this nuclear receptor favorably alters the transcription of several genes involved in glucose and lipid metabolism and energy homeostasis (including AMPK), restoring lost sensitivity to endogenous insulin signaling. Approved for T2DM, the first drug in this class Troglitazone (Rezulin) was withdrawn from the US market in 2000 after its adverse hepatic effects became known. Another drug, Rosiglitazone (Avandia), has been implicated in cardiovascular events and was placed under sales restrictions, but the FDA reversed this decision in 2013.

A second class of antidiabetic drugs for T2DM are the Biguanides, especially Metformin (Glucophage); the first-choice drug for obese and overweight patients currently prescribed to 100 million patients worldwide (Rena et al. 2013). T2DM patients have increased rates of endogenous hepatic glucose production, and metformin functions to reduce this gluconeogenesis (Hundal et al. 2000). The exact mechanism is yet to be fully elucidated, yet includes inhibition of complex I of the mitochondrial respiratory chain, activation of AMPK, potentially through an increase in the AMP:ATP ratio, and alterations to the gut microbiome (Rena et al. 2013; Burcelin 2013). Furthermore, metformin increases insulin sensitivity as well as insulin

receptor binding of insulin, and enhances peripheral glucose uptake (Baily & Turner 1996).

The third common class of antidiabetics is the Sulfonylureas, which function by promoting the release of insulin. Often coupled with other antidiabetic agents, these drugs bind to ATP-sensitive K^+ channels on pancreatic beta cells, depolarizing the cells, thus stimulating an increase in intracellular Ca^{2+} concentrations and the fusion of insulin granulae with the cell membrane and the release of insulin.

An additional class of therapeutics for diabetes is the Glucagon-Like Peptide-1 (GLP-1) mimetics, which mimic endogenous GLP-1 by increasing the post-prandial release of insulin and inhibiting glucagon release. These drugs have been further demonstrated to reduced inflammation of endothelial cells and activate AMPK, thereby protecting the bioenergetics of the vasculature (Krasner et al. 2014).

Alternative treatments have focused on the mitochondrial etiology of the disease and have thus viewed mitochondrial protection as a means to prevent end-organ dysfunction. The most researched of these is MitoQ, a ubiquinone moiety linked to a triphenylphosphonium (TPP) cation by a ten-carbon alkyl chain. TPP is thus used as a lipophilic cation to deliver ubiquinol to the mitochondria where it functions as an antioxidant, preventing lipid peroxidation and damage from peroxynitrite and superoxide (Smith & Murphy 2011). Promising results have been demonstrated in animal models of mitochondrial oxidative damage, yet MitoQ failed in its only Phase II trial in 2010 (NCT01167088).

More recent studies have also found potential for other mitochondria-targeted therapeutics. TT01001, a novel ligand of the OMM protein mitoNEET, has been

demonstrated to restore proper glucose metabolism and mitochondrial function in a diabetic mouse model (Takahashi et al. 2014). The AMPK-activating compound 5-aminoimidazole-4-carboxamide riboside (AICAR) has been demonstrated to ameliorate glucoregulatory defecits and attenuate hyperglycemia-induced effects in animal models, as well as reduce hepatic glucose output, lower blood glucose levels and reduce plasma FFA concentrations in human subjects (Winder 2009; Boon et al. 2008).

A novel strategy

Combating visual degeneration by protecting the RPE has been attempted in a myriad of ways, yet no treatment has proven useful to human patients. Here, we investigated the use of SS-31 (MTP-131, Bendavia, Ocuvia) as a potential therapeutic to combat DR via mitochondrial protection.

Discovered serendipitously during synthetic opioid research, the Szeto-Schiller (SS) peptides are highly polar, water-soluble, four amino acid long peptides with remarkable cell permeability (Szeto & Birk 2014). Despite a 3^+ charge, high molecular weight (640 kDa) and polar peptide backbone, an SS peptide (a fluorescent analog of SS-02) was taken up by numerous cell types and localized to the mitochondria (Zhao et al. 2004). The uptake does not rely on mitochondrial potential, unlike TPP-based compounds (eg: MitoQ), and selectively partitions to the IMM with little presence elsewhere in the mitochondria, all without causing mitochondrial

depolarization (Zhao et al. 2004). Among this class of peptides is SS-31 (H-d-Arg-Dmt-Lys-Phe-NH2, also known as MTP-131 as a acetate salt, or "Bendavia"), which has been demonstrated to selectively target the mitochondrial phospholipid cardiolipin, which is present exclusively on the IMM (Birk et al. 2013). Alterations to cardiolipin, including its oxidation and depletion, deleteriously impact the membrane curvature necessary for proper cristae formation (Acehan et al. 2007). Through both electrostatic and hydrophobic interaction with cardiolipin, SS-31 localizes to the inner mitochondrial membrane and prevents cardiolipin peroxidation and promotes proper cristae formation, allowing adequate respiratory complex association (Szeto 2014). This optimization of respiratory complex assembly and function optimizes the ETC, reducing the generation of ROS while improving electron transfer and thus ATP production.

SS-31 has shown promise in combating cellular deterioration in disease states associated with bioenergetic failure, including animal models of ischemia-reperfusion, age-related muscle weakness, kidney failure and neurodegeneration (Birk et al. 2013; Siegel et al. 2013; Eirin et al. 2012; Yang et al. 2009). There has been a focus on research of ischemic and hypoxic disease states, such as in ischemic heart injury where SS-31 was shown to protect cardiac mitochondria and improve myocardial ATP synthesis, and in transverse aortic constriction-induced heart failure where similar mitochondrial protection was proteomically observed (Dai et al. 2013; Sabbah et al. 2013). Similar results were seen in isolated perfused hearts, where SS-31 treatment decreased total heart lipid peroxidation and preserved ATP content (Szeto 2008). Prevention of the deleterious effects of ischemia was further demonstrated in a renal

artery occlusion model, where SS-31 maintained mitochondrial structure and ATP production, as well as decreased lipid peroxidation and tubular apoptosis (Szeto et al. 2011). SS-31's mitochondrial protective effects during ischemia have been recognized to protect microvasculature during energy and oxygen deficiency. In a renal artery stenosis model treated with SS-31 during the renal angioplasty, a reduction in oxidative stress, fibrosis and microvascular rarefaction was seen four weeks later (Eirin et al. 2012). Similar microvascular-protective effects were demonstrated in attenuation of no-reflow effects in a rabbit model, even with SS-31 dosage after the onset of ischemia (Kloner et al. 2012). This SS-31-based protection of the microvasculature and subsequent preservation of organ function after blood flow deprivation was further demonstrated in rat model of acute renal ischemia where protection of endothelial mitochondria prevented inflammatory and fibrotic damage typical of tissue hypoxia (Liu et al. 2014). This microvascular-protective effect in hypoxic conditions provides a well-supported basis for SS-31's investigation in diabetic retinopathy, a disease where microvascular dysfunction drives visual degeneration.

SS-31 has been further shown to block the development of insulin resistance in the skeletal muscle of mice fed a high-fat diet while reducing H_2O_2 emission and preventing the increase in GSSG and decrease in GSH/GSSG ratio in response to glucose ingestion (Anderson et al. 2009). The link between mitochondrial bioenergetics protection and insulin sensitivity, coupled with SS-31's proven ability to protect microvasculature and therefore the functionality of the surrounding tissue, positions it to fill an unmet need in the treatment of diabetic retinopathy.

A preliminary study found SS-31 to protect the inner retina from oxidative stress after a four-week daily injection in an STZ model (Huang et al. 2013). Eneucleated eyes showed improved distribution of claudin-5 and occludin, as well as decreased retinal leakage in an Evans blue assay; all indicating SS-31 preserved the integrity of the microvasculature. SS-31 has additionally been documented to protect cultured human lens cells against oxidative stress (Cai et al. 2014). Importantly, we have now linked these observations regarding retinal blood supply failures to functional visual measurements, confirming their findings that SS-31 exerts a protective effect in the eye.

A topical, eye drop formulation of SS-31 has been created in order to facilitate treatment. Despite SS-31's 3^+ net charge, excellent corneal penetration was achieved. Rapid intraocular wall distribution was observed with high levels of SS-31 in the anterior compartment (conjunctiva, cornea and sclera), indicating potential uptake via the episcleral veins of the conjunctival epithelium. With low drug concentrations observed in the vitreous, it is likely that the drug is absorbed systemically and thus distributes to the posterior compartment of the eye through blood circulation to the choroid and RPE. Peak blood levels occur after 2 hours, with peak levels in the choroid and retina following at 4 hours post application.

Table 1. Distribution of [^{14}C] SS-31 in New Zealand white rabbits in ocular tissues. Rabbits are >12 weeks of age, 2.5 – 3.43 kg, n>3.

	3 kg NZW Rabbits n= 3 eyes/group	Mean Total ^{14}C from 40 µl/eye of 1% Eyedrops of ^{14}C-MTP-131 (ng-equi/g) Time post-dose (hours)						
	Tissues	**0.25**	**0.5**	**2**	**4**	**6**	**8**	**24**
1	**Conjunctiva**	3139.0	**7425.0**	2534.0	2059.0	1806.0	1774.0	744.0
2	**Cornea**	613.0	**1976.0**	778.0	**1253.0**	489.0	462.0	389.0
3	**Sclera**	218.0	**917.0**	297.0	**442.0**	224.0	235.0	119.0
4	**Choroid**	24.2	**157.0**	69.6	**208.0**	113.0	88.8	24.3
5	**Blood**	1.1	15.0	**116.0**	**115.0**	98.0	59.2	4.7
6	**Iris/Ciliary Body**	6.4	56.7	146.0	**343.0**	198.0	115.0	40.9
7	**Aqueous Humor**	5.3	32.8	137.0	**314.0**	212.0	130.0	12.6
8	**Retina**	4.5	25.2	49.4	**96.7**	75.5	54.3	11.8
9	**Lens**	0.2	2.0	20.6	**185.0**	156.0	90.4	149.0
10	**Vitreous Humor**	0.2	0.6	3.9	**19.8**	16.5	13.3	3.2

Measurement of vision

A variety of visual deficits are among the earliest symptoms of diabetic retinopathy, often occurring ahead of detectable vascular lesions or macular edema (Jackson et al. 2012). Functional deficits, including color perception, loss of blue-sensitive color vision, and reduced dark adaptation are present before alterations to the microvasculature or retinal structure (Hardy et al. 1992; Henson & North 1979; Daley et al. 1987; Jackson et al. 2012). Visual function in animal models of diabetes, as measured by optokinetic tracking (OKT), shows a loss of visual acuity as early as 3

weeks and contrast sensitivity within 9 weeks after STZ treatment when controlling for cataract formation, all before detectable physical lesions including vascular leakage, pericyte dropout, and acellular capillaries (Aung et al. 2013; Kirwin et al. 2011)

Visual degeneration can be detected through the sensitive assessment technique of optokinetic tracking. Developed by Glen Prusky, this practice utilizes a rotating virtual cylinder to assess both contrast sensitivity and spatial frequency (Prusky et al. 2004). Here, we utilize this technique in order to assess the degeneration of vision in models of diabetes in mice, as well as the utility of SS-31.

We have carefully selected a model mouse to recapitulate the human early diabetic phenotype for this retinopathy study. Our model combines a moderate dose of streptozotocin in order to destroy a fraction of the pancreatic beta cells and thus reduce insulin secretion. More importantly, the high-fat diet, begun at an early age, induces insulin resistance and ultimately glucose intolerance, hyperglycemia and weight gain. Vasculopathy develops, and the choroidal blood flow ceases to support the outer retina, resulting in visual degeneration without requiring genetic manipulation.

The work in this thesis presents a deeper understanding of diabetic retinopathy, combined with positive results from a novel therapeutic tailored to this new understanding. Using a mitochondria-targeted therapeutic to halt the feed-forward cycle of bioenergetics breakdown protects the retina's vasculature and RPE, allowing the retina-sustaining functions to resist failure. Protecting these vital sections of the retina, without reversing hyperglycemia, weight gain and insulin resistance shows

promise in a disease that threatens the vision of hundreds of millions of people. Reversing or preventing the loss of contrast sensitivity and visual acuity, events that occur before the larger-scale edema and neovascularization, represents a paradigm shift in the treatment of diabetic retinopathy. Formulated into a topical ophthalmic solution ("Ocuvia™") a phase 1/2 clinical trial (NCT02314299) has begun with an estimated completion date of July 2015.

REFERENCES

Acehan, D. et al., 2007. Comparison of lymphoblast mitochondria from normal subjects and patients with Barth syndrome using electron microscopic tomography. *Laboratory investigation; a journal of technical methods and pathology*, 87(1), pp.40–48.

Aguiree, F. et al., 2013. *IDF Diabetes Atlas*, Available at: http://scholar.google.com/scholar?hl=en&btnG=Search&q=intitle:Diabetes+Atlas#5\nhttp://dro.deakin.edu.au/view/DU:30060687\nhttp://hdl.handle.net/10536/DRO/DU:30060687.

Ahmed, A., 2002. History of diabetes mellitus. *Saudi Med J.*, 23(4), pp.373–8.

Aiello, L. et al., 1994. Vascular endothelial growth factor in ocular fluid of patients with diabetic retinopathy and other retinal disorders. *The New England Journal of Medicine*, 331(22), pp.1480–1487.

Ambati, J. & Fowler, B.J., 2012. Mechanisms of Age-Related Macular Degeneration. *Neuron*, 75(July 12), pp.26–39.

Anderson, E.J. et al., 2009. Mitochondrial H2O2 emission and cellular redox state link excess fat intake to insulin resistance in both rodents and humans. *The Journal of Clinical Investigation*, 119(3), pp.573–581.

Antonetti, D. a, Klein, R. & Gardner, T.W., 2012. Diabetic retinopathy. *The New England Journal of Medicine*, 366(13), pp.1227–39. Available at: http://www.ncbi.nlm.nih.gov/pubmed/23275374.

Ashcroft, F.M. & Rorsman, P., 2012. Diabetes mellitus and the Beta cell: The last ten years. *Cell*, 148(6), pp.1160–1171. Available at: http://dx.doi.org/10.1016/j.cell.2012.02.010.

Aung, M.H. et al., 2013. Early visual deficits in streptozotocin-induced diabetic long evans rats. *Investigative Ophthalmology & Visual Science*, 54(2), pp.1370–7. Available at: http://www.pubmedcentral.nih.gov/articlerender.fcgi?artid=3597194&tool=pmcentrez&rendertype=abstract [Accessed May 19, 2014].

Baily, C.J. & Turner, R.C., 1996. Metformin. *The New England Journal of Medicine*, 334(9), pp.574–570.

Bakker, W. et al., 2009. Endothelial dysfunction and diabetes: Roles of hyperglycemia, impaired insulin signaling and obesity. *Cell and Tissue Research*, 335, pp.165–189.

Bergamini, C.M. et al., 2004. Oxygen, reactive oxygen species and tissue damage. *Current pharmaceutical design*, 10, pp.1611–1626.

Birk, A. V et al., 2013. The Mitochondrial-Targeted Compound SS-31 Re-Energizes Ischemic Mitochondria by Interacting with Cardiolipin. *Journal of the American Society of Nephrology : JASN*, 24(8), pp.1250–61. Available at: http://www.ncbi.nlm.nih.gov/pubmed/23813215 [Accessed September 18, 2013].

Boon, H. et al., 2008. Intravenous AICAR administration reduces hepatic glucose output and inhibits whole body lipolysis in type 2 diabetic patients. *Diabetologia*, 51, pp.1893–1900.

Brownlee, M., 2001. Biochemistry and molecular cell biology of diabetic complications. *Nature*, 414(December), pp.813–820.

Burcelin, R., 2013. The antidiabetic gutsy role of metformin uncovered? *Gut*, 2013(5), pp.9–10. Available at: http://www.ncbi.nlm.nih.gov/pubmed/23840042.

Cai, M. et al., 2014. Mitochondria-Targeted Antioxidant Peptide SS31 Protects Cultured Human Lens Epithelial Cells against Oxidative Stress. *Current eye research*, 00(00), pp.1–8. Available at: http://www.ncbi.nlm.nih.gov/pubmed/25310141 [Accessed October 15, 2014].

Chen, J. et al., 2007. Premature vascular senescence in metabolic syndrome: Could it be prevented and reversed by a selenorganic antioxidant and peroxynitrite scavenger ebselen? *Drug Discovery Today: Therapeutic Strategies*, 4(1), pp.93–99.

Costa, P.Z. & Soares, R., 2013. Neovascularization in diabetes and its complications. Unraveling the angiogenic paradox. *Life sciences*, 92(22), pp.1037–45. Available at: http://www.ncbi.nlm.nih.gov/pubmed/23603139 [Accessed October 19, 2013].

Croston, T.L. et al., 2014. Functional Deficiencies of Subsarcolemmal Mitochondria in the Type 2 Diabetic Human Heart. *American journal of physiology. Heart and circulatory physiology*, pp.54–65.

Dai, D.-F. et al., 2013. Global Proteomics and Pathway Analysis of Pressure-overload Induced Heart Failure and Its Attenuation by Mitochondrial Targeted Peptides Dao-Fu. *Circ Heart Fail.*, 6(5), pp.417–428.

Daley, M.L., Watzke, R.C. & Riddle, M.C., 1987. Early loss of blue-sensitive color vision in patients with type I diabetes. *Diabetes Care*, 10(6), pp.777–781.

Du, X.L. et al., 2001. Hyperglycemia inhibits endothelial nitric oxide synthase activity by posttranslational modification at the Akt site.[comment]. *Journal of Clinical Investigation*, 108(9), pp.1341–1348.

Du, Y., Miller, C.M. & Kern, T.., 2003. Hyperglycemia increases mitochondrial superoxide in retina and retinal cells. *Free Radical Biology and Medicine*, 35(11), pp.1491–1499. Available at: http://linkinghub.elsevier.com/retrieve/pii/S0891584903005665 [Accessed May 20, 2014].

Dugan, L.L. et al., 2013. AMPK dysregulation promotes diabetes- related reduction of superoxide and mitochondrial function. *The Journal of Clinical Investigation*, 123(11).

Duh, E., 2008. *Diabetic Retinopathy* A. Veves, ed.,

Eirin, A. et al., 2012. A mitochondrial permeability transition pore inhibitor improves renal outcomes after revascularization in experimental atherosclerotic renal artery stenosis. *Hypertension*, 60, pp.1242–1249.

Ferreira, R. et al., 2013. Lipidomic characterization of streptozotocin-induced heart mitochondrial dysfunction. *Mitochondrion*, 13(6), pp.762–71. Available at: http://www.ncbi.nlm.nih.gov/pubmed/23665486 [Accessed June 9, 2014].

Funnell, M.M., 2007. Overcoming Barriers to the Initiation of Insulin Therapy. *Clinical Diabetes*, 25(1), pp.36–38.

Giacco, F. & Brownlee, M., 2010. Oxidative stress and diabetic complications. *Circulation research*, 107(9), pp.1058–70. Available at: http://www.pubmedcentral.nih.gov/articlerender.fcgi?artid=2996922&tool=pmcentrez&rendertype=abstract [Accessed May 6, 2014].

Gupta, N. et al., 2013. Diabetic retinopathy and VEGF. *The open ophthalmology journal*, 7, pp.4–10. Available at: http://www.pubmedcentral.nih.gov/articlerender.fcgi?artid=3580758&tool=pmcentrez&rendertype=abstract.

Hardy, K.J. et al., 1992. Detection of colour vision abnormalities in uncomplicated type 1 diabetic patients with angiographically normal retinas. *The British Journal of Ophthalmology*, 76(8), pp.461–4. Available at: http://www.pubmedcentral.nih.gov/articlerender.fcgi?artid=504317&tool=pmcentrez&rendertype=abstract.

He, Q. & Han, X., 2014. Cardiolipin remodeling in diabetic heart. *Chemistry and physics of lipids*, 179, pp.75–81. Available at: http://www.ncbi.nlm.nih.gov/pubmed/24189589 [Accessed May 29, 2014].

He, Y. et al., 2011. Mitochondria impairment correlates with increased sensitivity of aging RPE cells to oxidative stress. *Journal of Ocular Biology, Diseases, and Informatics*, 3(3), pp.92–108. Available at: http://www.pubmedcentral.nih.gov/articlerender.fcgi?artid=3372610&tool=pmcentrez&rendertype=abstract [Accessed December 7, 2012].

Henson, D.B. & North, R. V, 1979. Dark adaptation in diabetes mellitus. *The British Journal of Ophthalmology*, 63(8), pp.539–41. Available at:

http://www.pubmedcentral.nih.gov/articlerender.fcgi?artid=1043544&tool=pmcentrez&rendertype=abstract.

Houtkooper, R.H. & Vaz, F.M., 2008. Cardiolipin, the heart of mitochondrial metabolism. *Cellular and Molecular Life Sciences*, 65, pp.2493–2506.

Huang, J. et al., 2013. Mitochondria-Targeted Antioxidant Peptide SS31 Protects the Retinas of Diabetic Rats. *Current Molecular Medicine*, 13, pp.935–945.

Hundal, R.S. et al., 2000. Mechanism by which metformin reduces glucose production in type 2 diabetes. *Diabetes*, 49, pp.2063–2069.

Jackson, G.R. et al., 2012. Inner retinal visual dysfunction is a sensitive marker of non-proliferative diabetic retinopathy. *The British Journal of Ophthalmology*, 96(5), pp.699–703. Available at: http://www.ncbi.nlm.nih.gov/pubmed/22174096 [Accessed May 20, 2014].

Kennedy, C.J., Rakoczy, P.E. & Constable, I.J., 1995. Lipofuscin of the retinal pigment epithelium: a review. *Eye (London, England)*, 9 (Pt 6), pp.763–771.

Kirwin, S.J. et al., 2011. Retinal gene expression and visually evoked behavior in diabetic long evans rats. *Investigative Ophthalmology & Visual Science*, 52(10), pp.7654–63. Available at: http://www.ncbi.nlm.nih.gov/pubmed/21862641 [Accessed May 20, 2014].

Kloner, R. a. et al., 2012. Reduction of Ischemia/Reperfusion Injury With Bendavia, a Mitochondria-Targeting Cytoprotective Peptide. *Journal of the American Heart Association*, 1, pp.e001644–e001644. Available at: http://jaha.ahajournals.org/cgi/doi/10.1161/JAHA.112.001644.

Kovach, J. & Schwartz, S., 2009. Novel Pharmacologic Approaches for the Management of Diabetic Retinopathy. *Mol Cell Pharmacol.*, 1(4), pp.222–227.

Kowluru, R. a et al., 2011. Abrogation of MMP-9 gene protects against the development of retinopathy in diabetic mice by preventing mitochondrial damage. *Diabetes*, 60(11), pp.3023–33. Available at: http://www.pubmedcentral.nih.gov/articlerender.fcgi?artid=3198054&tool=pmcentrez&rendertype=abstract [Accessed January 12, 2015].

Kowluru, R. a & Chan, P.-S., 2007. Oxidative stress and diabetic retinopathy. *Experimental diabetes research*, 2007, p.43603.

Kowluru, R.A., 2005. Diabetic Retinopathy: Mitochondrial Dysfunction and Retinal Capillary Cell Death. *Antioxidants & Redox Signaling*, 7(11&12), pp.1581–1587.

Krasner, N.M. et al., 2014. Glucagon-Like Peptide-1 (GLP-1) analog liraglutide inhibits endothelial cell inflammation through a calcium and AMPK dependent mechanism. *PLoS ONE*, 9(5), pp.1–11.

Kurihara, T. et al., 2012. Targeted deletion of Vegfa in adult mice induces vision loss. *Journal of Clinical Investigation*, 122(11), pp.4213–4217.

Liu, S. et al., 2014. Novel cardiolipin therapeutic protects endothelial mitochondria during renal ischemia and mitigates microvascular rarefaction, inflammation, and fibrosis. *American journal of physiology. Renal physiology*, 306(9), pp.F970–80. Available at: http://www.ncbi.nlm.nih.gov/pubmed/24553434 [Accessed June 9, 2014].

Lu, H. & Koshkin, V., 2010. Molecular and metabolic evidence for mitochondrial defects associated with β-cell dysfunction in a mouse model of type 2 diabetes. *Diabetes*, 59(February).

Luderitz, B., 1993. *Principles of Diabetes Mellitus*, Springer.

Madsen-Bouterse, S. a et al., 2010. Role of mitochondrial DNA damage in the development of diabetic retinopathy, and the metabolic memory phenomenon associated with its progression. *Antioxidants & Redox Signaling*, 13(6), pp.797–805. Available at: http://www.pubmedcentral.nih.gov/articlerender.fcgi?artid=2935337&tool=pmcentrez&rendertype=abstract.

Mather, K.J., Steinberg, H.O. & Baron, A.D., 2013. Insulin resistance in the vasculature. *The Journal of Clinical Investigation*, 123(3), pp.1003–1004.

Miller, J.W. et al., 1994. Vascular endothelial growth factor/vascular permeability factor is temporally and spatially correlated with ocular angiogenesis in a primate model. *The American journal of pathology*, 145(3), pp.574–584.

Mootha, V.K. et al., 2003. PGC-1alpha-responsive genes involved in oxidative phosphorylation are coordinately downregulated in human diabetes. *Nature genetics*, 34(3), pp.267–273.

Muoio, D.M., 2014. Metabolic Inflexibility: When Mitochondrial Indecision Leads to Metabolic Gridlock. *Cell*, 159(6), pp.1253–1262. Available at: http://linkinghub.elsevier.com/retrieve/pii/S0092867414015116 [Accessed December 5, 2014].

Nakamura, S. et al., 1997. Progression of nephropathy in spontaneous diabetic rats is prevented by OPB-9195, a novel inhibitor of advanced glycation. *Diabetes*, 46, pp.895–899.

Nathan, D. et al., 2009. Modern-Day Clinical Course of Type 1 Diabetes Mellitus After 30 Years' Duration. *Arch Intern Med*, 169(14), pp.1307–1316.

Nickla, D. & Wallman, J., 2011. The Multifunctional Choroid. *Prog Retin Eye Res*, 29(2), pp.144–168.

Polonsky, K.S., 2012. The Past 200 Years in Diabetes. *New England Journal of Medicine*, 367, pp.1332–1340.

Potenza, M.A. et al., 2009. Endothelial Dysfunction in Diabetes : From Mechanisms to Therapeutic Targets. *Current Medicinal Chemistry*, 16, pp.94–112.

Prusky, G.T. et al., 2004. Rapid quantification of adult and developing mouse spatial vision using a virtual optomotor system. *Investigative ophthalmology & visual science*, 45(12), pp.4611–6. Available at: http://www.ncbi.nlm.nih.gov/pubmed/15557474 [Accessed November 7, 2012].

Rena, G., Pearson, E.R. & Sakamoto, K., 2013. Molecular mechanism of action of metformin: Old or new insights? *Diabetologia*, 56, pp.1898–1906.

Ristow, M. & Zarse, K., 2010. How increased oxidative stress promotes longevity and metabolic health: The concept of mitochondrial hormesis (mitohormesis). *Experimental Gerontology*, 45(6), pp.410–418. Available at: http://dx.doi.org/10.1016/j.exger.2010.03.014.

Sabbah, H.N. et al., 2013. Long-Term Therapy With Bendavia (Mtp-131), a Novel Mitochondria-Targeting Peptide, Reverses Mitochondrial Functional Abnormalities in Left Ventricular Myocardium of Dogs With Advanced Heart Failure. *Journal of the American College of Cardiology*, 61(10), p.E709. Available at: http://linkinghub.elsevier.com/retrieve/pii/S0735109713607093.

Saltiel, A.R. & Kahn, C.R., 2001. Glucose and Lipid Metabolism. , 414(December), pp.799–806.

Samuel, V.T. & Shulman, G.I., 2012. Mechanisms for insulin resistance: Common threads and missing links. *Cell*, 148(5), pp.852–871. Available at: http://dx.doi.org/10.1016/j.cell.2012.02.017.

Santos, J.M. & Kowluru, R.A., 2013. Impaired Transport of Mitochondrial Transcription Factor and the Metabolic Memory Phenomenon Associated with the Progression of Diabetic Retinopathy. *Diabetes Metab Res Rev.*, 29(3), pp.204–213.

Schütt, F. et al., 2012. Moderately reduced ATP levels promote oxidative stress and debilitate autophagic and phagocytic capacities in human RPE cells. *Investigative Ophthalmology and Visual Science*, 53, pp.5354–5361.

Sharma, K., 2015. Mitochondrial Hormesis and Diabetic Complications: Figure 1. *Diabetes*, 64(October 2014), pp.663–672. Available at: http://diabetes.diabetesjournals.org/lookup/doi/10.2337/db14-0874.

Shulman, G.I., 2014. Ectopic Fat in Insulin Resistance, Dyslipidemia, and Cardiometabolic Disease. *The New England Journal of Medicine*, 31, pp.1131–1141.

Shweiki, D. et al., 1992. Vascular endothelial growth factor induced by hypoxia may mediate hypoxia-initiated angiogenesis. *Nature*, 359, pp.843–845.

Siegel, M.P. et al., 2013. Mitochondrial-targeted peptide rapidly improves mitochondrial energetics and skeletal muscle performance in aged mice. *Aging cell*, 12(5), pp.763–71. Available at: http://www.ncbi.nlm.nih.gov/pubmed/23692570 [Accessed June 9, 2014].

Skugor, M., 2014. Diabetes Mellitus Treatment. *Cleveland Clinic Center for Continuing Education*. Available at: http://www.clevelandclinicmeded.com/medicalpubs/diseasemanagement/endocrinology/diabetes-mellitus-treatment/ [Accessed March 1, 2015].

Sleigh, A. et al., 2011. Brief report Mitochondrial dysfunction in patients with primary congenital insulin resistance. *The Journal of Clinical InvestigationJournal of Clinical Investigation*, 121(6), pp.2457–2461.

Smith, R.A.J. & Murphy, M.P., 2011. Mitochondria-targeted Antioxidants as Therapies. *Discov Med.*, 11(57).

Snodderly, D.M. et al., 2002. Retinal pigment epithelial cell distribution in central retina of rhesus monkeys. *Investigative ophthalmology & visual science*, 43, pp.2815–2818.

Soulis-liparota, T. et al., 1991. Retardation by aminoguanidine of development of albuminuria, mesangial expansion, and tissue fluorescence in streptozocin-induced diabetic rat. *Diabetes*, 40, pp.1328–1334.

Strauss, O., 2005. The Retinal Pigment Epithelium in Visual Function. *Physiol Rev*, 85, pp.845–881.

Szendroedi, J., Phielix, E. & Roden, M., 2011. The role of mitochondria in insulin resistance and type 2 diabetes mellitus. *Nature Reviews Endocrinology*, 8(2), pp.92–103. Available at: http://dx.doi.org/10.1038/nrendo.2011.138.

Szeto, H. & Birk, A., 2014. Serendipity and the Discovery of Novel Compounds That Restore Mitochondrial Plasticity. *Clin Pharmacol Ther. Author*, 96(6), pp.997–1003.

Szeto, H.H., 2014. First-in-class cardiolipin-protective compound as a therapeutic agent to restore mitochondrial bioenergetics. *British Journal of Pharmacology*, 171, pp.2029–2050.

Szeto, H.H., 2008. Mitochondria-targeted cytoprotective peptides for ischemia-reperfusion injury. *Antioxidants & redox signaling*, 10(3), pp.601–619.

Szeto, H.H. et al., 2011. Mitochondria-targeted peptide accelerates ATP recovery and reduces ischemic kidney injury. *Journal of the American Society of Nephrology : JASN*, 22(6), pp.1041–52. Available at: http://www.pubmedcentral.nih.gov/articlerender.fcgi?artid=3103724&tool=pmcentrez&rendertype=abstract [Accessed January 13, 2013].

Takahashi, T. et al., 2014. A Novel MitoNEET Ligand, TT01001, Improves Diabetes and Ameliorates Mitochondrial Function in db/db Mice. *Journal of Pharmacology and Experimental Therapeutics*, 352, pp.338–345. Available at: http://jpet.aspetjournals.org/cgi/doi/10.1124/jpet.114.220673.

Thierry, M. et al., 2014. Metabolic syndrome triggered by high-fructose diet favors choroidal neovascularization and impairs retinal light sensitivity in the rat. *PloS one*, 9(11), p.e112450. Available at: http://www.pubmedcentral.nih.gov/articlerender.fcgi?artid=4224482&tool=pmcentrez&rendertype=abstract [Accessed January 14, 2015].

Vicent, D. et al., 2003. The role of endothelial insulin signaling in the regulation of vascular tone and insulin resistance. *J Clin Invest*, 111(9), pp.1373–1380.

Wilcox, G., 2005. Insulin and insulin resistance. *The Clinical biochemist. Reviews / Australian Association of Clinical Biochemists*, 26(May), pp.19–39.

Winder, W.W., 2009. Can Patients with Type 2 Diabetes Be Treated with AMPK-Activators? *Diabetologia*, 51(10), pp.1761–1764.

Xie, L. et al., 2008. Mitochondrial DNA oxidative damage triggering mitochondrial dysfunction and apoptosis in high glucose-induced HRECs. *Investigative Ophthalmology & Visual Science*, 49(9), pp.4203–9. Available at: http://www.ncbi.nlm.nih.gov/pubmed/18539942 [Accessed May 20, 2014].

Yang, L. et al., 2009. Mitochondria targeted peptides protect against 1-methyl-4-phenyl-1,2,3,6-tetrahydropyridine neurotoxicity. *Antioxidants & redox signaling*, 11(9), pp.2095–2104.

Zhang, H., Dellsperger, K.C. & Zhang, C., 2012. The link between metabolic abnormalities and endothelial dysfunction in type 2 diabetes: An update. *Basic Research in Cardiology*, 107(1), p.237. Available at: http://www.ncbi.nlm.nih.gov/pubmed/22189563 [Accessed January 4, 2015].

Zhang, W. et al., 2011. Inflammation and diabetic retinal microvascular complications. *Journal of cardiovascular disease research*, 2(2), pp.96–103. Available at: http://www.pubmedcentral.nih.gov/articlerender.fcgi?artid=3144626&tool=pmcentrez&rendertype=abstract [Accessed October 29, 2013].

Zhao, K. et al., 2004. Cell-permeable peptide antioxidants targeted to inner mitochondrial membrane inhibit mitochondrial swelling, oxidative cell death, and reperfusion injury. *The Journal of biological chemistry*, 279(33), pp.34682–90. Available at: http://www.ncbi.nlm.nih.gov/pubmed/15178689 [Accessed November 12, 2012].

Zhong, Q. & Kowluru, R. a, 2011. Diabetic retinopathy and damage to mitochondrial structure and transport machinery. *Investigative Ophthalmology & Visual Science*, 52(12), pp.8739–46. Available at: http://www.pubmedcentral.nih.gov/articlerender.fcgi?artid=3263781&tool=pmcentrez&rendertype=abstract [Accessed May 20, 2014].

Title: MITOCHONDRIAL ENERGY FAILURE IN THE RPE INDUCES LOSS OF VISUAL ACUITY IN EARLY METABOLIC SYNDROME: A NOVEL THERAPEUTIC TARGET

Short Running Title: Mitochondrial-targeted restoration of vision.

Authors: William C. Mills IV[1], Nazia M. Alam[2,3], Ryan P. Schreiner[4], Glen T. Prusky[2,3], Hazel H. Szeto[1]

Affiliations:

[1] Research Program in Mitochondrial Therapeutics, Department of Pharmacology, Weill Cornell Medical College, New York, NY, USA

[2] Dept of Physiology and Biophysics, Weill Cornell Medical College, New York, NY, USA

[3]Burke-Cornell Medical Research Institute, White Plains, NY, USA

[4]Department of Ophthalmology, Department of Cell and Developmental Biology, Department of Physiology and Biophysics, Margaret Dyson Vision Research Institute, Weill Cornell Medical College, New York, NY

Corresponding Author: William C. Mills, 1300 York Avenue, New York, NY 10065, 978 505 7675, wcm2002@med.cornell.edu

Key Words: diabetic retinopathy, RPE, SS-31, MTP-131, Bendavia, Ocuvia, insulin resistance, hyperglycemia, neovascularization, optomotor, spatial vision, cardiolipin, OKT, mouse

Disclosures

The peptide described in this article has been licensed for commercial research and development to Stealth Peptides Inc, a clinical stage biopharmaceutical company, in which H.H.S. and the Cornell Research Foundation have financial interests. Equipment and software in this article has been purchased from CerebralMechanics Inc., of which GTP is a principal.

Word Count: ~3900

Number of Tables/Figures: 7

Acknowledgements

We would like to thank Lee Cohen-Gould of the Weill Cornell Optical Microscopy Facility for her support with EM imaging. Guillermo L. Lehmann Mántaras, M.D., Ph.D. was instrumental in flat mounting and confocal imaging. The lab of Enrique Rodriguez-Boulan, M.D., with funding from the Tri-Institutional Training Program in Vision Research by the National Eye Institute of the National Institutes of Health under Award Number T32EY007138 was especially helpful throughout the process.

ABSTRACT

Subtle changes in the neural retina can be detected much earlier than retinal vasculopathy in diabetic retinopathy. In mice fed a high fat diet, we have found early and progressive decline in visual acuity, as measured by optokinetic tracking, even before significant weight gain and hyperglycemia. Fundus examination was normal and fluorescein angiography showed normal retinal vasculature. The only major histologic findings were swollen mitochondria, edema and degenerative changes in the retinal pigment epithelium (RPE). Outer retinal ischemia and inflammation are supported by elevated VEGF, TNFa, MCP-1, and choroidal neovascular tufts. Treatment with a mitochondria-targeted tetrapeptide (SS-31/MTP-131) reversed visual decline without reducing blood glucose, body weight or insulin resistance. SS-31 is known to target cardiolipin and promote electron transfer and ATP synthesis. SS-31 preserved mitochondrial morphology and integrity of the RPE, reduced inflammatory markers, and prevented choroidal neovascularization. These results demonstrate a causal relationship between RPE mitochondrial energy failure and loss of visual acuity in early metabolic syndrome, and support a bioenergetics-based approach for preventing diabetic complications. A topical formulation of SS-31 (Ocuvia^{TM}) is in Phase 2 clinical trial for diabetic macula edema and non-proliferative age-related macular degeneration.

INTRODUCTION

Diabetic Retinopathy (DR can manifest as diabetic macular edema in the non-proliferative phase, and retinal neovascularization with vascular hemorrhage in the proliferative phase. Intensive metabolic control reduces the incidence and progression of DR, but proliferative DR still develops in up to 20% of persons with diabetes despite intensive metabolic control (1). Vascular endothelial growth factor (VEGF) has been implicated in the pathogenesis of macular edema and neovascularization, and agents that block VEGF are currently the most effective treatment for DR when metabolic control is insufficient. Although these anti-VEGF therapies are effective in regression of neovascularization in some patients, they only provide small gains in visual acuity and require repeat intravitreal injections with the additional concern of systemic adverse effects due to the pleiotrophic actions of VEGF.

There is growing recognition that retinal dysfunction and impaired visual behavior, including loss of contrast sensitivity and dark adaptation, are present in human patients and diabetic animal models before retinal vascular changes become evident (2-7). Furthermore, abnormal electroretinography (ERG) has been found in both type 1 and type 2 diabetics who have no clinical vascular lesions, as well as diabetic animal models (6; 8; 9). We recently reported very early decline in spatial visual function in a mouse model of high fat feeding (10). Reduction in spatial frequency and contrast sensitivity was apparent after just 4 weeks of high-fat diet (HFD), before there was any increase in blood glucose. Abnormal glucose tolerance

tests (GTT) suggest that the onset of visual function may be associated with insulin resistance rather than glucose toxicity. However, the addition of a modest dose of STZ (HFD+STZ) potentiated the rate and magnitude of visual degeneration in HFD mice, suggesting a synergistic mechanism between insulin resistance and hyperglycemia.

Hyperglycemia, by increasing substrate flux through mitochondria, increases production of reactive oxygen species (ROS), causing oxidative damage to mitochondrial lipids and proteins and reducing ATP generation (11-14). As mitochondrial damage accrues, endogenous antioxidant systems fail to keep pace with elevated ROS levels, creating a feed-forward cycle of oxidative stress. Once this cycle has begun, bioenergetics failure in the retinal pigment epithelium (RPE) impairs its critical barrier, secretory, transport and visual cycle functions, as well as the phagocytic capability required for the daily metabolism of shed photoreceptor outer segments, ultimately resulting in loss of visual function and cell death (15). To test the hypothesis that mitochondrial dysfunction and oxidative stress may underlie this visual decline, we treated both HFD and HFD+STZ mice with the mitochondria-targeted antioxidant SS-31 (also known as MTP-131) (16; 17). Treatment with SS-31 after onset of visual decline led to recovery of visual function, while having no effect on blood glucose levels, body weight or glucose clearance (10). We further demonstrated a similar preservation of spatial frequency and contrast sensitivity utilizing a topical ophthalmic formulation of SS-31 (10). These findings suggest that SS-31 is acting directly to protect the retina from insulin resistance and glucose toxicity. In this study, we report that the decline in spatial visual function is associated

with choroidal neovascularization, retinal hypoxia and inflammation, and degeneration of the RPE. Treatment with SS-31 preserved the choroidal vasculature and protected RPE structure and function, and restored visual function.

RESEARCH DESIGN AND METHODS

Animals and Diets

Experimental procedures on animals were conducted in accordance with the policies of the Weill Cornell Medical College IACUC Committee. Male C57BL/6 mice were obtained from Charles River Laboratories at 3 weeks of age. They were maintained on a 12 hour light/dark cycle. Mice were fed a normal diet (ND; LabDiet Picolab Rodent Diet 5053; 4.5% fat, 60% carbohydrate, 20% protein,) or a high-fat diet (HFD; Bio-Serv Mouse Diet F3282; 36.0% fat, 35.7 % carbohydrate, 20.5% protein) *ad libitum* from 4 weeks of age. Streptozotocin (STZ; 40 mg/kg, *i.p.*) was administered to HFD mice (HFD+STZ) at 8 weeks of age for 5 consecutive days.

Study Design

Body weight, non-fasted blood glucose, and visual behavior were assessed weekly in all mice starting at 4 weeks. A glucose tolerance test (GTT) was administered at 12 weeks and 30 weeks of age as described previously (10). After the first GTT at 12 weeks, HFD+STZ mice received either 5 μl of 0.01 M SS-31 (D-Arg-2'6'-dimethylTyr-Lys-Phe-NH_2; Stealth Peptides, Newton, MA) or vehicle (sodium acetate, pH 6.0) in each eye daily from 12 to 32 weeks of age.

Test of Spatial Visual Function

Spatial thresholds for optokinetic tracking (OKT) of sine-wave gratings were measured weekly from 4 weeks to 32 weeks of age using a virtual optokinetic system

(OptoMotry, CerebralMechanics Inc., Medicine Hat, Alberta, Canada). Details of this method can be found in our previous publications (10; 18; 19). A spatial frequency (SF) threshold was generated under scotopic conditions (1 lux) through each eye separately in a testing session.

Fundus Photography and Fluorescein Angiography

Fundus images were taken on isoflurane-anesthetized mice at 32 weeks with the Micron III system (Phoenix Research Laboratories, Pleasanton, CA). Briefly, the pupils were dilated with tropicamide and phenylephrine hydrochloride, followed by Goniosoft (Hydroxypropyl Methylcellulose 2.5%) medium for protection. A series of 5-15 images was taken for each eye. Fluorescein angiography followed the fundus protocol. A series of 5-15 images per eye was taken starting 1 minute after 0.05-0.1 ml of 2.5% sodium fluorescein (*i.p.*). Fundus and FA images were graded on a standard scale.

Tissue Handling and Histological Evaluations

Mice were sacrificed by anesthetic overdose and cervical dislocation, followed by decapitation and eye excision. For assessment of retinal architecture, eyes were fixed in Davidson's Fixative for two days, followed by post-fixation in 4% paraformaldehyde, 2% ZnCl and 20% isopropyl alcohol for >48 h. Eyes were then processed by Excalibur Pathology Inc. according to a standard protocol. The H&E stained sections were photographed with a light microscope (Zeiss Axio Observer Z1 with an AxioCam ERc 5s color CMOS camera) and examined for laminar

abnormalities. Whole flat mounts of the outer retina were prepared for detailed analysis of the RPE monolayer (20). Briefly, eyes were enucleated and the retinas were carefully removed with tweezers. Eye cups were fixed for 1 hour, washed in cold ICC buffer and stained for 15 minutes in 1:100 Alexa Fluor® 488 Phalloidin (Life Technologies, Carlsbad, CA) and a 1:100 of a 1μg/1μL solution of isolectin IB4 conjugated with Alexa Fluor 568 (Life Technologies, Carlsbad, CA) in ICC buffer. Imaging was accomplished with both a Zeiss Cell Observer SD equipped with dual Photometrics Evolve 512 EMCCD cameras on the Yokogawa CSU-X1 confocal scanner unit and a Zeiss Axio Observer. Images were stitched together at maximum intensity projection with Zeiss Zen software to view the entire flat mount with high resolution. Stacks of images spanning the retinal vasculature and RPE, and three-dimensional images were obtained using Zeiss Zen image analysis software (Carl Zeiss AG, Oberkochen, Germany). RPE cell size was quantified using ImageJ (National Institutes of Health, Bethesda, MD). Twenty areas were scored from three eyes per group, with five representative cells quantified per area. Neovascular tuft counts were performed by tallying the number of isolectin-labeled tufts around the optic nerve in five flat mounted eyes per group.

Transmission Electron Microscopy (TEM) of Retina

Eyes were punctured with a fine gauge needle through the pupil, and placed in Yellow Fixative on ice for 24 hours then transferred and stored in 0.1M sodium cacodylate at RT until being processed. Eyes were immersed in 1% osmium tetroxide for 1 h, dehydrated in acetone, stained in 1.5% uranyl acetate for 1 h, and then embedded in

Epon. 1μM sections of the block were cut and stained with 0.1% toluene blue, then sections were further cut to 70 nM and stained with lead citrate (21). Specimens were examined with a digital TEM (JEOL JEM-1400). To calculate mitochondrial cristae morphology, mitochondrial density was quantified using Mean Grey Value on an inverted-color image (ImageJ). 25-30 total representative mitochondria were assessed per treatment group from 3 or more eyes.

Protein Expression in the RPE/Choroid

Eyes were enucleated and the cornea removed in order to detach the lens and retina. The RPE/choroid complex was scraped from the sclera carefully using a scalpel and collected in cold PBS, homogenized and stored at -80^{o}C. Homogenate was suspended in loading buffer and subjected to a 4-15% sodium dodecyl sulfate polyacrylamide gel electrophoresis. The resolved proteins were transferred to a polyvinylidene fluoride membrane. After electroblotting, the membrane was incubated overnight with one of the following antibodies: anti-VEGF (1:250) (Millipore, Billerica, MA), anti-TNFα (1:250) (Abcam, Cambridge, MA), anti-CCL2/MCP-1 (1:2000) (Abcam, Cambridge, MA), anti-eNOS (1:500) (Abcam, Cambridge, MA), anti-AMPK (1:500) (R&D Systems, Minneapolis, MN), or anti-β-actin (1:5000) (Santa Cruz, Dallas, TX). Membranes were further incubated for 1 hour with their respective HRP-conjugated antibodies. Protein bands were detected with an enhanced chemiluminescence detection system (Cell Signaling, Danvers, MA). Bands were evaluated for integrated density values with ImageJ software. AMPK [p-172] levels were quantified using the

AMPK [pT172] ELISA Kit (Life Technologies, Carlsbad, CA) according to manufacturer's protocol.

Statistical Analyses

All data are presented as mean ± S.E. One-way analysis of variance (ANOVA) was used for group comparisons. Post-hoc multiple comparisons were performed using Tukey's correction methods (GraphPad Software, Inc., San Diego, CA). Statistical comparisons were considered significantly different at $P < 0.05$.

RESULTS

Longitudinal changes in spatial visual function during high fat feeding

There was no change in SF threshold in ND mice over the course of this study, from 4 weeks through 32 weeks of age (Fig. 1*A*). A decrease in SF threshold was apparent after just 4 weeks of HFD, even before the administration of STZ. Spatial vision deteriorated markedly by 12 weeks and continued to decline throughout the study period, reaching 0.25 c/d by 32 weeks (Fig. 1*A*). Daily topical application of SS-31 starting at 12 weeks arrested the decline in SF in HFD+STZ mice, and gradually restored visual function to normal levels by 20 weeks.

Basal metabolic parameters during high fat feeding

Body weight in the HFD+STZ mice (n=6) was not different from ND mice (n=5) at 12 weeks (29.5 ± 0.07 *vs* 25.2 ± 0.29 g), at the time when there was significant decline in visual function. Body weight was significantly higher in HFD+STZ mice by 30 weeks (59.4 ± 0.15 *vs* 33.0 ± 0.23 g; $P < 0.001$) (Fig. 1*B*). Daily topical application of SS-31 starting at 12 weeks had no effect on body weight in HFD+STZ mice at 30 weeks (59.1 ± 0.22 g vs 59.4 ± 0.15 g; n=6) (Fig. 1*B*). Non-fasted blood glucose was slightly elevated in HFD+STZ mice at 12 weeks (202 ± 1.7 *vs* 184 ± 0.5 mg/dl), but was significantly elevated at 30 weeks (291 ± 2.0 mg/dl *vs* 190 ± 5.3; $P < 0.001$) (Fig. 1*C*). Daily topical application of SS-31 starting at 12 weeks had no effect on blood glucose in HFD+STZ mice at 30 weeks (287.5 ± 5.2 mg/dl). Glucose clearance, as determined

by GTT, was impaired by 12 weeks and persisted through 30 weeks, and was unaffected by SS-31 (Fig. 1*D* and *E*).

Disruption of RPE morphology during high fat feeding The delicate laminar architecture of the retina was relatively unaltered in HFD+STZ mice when compared to ND mice at 32 weeks of age (Fig. 2*A*). Higher magnification revealed disruption of the single cell layer of the RPE in HFD+STZ mice (Fig. 2*B*, arrows). Examination of the RPE layer by TEM revealed occasional degenerating cells with loss of cell contents (Fig. 2*C*). The RPE layer was intact in HFD+STZ mice that received daily SS-31 treatment starting at 12 weeks (Fig. 2*A*-*C*). Flatmounts of the RPE layer was stained with phalloidin (F-actin) to visualize the hexagonal lattice. The RPE of ND mice showed relative homogeneity with respect to cell size (Fig. 2*D* and E). Significantly more variability was seen in the HFD+STZ group, with much larger and much smaller cells present. SS-31-treatment prevented the heterogeneity in cell size seen in the HFD+STZ group, maintaining a size distribution similar to the vehicle-treated mice (Fig. 2*D* and *E*).

RPE mitochondrial and cellular structure during high fat feeding

ND mice exhibited normal RPE morphology and ultrastructural histology at 32 weeks of age (Fig. 3*A*). The RPE layer maintained continuous cell-cell contact (white arrow) with numerous intricate basolateral infoldings (*). The cytoplasm was filled with pigmented granules (PG) and there was no sign of endoplasmic reticulum (ER) stress. Mitochondria (M) are elongated and clustered along the basal membrane infoldings

and along cell-cell junctions. In contrast, RPE cells from HFD+STZ mice exhibited an interrupted RPE barrier with breaks and spaces between cells (black arrow) (Fig.3*C* and 3*D*). Basolateral infoldings were edematous and swollen (**), and were occasionally filled with membrane-bound vesicles. ER stress was apparent, as were rounded and swollen mitochondria (M) that were depleted of cristae membranes (Fig. 3*C*). SS-31-treated HFD+STZ mice displayed RPE morphology similar to ND animals, with extensive basolateral infoldings, no edema, tight cell junctions (white arrow), elongated mitochondria (M), and no ER stress (Fig. 3*D*). Higher magnification of the RPE revealed notable differences in mitochondria structure among the three groups (Fig. 3*E*). Mice fed ND displayed elongated mitochondria densely packed with cristae membranes and electron-dense matrix. RPE from HFD+STZ mice featured swollen mitochondria with a rounded shape, with few cristae and an electron-lucent matrix. In contrast, SS-31-treated HFD+STZ mice exhibited mitochondrial morphology similar to ND mice. Mitochondrial density was significantly reduced in the HFD+STZ mitochondria, but there was no difference between HFD+STZ mice treated with SS-31 and ND mitochondria (Fig. 3*F*).

Choroidal neovascular tufts are seen with high fat feeding

Isolectin IB4 selectively labels endothelial cell glycocalyx, but the highly pigmented RPE and choroid of C57BL/6 mouse eyes normally prevent visualization of the choroidal capillaries. Notably, punctated staining was seen throughout the eye cup in HFD+STZ mice but not in ND or HFD+STZ mice treated with SS-31 (Fig. 4*A*). Higher magnification revealed these isolectin-stained cells to be single cells with

processes radiating outwards from a central tuft (Fig. 4*B*). Closer inspection with z-stack confocal microscopy revealed these tufts to be between the apical face of the RPE lattice and the photoreceptors of the neural retina (Fig. 4*C*). These neovascular tufts were not seen in ND mice or HFD-STZ mice treated with SS-31 (Fig. 4*D*).

Characterization of Fundus and Retinal Vasculature during high fat feeding

Fundus photography showed no difference in gross morphology between HFD+STZ mice and ND mice (Fig.5*A*). The retina appeared healthy in all animals with no signs of hypoxia or vascular abnormalities. Fluorescein angiography also showed no notable differences between the inner retinal vasculature among the three groups, with all animals lacking obvious signs of occlusion or leakage (Fig. 5*B* and *C*).

High fat feeding leads to loss of AMPK activity

There was a significant decrease in phosphorylated AMPK (pAMPKa) in HFD+STZ mice at 32 weeks (Fig. 6*A*). Treatment with SS-31 starting at 12 weeks partially restored pAMPKa in HFD+STZ mice (Fig. 6*A*). This reduction in pAMPKa reflects a reduction in AMPK activation rather than a decline in protein levels (Fig. 6*B*).

Upregulation of hypoxia and inflammatory markers in the retina during high fat feeding

Although VEGF is normally expressed in the RPE/choroid complex in ND mice, it was significantly upregulated in the HFD+STZ retinas (Fig. 6*C*). Treatment with SS-31 starting at 12 weeks prevented this upregulation of VEGF in HFD+STZ mice (Fig.

6*C*). The upregulation of VEGF is likely in response to hypoxia and indicates retinal ischemia during high fat feeding. Endothelial nitric oxide synthase (eNOS) is responsible for the production of nitric oxide (NO), a critical vasodilatory element that was significantly downregulated in HFD+STZ mice at 32 weeks, suggesting that high fat feeding dramatically compromises choroidal blood flow. This down-regulation of eNOS in HFD+STZ mice was completely prevented by treatment with SS-31 (Fig. 6*D*). Retinal inflammation is a prominent component of DR, and we find a significant increase in tumor necrosis factor-α (TNFα) and monocyte chemotactic protein 1 (MCP1) (also known as chemokine ligand 2 (CCL2)) in the choroid/RPE in HFD mice (Fig. 6*E* and 6*F*). Treatment with SS-31 completely abolished the upregulation of these proinflammatory markers in the RPE/choroid, suggesting that SS-31 has an anti-inflammatory action in the retina.

DISCUSSION

Our recent study was the first longitudinal study documenting the decline in SF threshold starting after just 4 weeks of HFD in mice (10). In this study, we show the lack of any change in the inner retinal vasculature even after 28 weeks of HFD. Instead, this early visual dysfunction is correlated with specific disruption of the RPE and choroidal neovasculature. Our results support a model whereby HFD induces choroidal endothelial cell dysfunction and downregulation of eNOS that results in decreased choroidal blood flow (Fig. 7). As the choroidal vasculature accounts for 80% of retinal blood flow, any reduction in choroidal blood flow greatly reduces blood supply to the RPE and decreases mitochondrial ATP production. Bioenergetics failure in the RPE compromises its myriad of ATP-dependent functions that result in photoreceptor dysfunction, retinal edema, inflammation and neovascularization (Fig. 7). Our study is the first to demonstrate that protection of the choroidal vasculature and RPE bioenergetics can arrest and reverse the visual decline seen in early metabolic syndrome. These findings are novel and have significant translational relevance. The treatment of diabetic vision loss is currently limited to VEGF inhibitors in the late stages of the disease. These anti-VEGF therapies are expensive, complicated to administer, marginally successful, and fail to mitigate the underlying basis of the disease. SS-31 represents a novel approach to the treatment of DR. First, SS-31 acts directly on the mitochondrial ETC to improve retinal bioenergetics (16; 17). Second, SS-31 can reverse diet-induced visual dysfunction without lowering body weight or

blood glucose. Third, SS-31 is highly effective in protecting endothelial and epithelial cells in ischemic conditions (22-24). Fourth, SS-31 can be easily administered as an eye drop, it has a rapid onset of action, and an excellent safety profile (16; 17; 25). Based on this research, topical SS-31 (Ocuvia^{TM}) has just entered Phase 2 clinical trial for diabetic macula edema (NCT02314299).

While hyperglycemia is often thought to be the driving force behind diabetic complications, our results show that decline in spatial visual function begins before any increase in blood glucose. Impaired glucose clearance at 12 weeks suggests that insulin resistance, rather than hyperglycemia, might be responsible for the initial visual decline. Extensive evidence support the development of insulin resistance after just a few weeks of high fat feeding, as demonstrated by elevated plasma insulin levels, insulin-stimulated glucose metabolism, and euglycemic-hyperinsulinemic clamp studies (26-28). Blunted Akt phosphorylation has been shown in retina and other organs (26; 27; 29). Thus impaired insulin sensitivity can develop rapidly with relatively short interval of HFD. The vascular endothelium is an important insulin target, and disruption of insulin signaling reduces the expression of endothelial nitric oxide synthase (eNOS) and inhibits nitric oxide (NO) production, resulting in endothelial dysfunction and ischemia (30-32). In this study, downregulation of eNOS in the RPE/choroid confirms retinal insulin resistance and endothelial dysfunction.

Retinal ischemia/hypoxia triggers the upregulation of VEGF and abnormal angiogenesis (33). Here we demonstrate a very early manifestation of this

neovascularization process, small neovascular tufts that are visible above the RPE. Similar early-stage neovascular tufts have been reported in rats fed a high-fructose diet (8). Additionally, microaneurysms have been seen in rabbits on high-fat and high-sucrose diet while gross retinal morphology remained intact (34). High fat feeding further triggers retinal inflammation (35; 36), and we found significant elevation of TNFα and MCP-1/CCL2 expression in HFD+STZ retinas, consistent with retinal hypoxia. TNFα is required for late breakdown of the BRB in diabetic mice (37), and MCP-1 plays an important role in recruiting monocytes and macrophages to the eye in DR (38).

Insulin resistance is especially problematic for the choroidal vasculature where constitutive insulin signaling is responsible for glucose uptake required for the metabolically active retina (39; 40). The RPE is highly dependent on mitochondrial ATP generation to support its numerous functions that are essential for the action and survival of photoreceptors (15). Even moderately reduced ATP levels greatly reduce phagocytic activity of human RPE cells (41). Our results show that even short-term high fat feeding cause mitochondrial swelling and loss of cristae membranes in the RPE, leading to insufficient ATP. Cellular edema, disruption of basal membrane infoldings, and loss of cell-cell contact, are typical signs of ATP depletion (42). Similar mitochondrial swelling led to apoptosis in retinal neurons of early diabetic rats (43). High fat feeding for 3 months was shown to decrease both outer and inner retina thickness and increase apoptosis in rats, indicating modest retinal degeneration (28). The change in RPE morphometrics with the appearance of some large cells with more

than 6 sides suggests that there has been some cell loss and surrounding cells are enlarged in an attempt to protect the BRB (44). Sporadic breakdown in the RPE sheet may allow the choroidal neovascular tufts to migrate above the RPE (45).

SS-31 is the first pharmacological agent that can arrest visual decline, and even restore visual function, in high fat feeding, despite having no effect on body weight, blood glucose, or systemic glucose clearance. We previously reported that HFD and insulin resistance in skeletal muscles is associated with increased mitochondrial H_2O_2 production, and by reducing mitochondrial ROS, SS-31 prevented insulin resistance in skeletal muscles (27). In this study, SS-31 was initiated after onset of insulin resistance and visual decline, but it was able to normalize the expression of eNOS and VEGF in the RPE/choroid, suggesting that SS-31 can improve insulin sensitivity in retinal endothelial cells and preserve choroidal blood flow (Fig. 7). By preventing retinal hypoxia, choroidal neovascularization and inflammation were also prevented. In addition, SS-31 is known to minimize ischemic injury by protecting mitochondria cristae structure and maximizing ATP production under low substrate conditions in endothelial and epithelial cells (24; 42; 46). Here, mitochondria in the RPE appeared normal during high fat feeding, and the ATP-dependent processes of the RPE monolayer were maintained (42; 46). Thus, SS-31 also helps the RPE tolerate retinal ischemia better and maintain cellular structure and function (Fig. 7). Later when blood glucose becomes elevated, SS-31 may, in addition, protect against the detrimental effects of high glucose on retinal endothelial cells. This is supported by a prior study showing that SS-31 can stabilize mitochondrial potential, reduce ROS production, and

prevent cytochrome c release in human retinal endothelial cells subjected to high glucose conditions (47). Thus SS-31 provides a novel therapeutic approach for minimizing end-organ damage in diabetes by promoting mitochondrial bioenergetics rather than reducing blood glucose or increasing insulin sensitivity. AMPK, the fuel-sensing enzyme activated by low ATP levels, is known to be dysregulated in insulin resistance and diabetes, and strategies that activate AMPK can be helpful for these conditions (48). Interestingly, resveratrol normalized AMPK activity in retinas of diabetic mice and prevented retinal inflammation and VEGF upregulation without reducing blood glucose (49). Metformin, the diabetic drug that modestly improves insulin sensitivity, was reported to act as an AMPK activator, but it does so by inhibiting complex I of the ETC (50). AMPK activity was significantly down-regulated in the HFD+STZ mice, and treatment with SS-31 significantly improved phosphorylated AMPK levels in the retina. Unlike metformin, SS-31 promotes efficiency of the ETC to increase ATP production and reduce ROS emission (17). Restoration of the bioenergetic capacity of the retina may play a role beyond diabetic retinopathy. Impairment of the RPE and choroidal neovascularization are also hallmarks of age-related macula degeneration, and our results suggest that SS-31 may be beneficial for this disease.

FIGURE LEGENDS

Fig. 1. Longitudinal changes in spatial frequency threshold during high fat feeding. *A*. Spatial frequency stays constant in ND mice, but declines progressive in HFD+STZ animals starting at 8 weeks. SS-31 treatment starting at 12 weeks reverses the decline and restores SF threshold in HFD+STZ mice. *B*. Body weight showed no difference at 12 weeks, but was significantly elevated in the HFD+STZ animals at 30 weeks. *C*. Resting blood glucose was slightly elevated in HFD+STZ mice at 12 weeks, but was significantly increased at 30 weeks. *D & E*. Glucose clearance was significantly impaired in HFD+STZ at both 12 and 30 weeks. Daily treatment with topical SS-31 had no effect on body weight, blood glucose or glucose clearance in HFD+STZ mice.

Fig. 2. Disruption of RPE morphology during high fat feeding. *A*. Laminar architecture of the retina, with ganglion layer at top and choroid at bottom (x200). No notable disruptions to the laemellar architecture are obvious. *B.* The RPE single cell layer is disrupted in HFD+STZ mice (arrows) (x400). SS-31 treatment preserved the continuity of the RPE monolayer. *C.* Electron micrographs show occasional degenerating RPE cell in HFD+STZ mice. *D*. Representative flat mount images of the RPE with phalloidin (green) depicting the cell lattice. *E*. RPE cell size exhibited little variation in ND mice, but was much more variable in HFD+STZ animals. SS-31-treated mice showed distribution similar to ND mice.

Fig. 3. Electron micrographs of the RPE. *A*. RPE from ND mice demonstrate intricate basal membrane infoldings (*), tight cell-cell contact (white arrow), elongated cristae-dense mitochondria (M), and pigment granules (PG). *B & C*. RPE from HFD+STZ mice exhibit separation of cell-cell contact (black arrow), swollen mitochondria (M) and either edematous basal membrane infoldings or a total loss of infoldings. *D.* RPE from HFD+STZ mice treated with SS-31 have tight cell-cell contact (white arrow), elongated cristae-dense mitochondria (M), and proper membrane infoldings (*). *E.* Representative mitochondria from ND, HFD+STZ, and HFD+STZ mice treated with SS-31. *F.* Quantification of mitochondrial density. *** $P < 0.001$.

Fig. 4. Morphology of RPE and choroidal vasculature. *A*. Flat-mounted retinas labeled with phalloidin (*green*, depicting the hexagonal lattice of the RPE) and isolectin IB4 (*red*, depicting endothelial glycocalyx) around the optic nerve. Neovascular tufts are numerous in the HFD+STZ mice (see as red dots), but not in mice treated with SS-31. *B & C*. Higher magnification reveals neovascular tufts with spider-like processes in HFD+STZ mice. Z-stack shows the tufts sitting directly above the apical side of the RPE layer inside the retina, but under the photoreceptor outer segments. Images taken with the support of Guillermo Lehmann Mántaras, M.D., Ph.D. *D*. Quantification of neovascular tufts.

Fig. 5. *A*. Representative fundus photographs showing no difference in gross morphology with high fat feeding. The retina appeared healthy with no signs of

no notable differences in the inner retinal vasculature with high fat feeding, with no obvious signs of occlusion or leakage. *C.* Magnification of inset shown in *B*.

Fig. 6. Protein expression in the RPE/choroid. *A*. pAMPKα. *B*. AMPKa. *C*. VEGF. *D*. eNOS. *E*. TNFα. *F*. MCP-1 or CCL2. * $P < 0.05$; ** $P < 0.01$; *** $P < 0.001$.

Fig. 7. Schematic summarizing the progression from early endothelial cell damage in the choroid and RPE bioenergetics failure to retinal edema, inflammation, and choroidal neovascularization in DR. SS-31 protects choroidal endothelial cells and protects choroidal blood flow, thereby preventing injury to the RPE, retinal inflammation and choroidal neovascularization. In addition, SS-31 protects the RPE from ischemic injury.

Fig. 1. Longitudinal changes in spatial frequency threshold during high fat feeding.

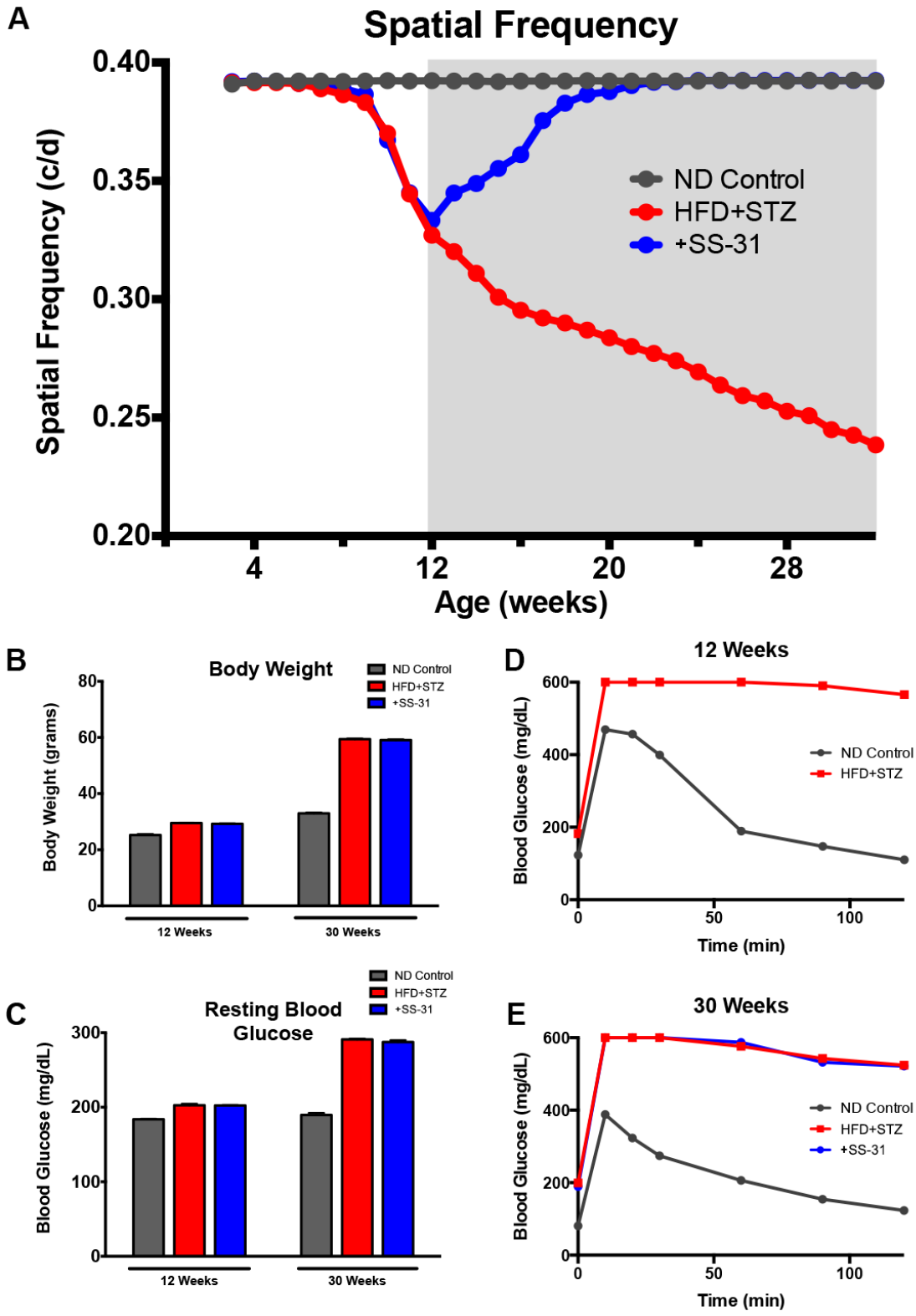

Fig. 2. Disruption of RPE morphology during high fat feeding.

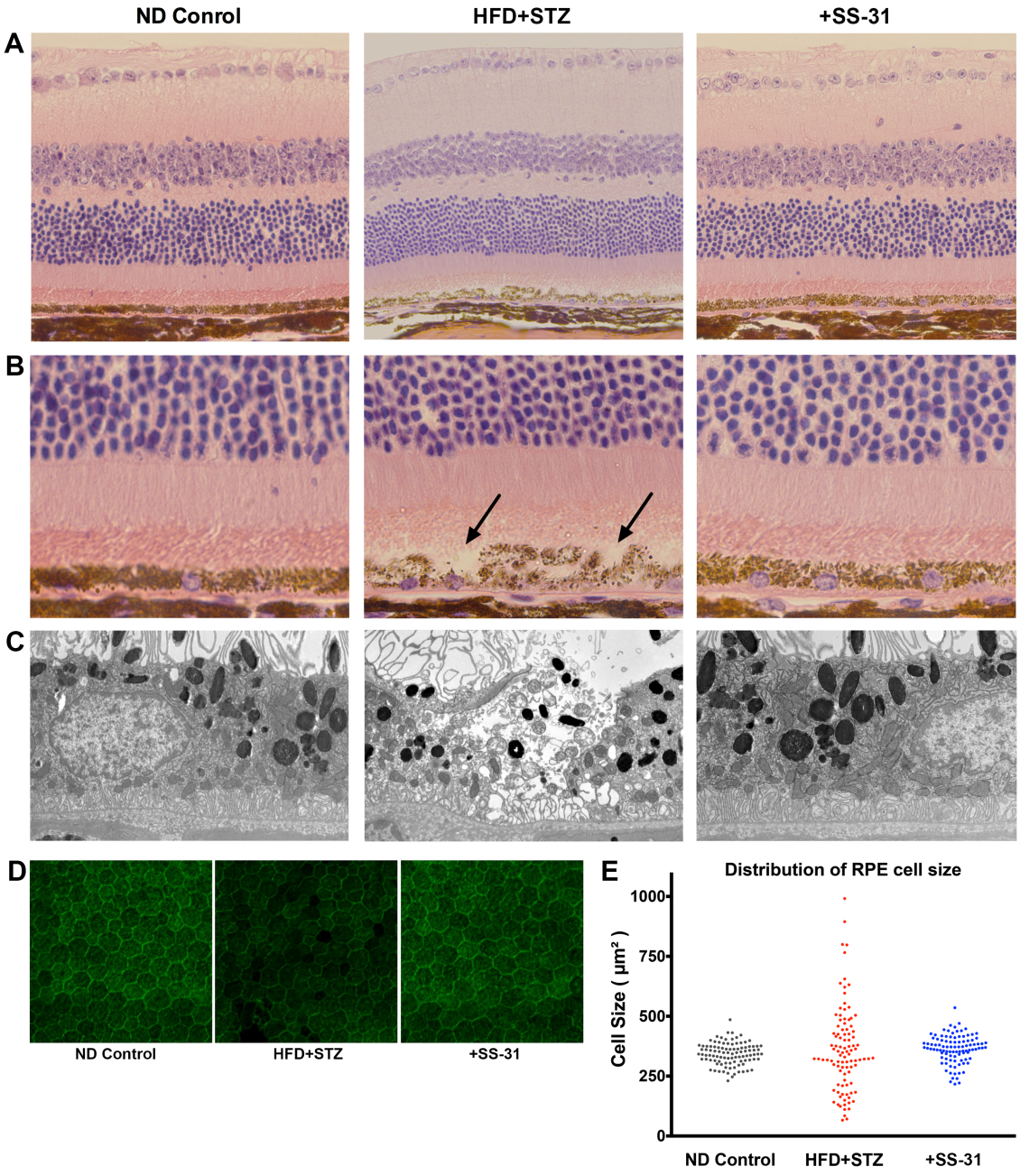

Fig. 3. Electron micrographs of the RPE.

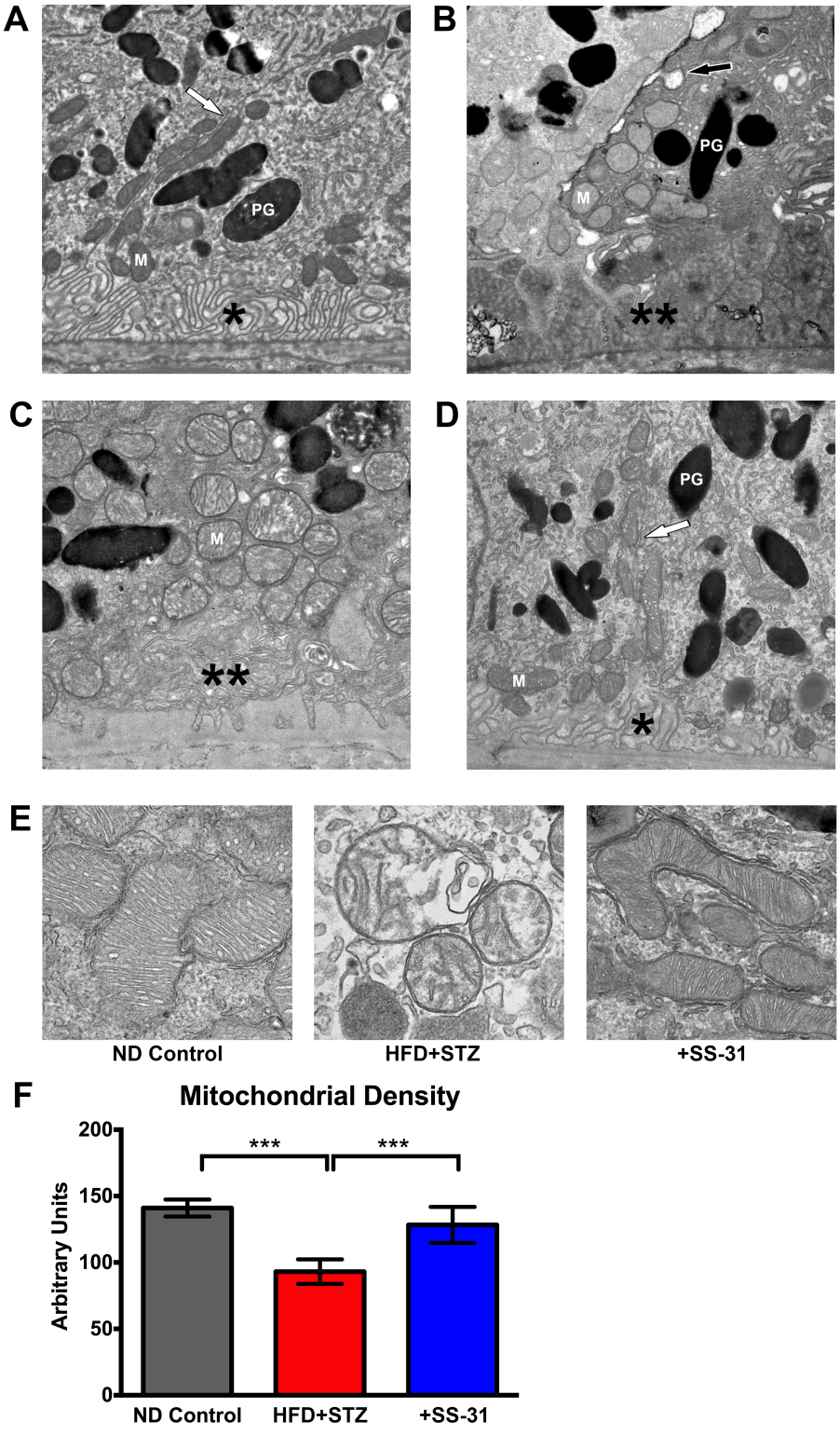

Fig. 4. Morphology of RPE and choroidal vasculature.

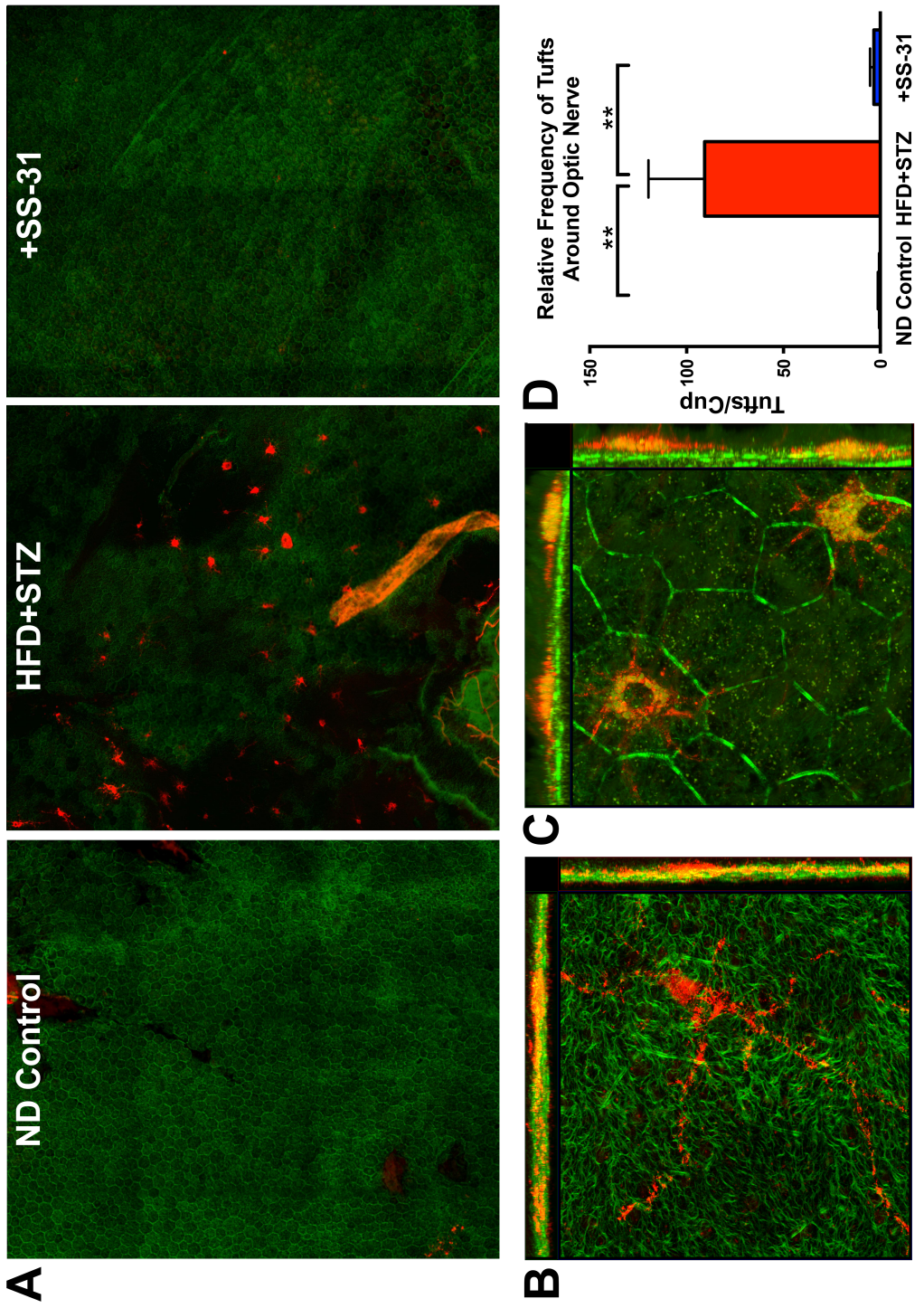

Fig. 5. *A*. Representative fundus photographs.

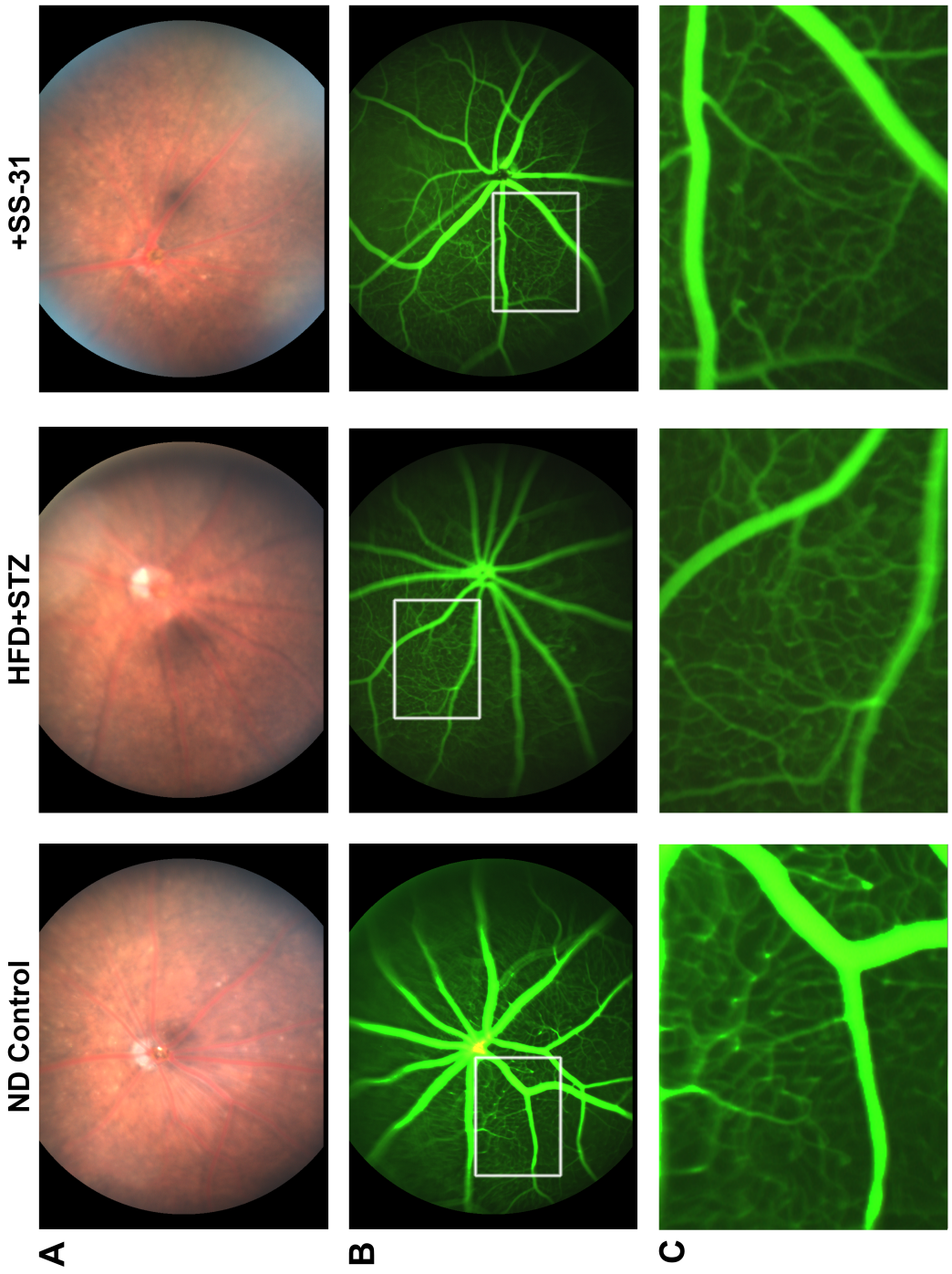

Fig. 6. Protein expression in the RPE/choroid.

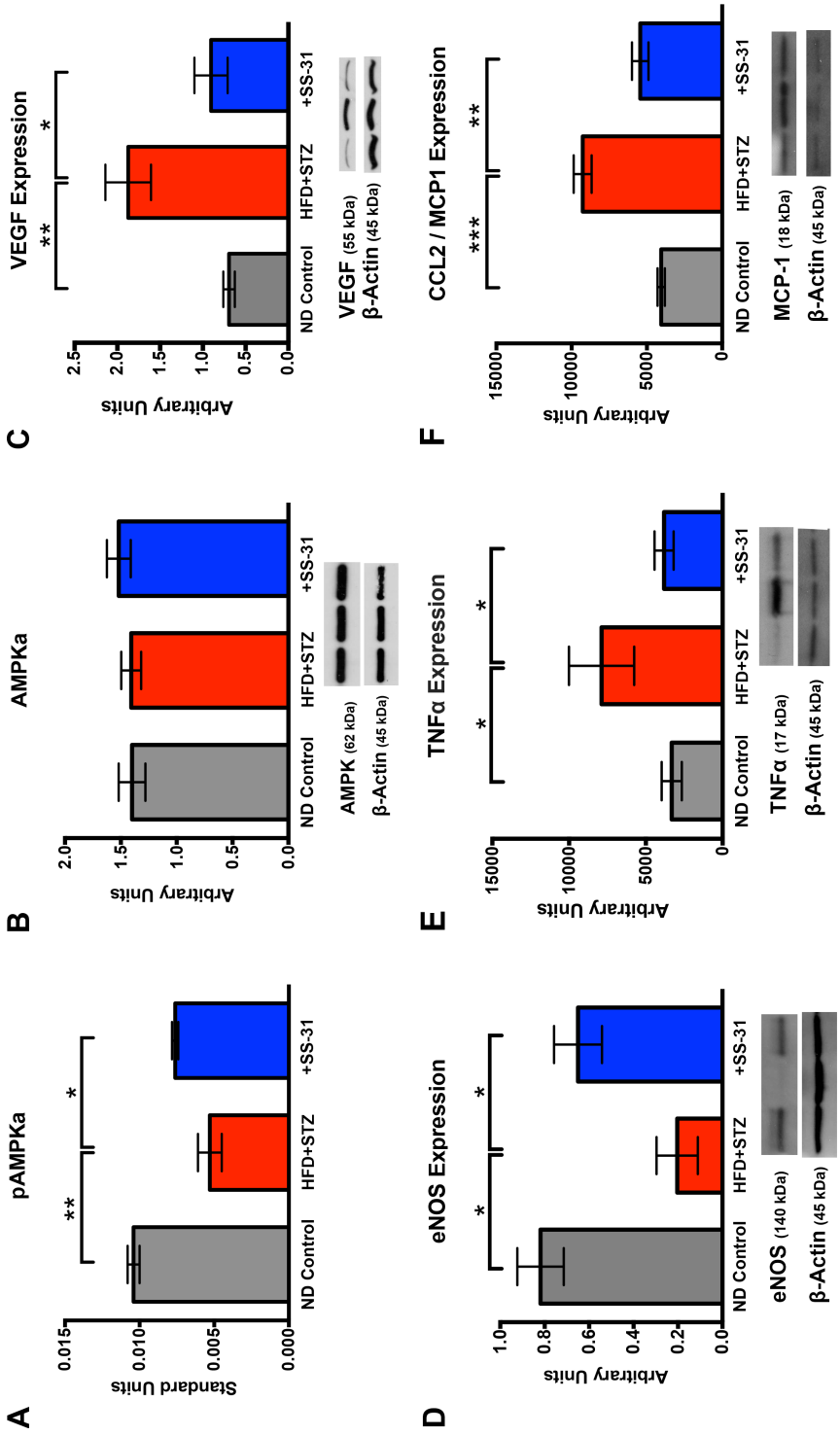

Fig. 7. Summary schematic.

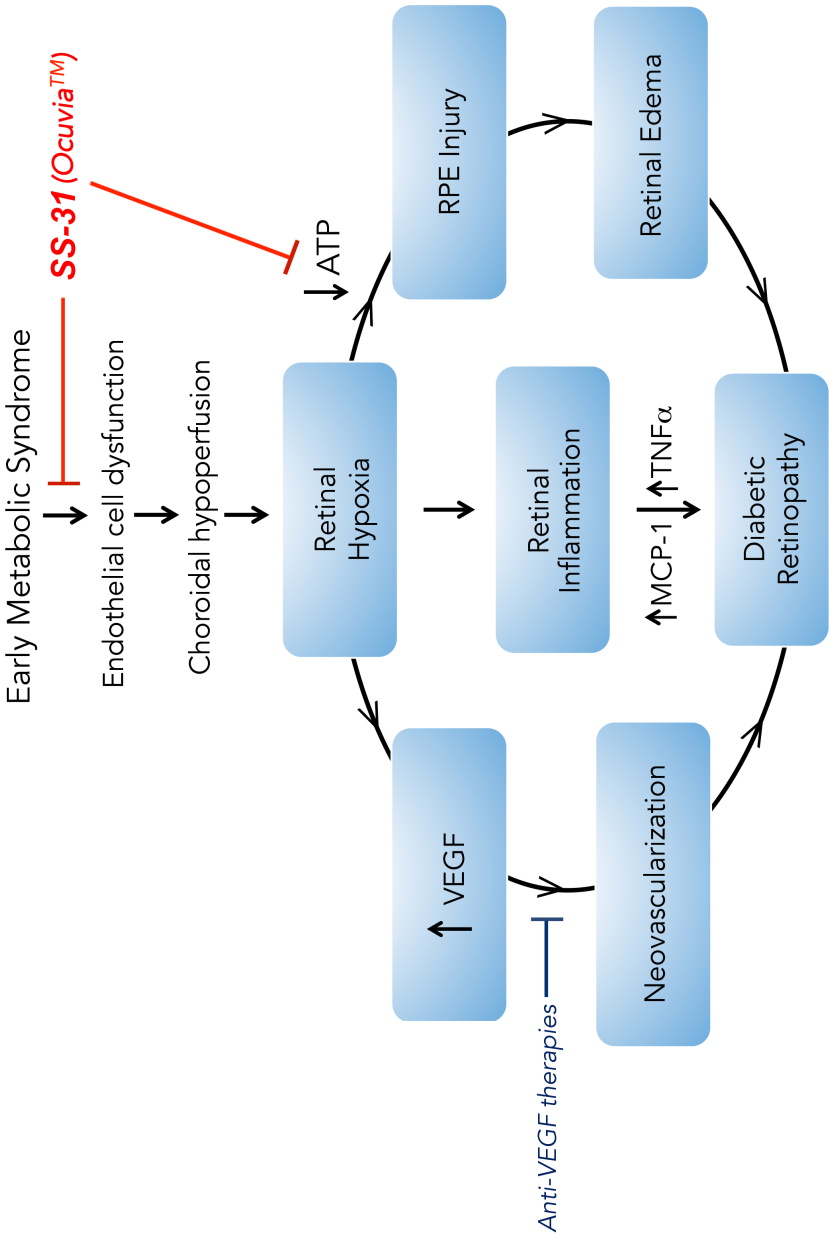

REFERENCES

1. Nathan DM, Zinman B, Cleary PA, Backlund JY, Genuth S, Miller R, Orchard TJ: Modern-day clinical course of type 1 diabetes mellitus after 30 years' duration: the diabetes control and complications trial/epidemiology of diabetes interventions and complications and Pittsburgh epidemiology of diabetes complications experience (1983-2005). Arch Intern Med 2009;169:1307-1316

2. Dosso AA, Yenice-Ustun F, Sommerhalder J, Golay A, Morel Y, Leuenberger PM: Contrast sensitivity in obese dyslipidemic patients with insulin resistance. Arch Ophthalmol 1998;116:1316-1320

3. Jackson GR, Scott IU, Quillen DA, Walter LE, Gardner TW: Inner retinal visual dysfunction is a sensitive marker of non-proliferative diabetic retinopathy. Br J Ophthalmol 2012;96:699-703

4. Hellgren KJ, Agardh E, Bengtsson B: Progression of early retinal dysfunction in diabetes over time: results of a long-term prospective clinical study. Diabetes 2014;63:3104-3111

5. Kirwin SJ, Kanaly ST, Hansen CR, Cairns BJ, Ren M, Edelman JL: Retinal gene expression and visually evoked behavior in diabetic long evans rats. Invest Ophthalmol Vis Sci 2011;52:7654-7663

6. Aung MH, Kim MK, Olson DE, Thule PM, Pardue MT: Early visual deficits in streptozotocin-induced diabetic long evans rats. Invest Ophthalmol Vis Sci 2013;54:1370-1377

7. Akimov NP, Renteria RC: Spatial frequency threshold and contrast sensitivity of an optomotor behavior are impaired in the Ins2Akita mouse model of diabetes. Behav Brain Res 2012;226:601-605

8. Thierry M, Pasquis B, Acar N, Gregoire S, Febvret V, Buteau B, Gambert-Nicot S, Bron AM, Creuzot-Garcher CP, Bretillon L: Metabolic syndrome triggered by high-fructose diet favors choroidal neovascularization and impairs retinal light sensitivity in the rat. PLoS One 2014;9:e112450

9. Samuels IS, Bell BA, Pereira A, Saxon J, Peachey NS: Early retinal pigment epithelium dysfunction is concomitant with hyperglycemia in mouse models of type 1 and type 2 diabetes. J Neurophysiol 2015;113:1085-1099

10. Alam NM, Mills, W.C., Wong, A.A., Douglas, R.M., Szeto, H.H., Prusky, D.T.: A mitochondrial therapeutic reverses diabetic visual decline. Disease Model and Mechanisms 2015;

11. Du Y, Miller CM, Kern TS: Hyperglycemia increases mitochondrial superoxide in retina and retinal cells. Free Radic Biol Med 2003;35:1491-1499

12. Madsen-Bouterse SA, Mohammad G, Kanwar M, Kowluru RA: Role of mitochondrial DNA damage in the development of diabetic retinopathy, and the metabolic memory phenomenon associated with its progression. Antioxid Redox Signal 2010;13:797-805

13. Kanwar M, Chan PS, Kern TS, Kowluru RA: Oxidative damage in the retinal mitochondria of diabetic mice: possible protection by superoxide dismutase. Invest Ophthalmol Vis Sci 2007;48:3805-3811

14. Zhong Q, Kowluru RA: Diabetic retinopathy and damage to mitochondrial structure and transport machinery. Invest Ophthalmol Vis Sci 2011;52:8739-8746

15. Strauss O: The retinal pigment epithelium in visual function. Physiol Rev 2005;85:845-881

16. Szeto HH: First-in-class cardiolipin-protective compound as a therapeutic agent to restore mitochondrial bioenergetics. Br J Pharmacol 2014;171:2029-2050

17. Szeto HH, Birk AV: Serendipity and the discovery of novel compounds that restore mitochondrial plasticity. Clin Pharmacol Ther 2014;96:672-683

18. Prusky GT, Alam NM, Beekman S, Douglas RM: Rapid quantification of adult and developing mouse spatial vision using a virtual optomotor system. Invest Ophthalmol Vis Sci 2004;45:4611-4616

19. Douglas RM, Alam NM, Silver BD, McGill TJ, Tschetter WW, Prusky GT: Independent visual threshold measurements in the two eyes of freely moving rats and mice using a virtual-reality optokinetic system. Vis Neurosci 2005;22:677-684

20. Campos M, Amaral J, Becerra SP, Fariss RN: A novel imaging technique for experimental choroidal neovascularization. Invest Ophthalmol Vis Sci 2006;47:5163-5170

21. Nandrot EF, Kim Y, Brodie SE, Huang X, Sheppard D, Finnemann SC: Loss of synchronized retinal phagocytosis and age-related blindness in mice lacking alphavbeta5 integrin. J Exp Med 2004;200:1539-1545

22. Cho J, Won K, Wu D, Soong Y, Liu S, Szeto HH, Hong MK: Potent mitochondria-targeted peptides reduce myocardial infarction in rats. Coron Artery Dis 2007;18:215-220

23. Cho S, Szeto HH, Kim E, Kim H, Tolhurst AT, Pinto JT: A novel cell-permeable antioxidant peptide, SS31, attenuates ischemic brain injury by down-regulating CD36. J Biol Chem 2007;282:4634-4642

24. Szeto HH, Liu S, Soong Y, Wu D, Darrah SF, Cheng FY, Zhao Z, Ganger M, Tow CY, Seshan SV: Mitochondria-targeted peptide accelerates ATP recovery and reduces ischemic kidney injury. J Am Soc Nephrol 2011;22:1041-1052

25. Szeto HH, Schiller PW: Novel therapies targeting inner mitochondrial membrane--from discovery to clinical development. Pharm Res 2011;28:2669-2679

26. Park SY, Cho YR, Kim HJ, Higashimori T, Danton C, Lee MK, Dey A, Rothermel B, Kim YB, Kalinowski A, Russell KS, Kim JK: Unraveling the temporal pattern of diet-induced insulin resistance in individual organs and cardiac dysfunction in C57BL/6 mice. Diabetes 2005;54:3530-3540

27. Anderson EJ, Lustig ME, Boyle KE, Woodlief TL, Kane DA, Lin CT, Price JW, 3rd, Kang L, Rabinovitch PS, Szeto HH, Houmard JA, Cortright RN, Wasserman DH, Neufer PD: Mitochondrial H2O2 emission and cellular redox state link excess fat intake to insulin resistance in both rodents and humans. J Clin Invest 2009;119:573-581

28. Marcal AC, Leonelli M, Fiamoncini J, Deschamps FC, Rodrigues MA, Curi R, Carpinelli AR, Britto LR, Carvalho CR: Diet-induced obesity impairs AKT signalling in the retina and causes retinal degeneration. Cell Biochem Funct 2013;31:65-74

29. Reiter CE, Sandirasegarane L, Wolpert EB, Klinger M, Simpson IA, Barber AJ, Antonetti DA, Kester M, Gardner TW: Characterization of insulin signaling in rat retina in vivo and ex vivo. Am J Physiol Endocrinol Metab 2003;285:E763-774

30. Steinberg HO, Chaker H, Leaming R, Johnson A, Brechtel G, Baron AD: Obesity/insulin resistance is associated with endothelial dysfunction. Implications for the syndrome of insulin resistance. J Clin Invest 1996;97:2601-2610

31. Vicent D, Ilany J, Kondo T, Naruse K, Fisher SJ, Kisanuki YY, Bursell S, Yanagisawa M, King GL, Kahn CR: The role of endothelial insulin signaling in the regulation of vascular tone and insulin resistance. J Clin Invest 2003;111:1373-1380

32. Antonetti DA, Klein R, Gardner TW: Diabetic retinopathy. N Engl J Med 2012;366:1227-1239

33. Shweiki D, Itin A, Soffer D, Keshet E: Vascular endothelial growth factor induced by hypoxia may mediate hypoxia-initiated angiogenesis. Nature 1992;359:843-845

34. Helfenstein T, Fonseca FA, Ihara SS, Bottos JM, Moreira FT, Pott H, Jr., Farah ME, Martins MC, Izar MC: Impaired glucose tolerance plus hyperlipidaemia induced by diet promotes retina microaneurysms in New Zealand rabbits. Int J Exp Pathol 2011;92:40-49

35. Mancini JE, Ortiz G, Croxatto JO, Gallo JE: Retinal upregulation of inflammatory and proangiogenic markers in a model of neonatal diabetic rats fed on a high-fat-diet. BMC Ophthalmol 2013;13:14

36. Mima A, Qi W, Hiraoka-Yamomoto J, Park K, Matsumoto M, Kitada M, Li Q, Mizutani K, Yu E, Shimada T, Lee J, Shoelson SE, Jobin C, Rask-Madsen C, King GL: Retinal not systemic oxidative and inflammatory stress correlated with VEGF expression in rodent models of insulin resistance and diabetes. Invest Ophthalmol Vis Sci 2012;53:8424-8432

37. Huang H, Gandhi JK, Zhong X, Wei Y, Gong J, Duh EJ, Vinores SA: TNFalpha is required for late BRB breakdown in diabetic retinopathy, and its inhibition prevents leukostasis and protects vessels and neurons from apoptosis. Invest Ophthalmol Vis Sci 2011;52:1336-1344

38. Panee J: Monocyte Chemoattractant Protein 1 (MCP-1) in obesity and diabetes. Cytokine 2012;60:1-12

39. Reiter CE, Wu X, Sandirasegarane L, Nakamura M, Gilbert KA, Singh RS, Fort PE, Antonetti DA, Gardner TW: Diabetes reduces basal retinal insulin receptor signaling: reversal with systemic and local insulin. Diabetes 2006;55:1148-1156

40. Fort PE, Losiewicz MK, Reiter CE, Singh RS, Nakamura M, Abcouwer SF, Barber AJ, Gardner TW: Differential roles of hyperglycemia and hypoinsulinemia in diabetes induced retinal cell death: evidence for retinal insulin resistance. PLoS One 2011;6:e26498

41. Schutt F, Aretz S, Auffarth GU, Kopitz J: Moderately reduced ATP levels promote oxidative stress and debilitate autophagic and phagocytic capacities in human RPE cells. Invest Ophthalmol Vis Sci 2012;53:5354-5361

42. Birk AV, Liu S, Soong Y, Mills W, Singh P, Warren JD, Seshan SV, Pardee JD, Szeto HH: The mitochondrial-targeted compound SS-31 re-energizes ischemic mitochondria by interacting with cardiolipin. J Am Soc Nephrol 2013;24:1250-1261

43. Li X, Zhang M, Zhou H: The morphological features and mitochondrial oxidative stress mechanism of the retinal neurons apoptosis in early diabetic rats. J Diabetes Res 2014;2014:678123

44. Jiang Y, Qi X, Chrenek MA, Gardner C, Dalal N, Boatright JH, Grossniklaus HE, Nickerson JM: Analysis of mouse RPE sheet morphology gives discriminatory categories. Adv Exp Med Biol 2014;801:601-607

45. Xu HZ, Le YZ: Significance of outer blood-retina barrier breakdown in diabetes and ischemia. Invest Ophthalmol Vis Sci 2011;52:2160-2164

46. Liu S, Soong Y, Seshan SV, Szeto HH: Novel cardiolipin therapeutic protects endothelial mitochondria during renal ischemia and mitigates microvascular rarefaction, inflammation, and fibrosis. Am J Physiol Renal Physiol 2014;306:F970-980

47. Li J, Chen X, Xiao W, Ma W, Li T, Huang J, Liu X, Liang X, Tang S, Luo Y: Mitochondria-targeted antioxidant peptide SS31 attenuates high glucose-induced injury on human retinal endothelial cells. Biochem Biophys Res Commun 2011;404:349-356

48. Ruderman NB, Carling D, Prentki M, Cacicedo JM: AMPK, insulin resistance, and the metabolic syndrome. J Clin Invest 2013;123:2764-2772

49. Kubota S, Ozawa Y, Kurihara T, Sasaki M, Yuki K, Miyake S, Noda K, Ishida S, Tsubota K: Roles of AMP-activated protein kinase in diabetes-induced retinal inflammation. Invest Ophthalmol Vis Sci 2011;52:9142-9148

50. Viollet B, Guigas B, Sanz Garcia N, Leclerc J, Foretz M, Andreelli F: Cellular and molecular mechanisms of metformin: an overview. Clin Sci (Lond) 2012;122:253-270

Title: A mitochondrial therapeutic reverses diabetic visual decline.

Authors: N.M. Alam[1,2]*, W. C. Mills IV[3], A.A. Wong[2], R.M. Douglas[4], H. H. Szeto[3], G. T. Prusky[1,2]

Affiliations:

[1]Department of Physiology and Biophysics, Weill Cornell Medical College, New York, NY, USA.

[2]Burke Medical Research Institute, White Plains, NY, USA.

[3]Research Program in Mitochondrial Therapeutics, Department of Pharmacology, Weill Cornell Medical College, New York, NY, USA.

[4]Department of Ophthalmology and Visual Sciences, University of British Columbia, Vancouver, BC, Canada.

*Corresponding Author

Nazia Alam

Weill Cornell Medical College

Burke Medical Research Institute

785 Mamaroneck Avenue

White Plains, NY 10605

nazia.alam@gmail.com

Running Title: Reversal of Diabetic Visual Decline

Key Words: diabetic retinopathy, RPE, SS-31, MTP-131, Bendavia, insulin resistance, hyperglycemia, optomotor, spatial vision, cardiolipin, OKT, mouse

ABSTRACT

Diabetic retinopathy is characterized by progressive vision loss and the advancement of retinal micoraneurysms, edema, and angiogenesis. Unfortunately, managing glycemia or targeting vascular complications with anti-vascular endothelial growth factor agents has shown only limited efficacy in treating the deterioration of vision in diabetic retinopathy. In light of growing evidence that mitochondrial dysfunction is an independent pathophysiology of diabetes and diabetic retinopathy, we investigated whether selectively targeting and improving mitochondrial dysfunction is a viable treatment for visual decline in diabetes. Measures of spatial visual behavior, blood glucose, bodyweight, and optical clarity were made in mouse models of diabetes. Treatment groups were administered MTP-131, a water-soluble tetrapeptide that selectively targets mitochondrial cardiolipin and promotes efficient electron transfer, either systemically or in eye drops. Progressive visual decline emerged in untreated animals before the overt symptoms of metabolic and ophthalmic abnormalities were manifest, but with time, visual dysfunction was accompanied by compromised glucose clearance, and elevated blood glucose and bodyweight. MTP-131 treatment reversed the visual decline without improving glycemic control or reducing bodyweight. These data provide evidence that visuomotor decline is an early complication of diabetes. They also indicate that selectively treating mitochondrial dysfunction with MTP-131 has the potential to remediate the visual dysfunction, and complement existing treatments for diabetic retinopathy.

INTRODUCTION

Diabetic retinopathy is a leading cause of progressive vision loss and blindness. It is characterized by occlusion and leakage of retinal vessels, which leads to macular edema in its non-proliferative phase, and angiogenesis and retinal detachment in its proliferative phase. Whereas vascular endothelial growth factor expression is necessary for the angiogenesis (Stefanini et al., 2014), treatment with anti- vascular endothelial growth factor agents is able to improve visual function in <30% of patients. Likewise, therapies aimed at managing the symptoms of metabolic dysfunction have shown limited efficacy in slowing the progression of diabetic retinopathy; diabetic complications develop in ~20% of patients under strict glycemic or blood-pressure control (Antonetti et al., 2012). Thus, earlier detection of risk for diabetes and diabetic retinopathy, and intervention with novel therapeutics before irreversible retinal damage occurs, has great potential to improve treatment.

There is growing recognition that retinal dysfunction (Barber et al., 2005; Ly et al., 2011; Martin et al., 2004; Murakami and Yoshimura, 2013; van Dijk et al., 2009) and impaired visual behavior is present in human diabetics and animal models before retinal vascular changes are evident (Akimov and Rentería, 2012; Aung et al., 2013; Hardy et al., 1992; Jackson et al., 2012; Kirwin et al., 2011). Thus, the identification of visual dysfunction early in the course of diabetes may provide an advanced opportunity for therapeutic intervention. A promising candidate for early intervention in diabetic retinopathy is the remediation of mitochondrial dysfunction. Diabetic complications in the non-proliferative phase of diabetic retinopathy are associated with metabolic pathways that are up-regulated by sustained hyperglycemia: increased polyol pathway flux, increased formation of advanced glycation end products and their receptors, activation of protein kinase C, and increased hexosamine pathway flux

(Forbes and Cooper, 2013). It has been proposed that the pathways are linked by the mitochondrial production of reactive oxygen species resulting from increased metabolic flux through the electron transport chain. This is supported by evidence that normalizing mitochondrial superoxide production can mitigate hyperglycemic damage (Brownlee, 2001; Nishikawa et al., 2000).

Indeed, mitochondria are simultaneously a major source of intracellular reactive oxygen species and the target of oxidative damage, and evidence of mitochondrial oxidative stress is present when histopathological abnormalities arise in diabetic retinopathy (Du et al., 2003; Kowluru and Zhong, 2011). Altered mitochondrial structure, including swelling and loss of cristae, the accumulation of defects in mitochondrial DNA, and a reduction of transport proteins (Kowluru and Zhong, 2011; Madsen-Bouterse et al., 2010b; Santos and Kowluru, 2013) which may be independent of hyperglycemia (Zhong and Kowluru, 2011), have also been reported. In addition, impairment of retinal pigment epithelium mitochondria is associated with increased oxidative stress, reduced ATP, and compromised autophagic and phagocytic capacities (He et al., 2010; Kanwar et al., 2007; Li et al., 2014; Madsen-Bouterse et al., 2010a). Taken together, these data indicate that apoptotic stress in the retina has the capacity to induce the hallmark microvascular injury of diabetic retinopathy, and that improving mitochondrial function may be an effective treatment.

Whereas antioxidants have shown promise in preclinical studies as a therapy for diabetic retinopathy (Huang et al., 2013; Nawaz et al., 2013; Xie et al., 2008), they have not been effective in clinical trials; possibly due to their inability to penetrate mitochondria. This problem can be overcome with the use of MTP-131 (also known as SS-31), a water-soluble mitochondria-targeting peptide that attenuates mitochondrial reactive oxygen species production and cytochrome c release (Huang et al., 2013; Li et

al., 2011; Szeto and Birk, 2014; Zhao et al., 2004). We thus tested the hypothesis here that MTP-131 can remediate visual impairment in mouse models of diabetes.

RESULTS

Characterization of Diabetic Mouse Models

Type-1 diabetes is an autoimmune disease that leads to loss of insulin-producing beta cells in the pancreas, which is often modeled in animal studies with injections of streptozotocin (STZ). We administered STZ to C57BL/6 mice fed a normal diet (ND) for 5 days at 8 weeks of age (ND+STZ). Type-2 diabetes is characterized by insulin resistance and the inability of β-cells to up-regulate their insulin production. For modeling this, mice were fed a diabetic diet (DD) high in fat and carbohydrates from 4 weeks of age, and a third group received both DD and STZ (DD+STZ). Control mice were fed a ND throughout the study.

Elevated resting blood glucose (non-fasted) was present in each diabetic model by 15 weeks, which was sustained at 32 weeks (Fig. 1A). Evidence of insulin resistance was also present in the results of a glucose tolerance test administered at 12 (Fig. 1B) and 30 weeks (Fig. 1C), with DD groups showing the greatest impairment. Elevated bodyweight emerged by 15 weeks in groups fed a DD, and by 32 weeks, mice in the DD groups were two-fold heavier than mice fed a ND (Fig. 1D, ~56g vs ~29g).

Progressive Decline of Visual Function in Diabetic Mouse Models

Spatial frequency (SF) and contrast thresholds for optokinetic tracking were measured through each eye once/week from 3-32 weeks, using a virtual optokinetic system (Prusky et al., 2004). SF thresholds near 0.39 cycles/degree (c/d) were measured in ND mice (Fig. 2A) up to 32 weeks; performance comparable to previously-published values (Prusky et al., 2004; Prusky et al., 2006). Loss-of-function emerged by 12 weeks in ND+STZ mice, which by 32 weeks, was reduced by 17%. Visual dysfunction emerged earlier (at 9 weeks) and declined more (29%) in DD

mice. In DD+STZ mice, visual dysfunction emerged the earliest (at 8 weeks), and declined the most (38%), by 32 weeks.

We have previously defined the luminance conditions in the virtual optokinetic system that are able isolate cone- and rod-only function (Alam et al., 2015; Altimus et al., 2010), and as such, the lighting conditions used to record the thresholds in Fig. 2A were selective for cone-mediated function. In order to measure rod-mediated function in the same animals, we configured the virtual optokinetic system to record rod-driven thresholds in low light conditions. Fig. 2B is a comparison of cone- and rod-selective function at 28 weeks. Whereas cone function was reduced by 16% in ND+ STZ mice, 27% in DD mice, and 36% in DD +STZ mice, rod function was proportionally less affected; ND+ STZ = 3%; DD = 10%, and DD +STZ = 18%. Thus, the loss of visual function in the diabetic models was primarily due to compromised cone-mediated responses.

Measures of CS also revealed evidence of visual decline that was graded by group. Adult-like CS (Douglas et al., 2005; Prusky et al., 2004) was present in ND mice at 4, 12, and 32 weeks (Fig. 2C). CS in ND+STZ mice (Fig. 2D) was normal at 4 and 12 weeks, but was slightly reduced by 32 weeks at SFs above 0.06 c/d. CS in DD mice was marginally lower at high SFs between 4 and 12 weeks, and by 32 weeks, was reduced at all SFs above 0.03 c/d (Fig. 2E). DD+STZ mice showed loss of function from 4-12 weeks comparable to DD mice, but showed a greater decline by 32 weeks (Fig. 2F).

MTP-131 Treatment Reversed Visual Decline in Diabetic Mouse Models

Treatment groups were injected with MTP-131 (1 mg/kg), (Veh; 0.9% saline), subcutaneously once/day from 12 weeks; an age by which evidence of visuomotor dysfunction had developed in each of the diabetic models (i.e. Fig. 2). The treatment

did not alter the level of non-fasted resting blood glucose (Fig. 3A), and did not change the rate of glucose clearance measured at 30 weeks (compared to Veh group; Fig. 3B). Likewise, the treatment did not correct the elevated bodyweight of the DD groups (Fig. 3C). Improvement of visual function, however, was present in each of the diabetic groups. Fig. 4A shows that improvement of the SF threshold for opto-kinetic tracking was present in DD+STZ mice 1 week after treatment, within 4 weeks in DD mice, and within 6 weeks in ND+STZ mice. Improvement continued thereafter in all groups until thresholds were restored to normal values by 24 weeks in DD+STZ mice, by 25 weeks in ND+STZ mice, and by 31 weeks in DD mice. MTP-131 treatment did not alter function in the control (ND) group. Cone-and rod selective dysfunction in the MTP-131 treated mice were both fully reversed in ND+STZ and DD+STZ groups, and substantially remediated in the DD group (Fig. 4B; compare with 28 weeks in Fig 2B). MTP-131 treatment improved CS in a similar manner; MTP-131 did not affect CS in ND mice (Fig. 4C), but it restored thresholds to near-normal values in ND+STZ (Fig. 4D), in DD (Fig. 4E), and DD+STZ mice (Fig. 4F). Ophthalmic examinations of mice presented in Figs. 3 & 4 revealed only sporadic ocular abnormalities, none of which were related to group or treatment. All animals were assessed at 12 weeks of age, prior to starting any treatment, and at 32 weeks prior to euthanasia, using a modification of the MacDonald-Shadduck Scoring System described elsewhere (Altmann et al., 2010). Ophthalmic examinations identified three animals with abnormal visual thresholds at 12 weeks, in the form of dense corneal infiltrates or central opacities, likely due to grooming or fighting. The mice were removed from the study. Two left eyes and two right eyes showed small punctate corneal opacities (less than 25% corneal involvement (score=1), either in the inferior or nasal region of 4 animals prior to 12 weeks of age, but that animals remained in the study and were randomly assigned into

groups. Ophthalmic examinations were performed again at 32 weeks of age, and no animals were identified with ocular problems.

Efficacy of MTP-131 Applied Via Eye Drops

We hypothesized that the benefit of systemic MTP-131 treatment was related to its action on the retina, since MTP-131 did not correct weight gain or high blood glucose. In an effort to deliver MTP-131 to the eye, we investigated whether eye drop application of the peptide would also treat diabetic visual dysfunction. Fig. 5A, B and C shows that resting blood glucose and body weight measures were unaffected by MTP-131 or placebo (Veh) eye drop application. In Fig. 5C, Veh-treated mice exhibited a SF threshold decline comparable to that with systemic Veh treatment (Fig. 2A, magenta line). However, decline in the MTP-131 eye drop-treated group was reversed after 1 week of treatment, and normal function was reinstated by 20 weeks- 4 weeks earlier than with systemic MTP-131 treatment in the same model.

In a separate cohort of mice, we investigated whether the timing and rate of visual recovery following the application of MTP-131 was dose-dependent (Fig. 5D). Improved function was observed within one week of treatment with 30 mg/ml, and within 5 weeks with 10 mg/ml. 1 mg/ml treatment did not lead to improvement. As with systemic MTP-131 treatment, the restoration of function with eye drop application of MTP-131 was independent of overt changes in the quality of the optical axis (data not shown).

MTP-131 Reversed More Severe Visual Dysfunction

To determine whether MTP-131 application was able to remediate more pronounced visual dysfunction than that at 12 weeks (i.e. Fig. 5), eye drop treatment with MTP-131 (30 mg/ml) was initiated in a group of DD+STZ mice at 34 weeks; an

age at which the SF threshold in untreated animals was reduced by ~50% (Fig. 6C). As in previous experiments, MTP-131 treatment had no effect on resting blood glucose (Fig. 6A) or body weight (Fig. 6B). Unlike the effect on visual function with treatment from 12 weeks, which showed a beneficial effect within 1 week (Fig. 5C), visual function continued to decline for 4 weeks after MTP-131 treatment in the group. At 5 weeks, however, visual decline was halted, followed by recovery at a rate similar to that with treatment from 12 weeks, reaching ~75% of normal by 52 weeks (Fig. 6C). As stipulated by our animal protocol, the study was terminated at 52 weeks, and thus, it is not known whether continued treatment would have led to more improvement. However, the rate of recovery appeared to slow after 48 weeks, likely indicating that complete recovery would not be achieved with more time. Whereas CS was measured in all of the eye drop studies, it changed in concert with measures of SF thresholds, and thus, the data is not presented here.

DISCUSSION

This study, which unfolded over the course of 2 years and utilized > 150 mice, is the most comprehensive examination to date of visual decline, and restoration with treatment, in rodent models of diabetes. It established a time course of the relationship between the emergence of metabolic dysfunction and visual decline in three diabetic models in the same mouse strain, it illuminated a role for mitochondrial dysfunction in the pathogenesis of diabetic visual complications, and it demonstrated a clinically-feasible approach to treating it.

We used a repeated low-dose STZ protocol to model type-1 diabetes, rather than the typical single high dose STZ protocol, to reduce the off-target toxic effects of STZ (Hayashi et al., 2006; Like and Rossini, 1976). This resulted in only a moderate increase in fed blood glucose (Hayashi et al., 2006; Leiter, 1982) and slightly abnormal glucose clearance, which may better model type-1 diabetes. Feeding a diet high in fat and carbohydrates was used to model type-2 diabetes, which led to an increase in body weight, abnormal glucose clearance, and mild hyperglycemia. Although we did not measure insulin in this study, an increase in plasma insulin has previously been reported in diet-induced models of diabetes (Park et al., 2005; Surwit et al., 1988). For example, a decrease in insulin-stimulated glucose uptake in the heart has been reported within 1.5 weeks of initiating a high fat diet in young C57BL/6 mice, which was reduced by ~90% after 20 weeks (Park et al., 2005). In addition, plasma insulin was elevated within 2 weeks in young mice fed a high fat diet, and remained elevated for up to 52 weeks (Park et al., 2005; Surwit et al., 1988; Winzell and Ahrén, 2004). Thus, the DD model enabled the ability to study the effect of insulin resistance on visual function. Indeed, the elevated blood glucose in DD mice most likely resulted from reduced glucose uptake by skeletal muscles and adipose

tissue, due to loss of insulin signaling (Winzell and Ahrén, 2004). A group that combined DD with STZ treatment provided a model of advanced type-2 diabetes, which is characterized by defects in insulin secretion and insulin resistance.

A decline of visuomotor function was detected in each experimental model before changes in resting blood glucose emerged- a common clinical indicator of susceptibility to diabetes. The onset of visual decline was most rapid in the DD+STZ group, and slowest in the ND+STZ group, suggesting that insulin resistance may have an early negative effect on visual function. Insulin receptors are expressed on both vascular and neural cells of the retina (Haskell et al., 1984), and are able to autophosphorylate and activate downstream kinases, as in other insulin-sensitive tissues (Reiter et al., 2003). Rats administered STZ have shown reduced insulin receptor signaling in the retina, especially in retinal endothelial cells, which may contribute to the early progression of diabetic retinopathy (Aizu et al., 2002; Fort et al., 2011; Kondo and Kahn, 2004; Reiter et al., 2003).

The study was designed such that daily MTP-131 treatment began 4 weeks after STZ treatment, or 8 weeks after the initiation of a DD. Since visual decline only began 4 weeks after STZ, MTP-131 treatment appeared to both reverse further decline, and prevent sustained visual dysfunction. MTP-131 treatment was also able to reverse more pronounced visual dysfunction in the DD group, but the time to full recovery was shortened. Unexpectedly, even though the DD+STZ mice had the most dramatic rate of visual decline; they had the most rapid response to MTP-131 treatment, showing improvement within one week of MTP-131 administration and full recovery after 12 weeks. The lack of effect of MTP-131 on blood glucose and body weight is in keeping with previous reports in STZ-administered rats (Huang et al., 2013). The more rapid onset of visual decline, and the slower treatment response in the DD group is also consistent with insulin resistance as a cause of diabetic visual dysfunction. Since

the addition of STZ has been shown to reduce diet-induced insulin resistance in C57BL/6 mice (Ning et al., 2011), this may account for the more rapid MTP-131 treatment effect in the DD+STZ group.

MTP-131 is a mitochondria-targeting peptide known to protect the structure of cristae and prevent mitochondrial swelling under ischemic conditions in numerous cell types (Birk et al., 2013; Liu et al., 2014; Szeto et al., 2011). By maintaining cristae membranes, MTP-131 treated tissues may be better able to sustain ATP synthesis and preserve vital ATP-dependent processes (Birk et al., 2013; Szeto et al., 2011). Although MTP-131 was known at the outset to selectively partition to the inner mitochondria membrane (Zhao et al., 2005), the mechanism by which MTP-131 protects mitochondrial cristae remained unclear until recently. It is now known, however, that MTP-131 has a high affinity for cardiolipin, a unique anionic phospholipid (Birk et al., 2013; Szeto, 2014). The conical shape of cardiolipin is required to maintain the curvature of cristae, and cardiolipin deficiency results in a loss of cristae and reduced mitochondrial respiration (Schlame and Ren, 2006). Since cardiolipin contains four unsaturated acyl chains, it is readily peroxidized under oxidative conditions, which is consistent with reports that increased cardiolipin peroxidation and cardiolipin depletion is present in diabetic hearts (Ferreira et al., 2013; He and Han, 2014). High glucose has also been postulated to increase mitochondrial reactive oxygen species (Brownlee, 2001), and thus, cardiolipin peroxidation could have the effect of reducing mitochondrial respiration. Interestingly, retinal mitochondria from diabetic mice show elevated superoxide levels and reduced glutathione, indicative of mitochondrial oxidative stress (Kanwar et al., 2007). In addition to a high reactive oxygen species environment, cardiolipin peroxidation is catalyzed by cytochrome c that is tightly bound to cardiolipin, and this [cyt c/cardiolipin] complex converts cytochrome c from an electron carrier to a peroxidase

that can peroxidize cardiolipin (Kagan et al., 2005; Sinibaldi et al., 2010; Snider et al., 2013). MTP-131 appears to protect the architecture of mitochondrial cristae by reducing mitochondrial oxidative stress and preventing cytochrome c peroxidase activity (Birk et al., 2013; Zhao et al., 2004).

Mitochondrial abnormalities have been documented in insulin-resistant and diabetic states in human and animal studies, and it has been proposed that mitochondrial dysfunction may be the primary defect in obesity-related insulin resistance (Patti and Corvera, 2010). The causal mechanism underlying the mitochondrial dysfunction, however, is not fully understood. Although it is often assumed that hyperglycemia causes mitochondrial oxidative stress in diabetes, a recent study reported lower mitochondrial superoxide and mitochondrial respiratory activity in the kidneys of diabetic mice after STZ treatment (Dugan et al., 2013), and suggests a loss of functional mitochondria in the latter stages of diabetes (Sharma, 2015) . MTP-131 could thus provide a novel approach for treating diabetes, based not on mitigating elevated blood glucose, but on enhancing mitochondrial bioenergetics through the preservation of mitochondrial cristae, and improved efficiency of the electron transfer chain. MTP-131 has displayed an exceptional safety profile in Phase 1 clinical trials, likely due to its lack of effect on the function of normal mitochondria (Siegel et al., 2013). Since the beneficial effects of MTP-131 appear to be independent of reducing circulating glucose, the treatment may also be useful in complementing therapies aimed at managing the typical symptoms of diabetes. Indeed, based on the results reported here, a clinical formulation of topical ophthalmic MTP-131 (Ocuvia^{TM}) has entered a clinical trial for treating diabetic macular edema.

MATERIALS AND METHODS

Animal Subjects

Experimental procedures on animals were conducted in accordance with the policies of the Weill Cornell Medical College Institutional Animal Care and Use Committee. 151 male C57BL/6 mice obtained from Charles River Laboratories at 3 weeks of age were group-housed at the Burke Medical Research Institute vivarium. They were maintained at 68°-76°F with 30-70% relative humidity, and a photoperiod of 12 hour light (6:00 lights on)/12 hour dark (18:00 lights off).

Disease Modeling

Mice in control groups were fed a ND (LabDiet Picolab Rodent Diet 5053 (min. protein = 20%, crude fat = 4.5%, max. crude fiber = 6.0%) *ad libitum* over the course of the study. Type 1 diabetes is an autoimmune disease that destroys insulin-producing pancreatic beta cells, which we modeled by administering the beta cell toxin STZ (Sigma S0130) to mice at 8 weeks of age fed a ND (ND+STZ; Arora et al., 2009; Gilbert et al., 2011). STZ was prepared in a 7.5 mg/ml sodium citrate buffer (pH 4.5) immediately prior to injection. On 5 consecutive days, mice were fasted 4 hours, anesthetized with inhaled isoflurane (induction at 2.5–4.5%, maintenance at 1–2% evaporated in 1-1.5 L/min O_2), before being administered 40 mg/kg intraperitoneal STZ.

Type-2 diabetes is characterized by insulin resistance and the inability of beta cells to up-regulate their function. To model this, mice were fed a DD (Bio-Serv Mouse Diet F3282; protein = 20.5%, crude fat = 36%, fiber = 0%, carbohydrates = 35.7%) *ad libitum* from 4 weeks of age. To model an accelerated version of type-2 diabetes, another group was fed a DD from 4 weeks and administered STZ at 8 weeks of age (DD+STZ).

MTP-131 Administration

In one experiment, mice were injected daily with a 1mg/kg solution of MTP-131 sub-cutaneously (provided by Stealth Peptides Inc, Newton, MA) dissolved in 0.9% sterile saline (pH 5.5-6.5), or with saline alone. In another experiment, mice were administered MTP-131 as an ophthalmic-formulated solution (Ocuvia^{TM}, provided by Stealth Peptides, Inc) daily via eye drops (in 0.01M sodium acetate buffer solution (pH 6.00); 5 ul/eye), or with buffer alone.

Measures of Weight and Blood Glucose

Mice were weighed, then lightly anesthetized with inhaled isoflurane, and a drop of blood was harvested from the tail or submandibular vein. Glucose in the drop was measured with a glucometer (AlphaTRAK II Blood Glucose Monitoring System, or One Touch Ultra Mini Blood Glucose Monitoring System). A glucose tolerance test was also administered periodically; animals were fasted overnight prior to receiving D-glucose (1.5 g/kg i.p.). Blood glucose was measured as above prior to and after 10, 20, 30, 60, and 120 minutes glucose administration.

Tests of Spatial Visual Function

Spatial thresholds for opto-kinetic tracking of sine-wave gratings were measured weekly using a virtual optokinetic system (OptoMotry, CerebralMechanics Inc., Medicine Hat, Alberta, Canada; (Prusky et al., 2004). Vertical sine wave gratings moving at 12 degrees/second, or gray of the same mean luminance, were projected on 4 monitors as a virtual cylinder, which surrounded an unrestrained mouse standing on a platform at the epicenter. The hub of the cylinder was continually centered between the eyes of the mouse to set the SF of the grating at the mouse's viewing position as it shifted its position. Gray was projected while the mouse was moving, but when

movement ceased, the gray was replaced with a grating. Grating rotation under these circumstances elicited reflexive tracking, which was scored via live video using a method of limits procedure with a yes/no criterion. A SF threshold, and contrast thresholds at 6 spatial frequencies (0.031, 0.064, 0.092, 0.103, 0.192, 0.272 c/d), were generated through each eye separately in a testing session (14 thresholds in ~ 30 minutes). Michelson contrast sensitivity (CS) was calculated using the average screen luminance (maximum –minimum)/(maximum + minimum). Most thresholds were generated under photopic lighting conditions (screen luminance= 54 lux), which selectively measures cone-based visual function. Rod-based visual function under scotopic conditions (1 lux) was also assessed in some animals after dark adaptation (>6 hours; Alam et al., 2015). For this, 6.3 ND filters (Lee Filters, USA) were placed on the monitors, and infrared lighting and an infrared-sensitive camera (Sony Handycam DCR-HC28, Sony, Japan) were used to image the animal.

Ophthalmic Assessments

A biomicroscope (slit lamp) was used to examine the cornea for clarity, size, surface texture, and vascularization, and the iris was inspected for pupil size, constriction, reflected luminescence, and synechia. The pupil was then dilated with a drop of 0.05% Tropicamide ophthalmic solution, and the lens was scored for cataract using a modified version of the Merriam-Focht scoring criterion (MERRIAM and FOCHT, 1962; Worgul et al., 1993). An indirect ophthalmoscope was also used to inspect the fundus for damage, degeneration, retinal vessel constriction, and optic nerve head abnormalities. A modified MacDonald-Shaddock Scoring System was used to score the optical quality of eyes at 12 and 32 weeks of age.

Statistical Analyses

Using Graphpad Prism 6 software, two-way, repeated-measures ANOVAs were used to make group comparisons. Post-hoc multiple comparisons were performed using the Tukey's or Bonferroni correction methods. Statistical comparisons were considered significantly different at $p < 0.05$.

Acknowledgements:

Funding: The research was supported by the Burke Foundation, Stealth Peptides Inc., and the Research Program in Mitochondrial Therapeutics at Weill Cornell Medical College. We thank the Stealth Peptides team for their expertise and valuable discussions, and Dr. Sunghee Cho for her assistance on the project. **Author contributions:** NMA, WCM and AAW designed and executed experiments, analyzed data and wrote manuscript. RMD participated in designing and executing experiments and editing the manuscript. GTP and HHS designed experiments and wrote and edited the manuscript.

Competing Interests: The peptide described in this article has been licensed for commercial research and development to Stealth Peptides Inc, a clinical stage biopharmaceutical company, in which H.H.S. and the Cornell Research Foundation have financial interests. The Research Program in Mitochondrial Therapeutics at Weill Cornell Medical College was established with a gift from Stealth Peptides International, Inc. Equipment and software in this article were purchased from CerebralMechanics Inc., of which GTP and RMD are Principals.

REFERENCES

Aizu, Y., Oyanagi, K., Hu, J. and Nakagawa, H. (2002). Degeneration of retinal neuronal processes and pigment epithelium in the early stage of the streptozotocin-diabetic rats. *Neuropathology* 22, 161–70.

Akimov, N. P. and Rentería, R. C. (2012). Spatial frequency threshold and contrast sensitivity of an optomotor behavior are impaired in the Ins2Akita mouse model of diabetes. *Behav. Brain Res.* 226, 601–5.

Alam, N. M., Altimus, C. M., Douglas, R. M., Hattar, S. and Prusky, G. T. (2015). Photoreceptor regulation of spatial visual behavior. *Invest Ophthalmol Vis Sci* in press.

Altimus, C. M., Güler, A. D., Alam, N. M., Arman, A. C., Prusky, G. T., Sampath, A. P. and Hattar, S. (2010). Rod photoreceptors drive circadian photoentrainment across a wide range of light intensities. *Nat. Neurosci.* 13, 1107–12.

Altmann, S., Emanuel, A., Toomey, M., McIntyre, K., Covert, J., Dubielzig, R. R., Leatherberry, G., Murphy, C. J., Kodihalli, S. and Brandt, C. R. (2010). A Quantitative Rabbit Model of Vaccinia Keratitis. *Invest. Ophthalmol. Vis. Sci.* 51, 4531–4540.

Antonetti, D. A., Klein, R. and Gardner, T. W. (2012). Diabetic retinopathy. *N. Engl. J. Med.* 366, 1227–39.

Arora, S., Ojha, S. K. and Vohora, D. (2009). Characterisation of Streptozotocin Induced Diabetes Mellitus in Swiss Albino Mice. 3, 81–84.

Aung, M. H., Kim, M. K., Olson, D. E., Thule, P. M. and Pardue, M. T. (2013). Early visual deficits in streptozotocin-induced diabetic long evans rats. *Invest. Ophthalmol. Vis. Sci.* 54, 1370–7.

Barber, A. J., Antonetti, D. A., Kern, T. S., Reiter, C. E. N., Soans, R. S., Krady, J. K., Levison, S. W., Gardner, T. W. and Bronson, S. K. (2005). The Ins2Akita mouse as a model of early retinal complications in diabetes. *Invest. Ophthalmol. Vis. Sci.* 46, 2210–8.

Birk, A. V, Liu, S., Soong, Y., Mills, W., Singh, P., Warren, J. D., Seshan, S. V, Pardee, J. D. and Szeto, H. H. (2013). The mitochondrial-targeted compound SS-31 re-energizes ischemic mitochondria by interacting with cardiolipin. *J. Am. Soc. Nephrol.* 24, 1250–61.

Brownlee, M. (2001). Biochemistry and molecular cell biology of diabetic complications. *Nature* 414, 813–20.

Douglas, R. M., Alam, N. M., Silver, B. D., McGill, T. J., Tschetter, W. W. and Prusky, G. T. (2005). Independent visual threshold measurements in the two eyes of freely moving rats and mice using a virtual-reality optokinetic system. *Vis. Neurosci.* 22, 677–84.

Du, Y., Miller, C. M. and Kern, T. S. (2003). Hyperglycemia increases mitochondrial superoxide in retina and retinal cells. *Free Radic. Biol. Med.* 35, 1491–9.

Dugan, L. L., You, Y.-H., Ali, S. S., Diamond-Stanic, M., Miyamoto, S., DeCleves, A.-E., Andreyev, A., Quach, T., Ly, S., Shekhtman, G., et al. (2013). AMPK dysregulation promotes diabetes-related reduction of superoxide and mitochondrial function. *J. Clin. Invest.* 123, 4888–99.

Ferreira, R., Guerra, G., Padrão, A. I., Melo, T., Vitorino, R., Duarte, J. A., Remião, F., Domingues, P., Amado, F. and Domingues, M. R. (2013). Lipidomic characterization of streptozotocin-induced heart mitochondrial dysfunction. *Mitochondrion* 13, 762–71.

Forbes, J. M. and Cooper, M. E. (2013). Mechanisms of diabetic complications. *Physiol. Rev.* 93, 137–88.

Fort, P. E., Losiewicz, M. K., Reiter, C. E. N., Singh, R. S. J., Nakamura, M., Abcouwer, S. F., Barber, A. J. and Gardner, T. W. (2011). Differential roles of hyperglycemia and hypoinsulinemia in diabetes induced retinal cell death: evidence for retinal insulin resistance. *PLoS One* 6, e26498.

Gilbert, E. R., Fu, Z. and Liu, D. (2011). Development of a nongenetic mouse model of type 2 diabetes. *Exp. Diabetes Res.* 2011, 416254.

Hardy, K. J., Lipton, J., Scase, M. O., Foster, D. H. and Scarpello, J. H. (1992). Detection of colour vision abnormalities in uncomplicated type 1 diabetic patients with angiographically normal retinas. *Br. J. Ophthalmol.* 76, 461–4.

Haskell, J. F., Meezan, E. and Pillion, D. J. (1984). Identification and characterization of the insulin receptor of bovine retinal microvessels. *Endocrinology* 115, 698–704.

Hayashi, K., Kojima, R. and Ito, M. (2006). Strain differences in the diabetogenic activity of streptozotocin in mice. *Biol. Pharm. Bull.* 29, 1110–9.

He, Q. and Han, X. (2014). Cardiolipin remodeling in diabetic heart. *Chem. Phys. Lipids* 179, 75–81.

He, Y., Ge, J., Burke, J. M., Myers, R. L., Dong, Z. Z. and Tombran-Tink, J. (2010). Mitochondria impairment correlates with increased sensitivity of aging RPE cells to oxidative stress. *J. Ocul. Biol. Dis. Infor.* 3, 92–108.

Huang, J., Li, X., Li, M., Li, J., Xiao, W., Ma, W., Chen, X., Liang, X., Tang, S. and Luo, Y. (2013). Mitochondria-targeted antioxidant peptide SS31 protects the retinas of diabetic rats. *Curr. Mol. Med.* 13, 935–45.

Jackson, G. R., Scott, I. U., Quillen, D. A., Walter, L. E. and Gardner, T. W. (2012). Inner retinal visual dysfunction is a sensitive marker of non-proliferative diabetic retinopathy. *Br. J. Ophthalmol.* 96, 699–703.

Kagan, V. E., Tyurin, V. A., Jiang, J., Tyurina, Y. Y., Ritov, V. B., Amoscato, A. A., Osipov, A. N., Belikova, N. A., Kapralov, A. A., Kini, V., et al. (2005). Cytochrome c acts as a cardiolipin oxygenase required for release of proapoptotic factors. *Nat. Chem. Biol.* 1, 223–32.

Kanwar, M., Chan, P.-S., Kern, T. S. and Kowluru, R. A. (2007). Oxidative damage in the retinal mitochondria of diabetic mice: possible protection by superoxide dismutase. *Invest. Ophthalmol. Vis. Sci.* 48, 3805–11.

Kirwin, S. J., Kanaly, S. T., Hansen, C. R., Cairns, B. J., Ren, M. and Edelman, J. L. (2011). Retinal gene expression and visually evoked behavior in diabetic long evans rats. *Invest. Ophthalmol. Vis. Sci.* 52, 7654–63.

Kondo, T. and Kahn, C. R. (2004). Altered insulin signaling in retinal tissue in diabetic states. *J. Biol. Chem.* 279, 37997–8006.

Kowluru, R. A. and Zhong, Q. (2011). Beyond AREDS: is there a place for antioxidant therapy in the prevention/treatment of eye disease? *Invest. Ophthalmol. Vis. Sci.* 52, 8665–71.

Leiter, E. H. (1982). Multiple low-dose streptozotocin-induced hyperglycemia and insulitis in C57BL mice: influence of inbred background, sex, and thymus. *Proc. Natl. Acad. Sci. U. S. A.* 79, 630–4.

Li, J., Chen, X., Xiao, W., Ma, W., Li, T., Huang, J., Liu, X., Liang, X., Tang, S. and Luo, Y. (2011). Mitochondria-targeted antioxidant peptide SS31 attenuates high glucose-induced injury on human retinal endothelial cells. *Biochem. Biophys. Res. Commun.* 404, 349–56.

Li, X., Zhang, M. and Zhou, H. (2014). The morphological features and mitochondrial oxidative stress mechanism of the retinal neurons apoptosis in early diabetic rats. *J. Diabetes Res.* 2014, 678123.

Like, A. A. and Rossini, A. A. (1976). Streptozotocin-induced pancreatic insulitis: new model of diabetes mellitus. *Science* 193, 415–7.

Liu, S., Soong, Y., Seshan, S. V and Szeto, H. H. (2014). Novel cardiolipin therapeutic protects endothelial mitochondria during renal ischemia and mitigates microvascular rarefaction, inflammation, and fibrosis. *Am. J. Physiol. Renal Physiol.* 306, F970–80.

Ly, A., Yee, P., Vessey, K. A., Phipps, J. A., Jobling, A. I. and Fletcher, E. L. (2011). Early inner retinal astrocyte dysfunction during diabetes and development of hypoxia, retinal stress, and neuronal functional loss. *Invest. Ophthalmol. Vis. Sci.* 52, 9316–26.

Madsen-Bouterse, S. A., Zhong, Q., Mohammad, G., Ho, Y.-S. and Kowluru, R. A. (2010a). Oxidative damage of mitochondrial DNA in diabetes and its protection by manganese superoxide dismutase. *Free Radic. Res.* 44, 313–21.

Madsen-Bouterse, S. A., Mohammad, G., Kanwar, M. and Kowluru, R. A. (2010b). Role of mitochondrial DNA damage in the development of diabetic retinopathy, and the metabolic memory phenomenon associated with its progression. *Antioxid. Redox Signal.* 13, 797–805.

Martin, P. M., Roon, P., Van Ells, T. K., Ganapathy, V. and Smith, S. B. (2004). Death of retinal neurons in streptozotocin-induced diabetic mice. *Invest. Ophthalmol. Vis. Sci.* 45, 3330–6.

MERRIAM, G. R. and FOCHT, E. F. (1962). A clinical and experimental study of the effect of single and divided doses of radiation on cataract production. *Trans. Am. Ophthalmol. Soc.* 60, 35–52.

Murakami, T. and Yoshimura, N. (2013). Structural changes in individual retinal layers in diabetic macular edema. *J. Diabetes Res.* 2013, 920713.

Nawaz, M. I., Abouammoh, M., Khan, H. A., Alhomida, A. S., Alfaran, M. F. and Ola, M. S. (2013). Novel drugs and their targets in the potential treatment of diabetic retinopathy. *Med. Sci. Monit.* 19, 300–8.

Ning, Y., Zhen, W., Fu, Z., Jiang, J., Liu, D., Belardinelli, L. and Dhalla, A. K. (2011). Ranolazine increases β-cell survival and improves glucose homeostasis in low-dose streptozotocin-induced diabetes in mice. *J. Pharmacol. Exp. Ther.* 337, 50–8.

Nishikawa, T., Edelstein, D., Du, X. L., Yamagishi, S., Matsumura, T., Kaneda, Y., Yorek, M. A., Beebe, D., Oates, P. J., Hammes, H. P., et al. (2000). Normalizing mitochondrial superoxide production blocks three pathways of hyperglycaemic damage. *Nature* 404, 787–90.

Park, S.-Y., Cho, Y.-R., Kim, H.-J., Higashimori, T., Danton, C., Lee, M.-K., Dey, A., Rothermel, B., Kim, Y.-B., Kalinowski, A., et al. (2005). Unraveling the temporal pattern of diet-induced insulin resistance in individual organs and cardiac dysfunction in C57BL/6 mice. *Diabetes* 54, 3530–40.

Patti, M.-E. and Corvera, S. (2010). The role of mitochondria in the pathogenesis of type 2 diabetes. *Endocr. Rev.* 31, 364–95.

Prusky, G. T., Alam, N. M., Beekman, S. and Douglas, R. M. (2004). Rapid quantification of adult and developing mouse spatial vision using a virtual optomotor system. *Invest Ophthalmol Vis Sci* 45, 4611–4616.

Prusky, G. T., Alam, N. M. and Douglas, R. M. (2006). Enhancement of vision by monocular deprivation in adult mice. *J. Neurosci.* 26, 11554–61.

Reiter, C. E. N., Sandirasegarane, L., Wolpert, E. B., Klinger, M., Simpson, I. A., Barber, A. J., Antonetti, D. A., Kester, M. and Gardner, T. W. (2003). Characterization of insulin signaling in rat retina in vivo and ex vivo. *Am. J. Physiol. Endocrinol. Metab.* 285, E763–74.

Santos, J. M. and Kowluru, R. A. (2013). Impaired transport of mitochondrial transcription factor A (TFAM) and the metabolic memory phenomenon associated with the progression of diabetic retinopathy. *Diabetes. Metab. Res. Rev.* 29, 204–13.

Schlame, M. and Ren, M. (2006). Barth syndrome, a human disorder of cardiolipin metabolism. *FEBS Lett.* 580, 5450–5.

Sharma, K. (2015). Mitochondrial hormesis and diabetic complications. *Diabetes* 64, 663–72.

Siegel, M. P., Kruse, S. E., Percival, J. M., Goh, J., White, C. C., Hopkins, H. C., Kavanagh, T. J., Szeto, H. H., Rabinovitch, P. S. and Marcinek, D. J. (2013). Mitochondrial-targeted peptide rapidly improves mitochondrial energetics and skeletal muscle performance in aged mice. *Aging Cell* 12, 763–71.

Sinibaldi, F., Howes, B. D., Piro, M. C., Polticelli, F., Bombelli, C., Ferri, T., Coletta, M., Smulevich, G. and Santucci, R. (2010). Extended cardiolipin anchorage to cytochrome c: a model for protein-mitochondrial membrane binding. *J. Biol. Inorg. Chem.* 15, 689–700.

Snider, E. J., Muenzner, J., Toffey, J. R., Hong, Y. and Pletneva, E. V (2013). Multifaceted effects of ATP on cardiolipin-bound cytochrome c. *Biochemistry* 52, 993–5.

Stefanini, F. R., Badaró, E., Falabella, P., Koss, M., Farah, M. E. and Maia, M. (2014). Anti-VEGF for the management of diabetic macular edema. *J. Immunol. Res.* 2014, 632307.

Surwit, R. S., Kuhn, C. M., Cochrane, C., McCubbin, J. A. and Feinglos, M. N. (1988). Diet-induced type II diabetes in C57BL/6J mice. *Diabetes* 37, 1163–7.

Szeto, H. H. (2014). First-in-class cardiolipin-protective compound as a therapeutic agent to restore mitochondrial bioenergetics. *Br. J. Pharmacol.* 171, 2029–50.

Szeto, H. H. and Birk, A. V (2014). Serendipity and the discovery of novel compounds that restore mitochondrial plasticity. *Clin. Pharmacol. Ther.* 96, 672–83.

Szeto, H. H., Liu, S., Soong, Y., Wu, D., Darrah, S. F., Cheng, F.-Y., Zhao, Z., Ganger, M., Tow, C. Y. and Seshan, S. V (2011). Mitochondria-targeted peptide

accelerates ATP recovery and reduces ischemic kidney injury. *J. Am. Soc. Nephrol.* 22, 1041–52.

Van Dijk, H. W., Kok, P. H. B., Garvin, M., Sonka, M., Devries, J. H., Michels, R. P. J., van Velthoven, M. E. J., Schlingemann, R. O., Verbraak, F. D. and Abràmoff, M. D. (2009). Selective loss of inner retinal layer thickness in type 1 diabetic patients with minimal diabetic retinopathy. *Invest. Ophthalmol. Vis. Sci.* 50, 3404–9.

Winzell, M. S. and Ahrén, B. (2004). The high-fat diet-fed mouse: a model for studying mechanisms and treatment of impaired glucose tolerance and type 2 diabetes. *Diabetes* 53 Suppl 3, S215–9.

Worgul, B. V, Brenner, D. J., Medvedovsky, C., Merriam, G. R. and Huang, Y. (1993). Accelerated heavy particles and the lens. VII: The cataractogenic potential of 450 MeV/amu iron ions. *Invest. Ophthalmol. Vis. Sci.* 34, 184–93.

Xie, L., Zhu, X., Hu, Y., Li, T., Gao, Y., Shi, Y. and Tang, S. (2008). Mitochondrial DNA oxidative damage triggering mitochondrial dysfunction and apoptosis in high glucose-induced HRECs. *Invest. Ophthalmol. Vis. Sci.* 49, 4203–9.

Zhao, K., Zhao, G.-M., Wu, D., Soong, Y., Birk, A. V, Schiller, P. W. and Szeto, H. H. (2004). Cell-permeable peptide antioxidants targeted to inner mitochondrial membrane inhibit mitochondrial swelling, oxidative cell death, and reperfusion injury. *J. Biol. Chem.* 279, 34682–90.

Zhao, K., Luo, G., Giannelli, S. and Szeto, H. H. (2005). Mitochondria-targeted peptide prevents mitochondrial depolarization and apoptosis induced by tert-butyl hydroperoxide in neuronal cell lines. *Biochem. Pharmacol.* 70, 1796–806.

Zhong, Q. and Kowluru, R. A. (2011). Diabetic retinopathy and damage to mitochondrial structure and transport machinery. *Invest. Ophthalmol. Vis. Sci.* 52, 8739–46.

FIGURE LEGENDS

Figure 1. Metabolic dysfunction in mouse models of diabetes. A. Elevated blood glucose emerged in ND+STZ, DD and DD+STZ groups by 15 weeks of age (DD = 215 mg/dL +/- 4.35 (n=7); DD+STZ = 235 mg/dL +/- 2.28 (n=6); ND+STZ = 205 mg/dL +/- 3.14; (n=12), significantly higher than ND = 161 mg/dL +/- 1.73 (n=7), $p<0.01$) and was sustained out to 32 weeks (DD = 263 mg/dL +/- 1.35 (n=4); DD+STZ = 253 mg/dL +/- 2.22 (n=3); ND+STZ = 208 mg/dL +/- 3.64 (n=9), significantly higher than ND = 164 mg/dL +/- 2.73 (n=5), $p<0.01$). B; C. Evidence of impaired glucose clearance on a glucose tolerance test was present in each diabetic model when measured at 12 (B; GTT1) and 30 weeks (C; GTT2), with DD groups being the most impaired. Dashed lines demarcate the upper limit of glucometer sensitivity. D. Abnormal weight gain emerged in the diabetic models by 15 weeks (DD = 35.2g +/- 3.11, DD+STZ = 41.3g +/- 1.42, ND+STZ = 24.9g +/- 2.31), which was significantly different than ND = 29.0g +/- 2.14, $p<0.05$. +/- SEMs are plotted in these and other panels but are often occluded by the data symbols.

Figure 2. Progressive decline of visuomotor function in diabetic models. A. SF thresholds under photopic (cone-mediated) conditions did not change in ND mice from 12 (0.393 c/d +/- 0.006, (n=7)) to 32 weeks (0.394 c/d +/- 0.001 (n=5), $p>0.05$). Reduced thresholds (average of both eyes) emerged in ND+STZ mice at 12 weeks (0.387 c/d +/- 0.003 (n=12), $p<0.05$), with 17% decline by 32 weeks (0.325 c/d +/- 0.001 (n=9), $p<0.01$). Reduced thresholds emerged in DD mice by 9 weeks (0.386 c/d +/- 0.002 (n=7), $p<0.01$), with 29% decline by 32 weeks (0.280 c/d +/- 0.001 (n=4), $p<0.01$), and emerged in DD+STZ mice at 8 weeks (0.327 c/d +/- 0.001 (n=6), $p<0.01$), with 38% decline by 32 weeks (0.244 c/d +/- 0.001c/d (n=3), $p<0.01$). B.

Cone-mediated function was more compromised than rod function in diabetic models at 28 weeks. As previously reported (Altimus et al., 2010), rod thresholds (Photopic; R) are significantly lower (0.19225 c/d +/- 0.000324) than cone (C) thresholds (0.3935c/d +/- 0.0006, $p<0.01$, n=4) in ND mice. Both rod and cone thresholds were reduced from normal in all diabetic models, with the most impairment in cone-mediated function: ND+STZ (cone: 0.331c/d +/- 0.0005 vs rod: 0.18624c/d +/- 0.0000342, $p<0.01$); DD (cone: 0.286c/d +/- 0.00634 vs rod: 0.17268c/d +/- 0.000325, $p<0.01$); DD+STZ (cone: 0.253c/d +/- 0.0000233 vs rod: 0.15813c/d +/- 0.000435, $p<0.01$). C; D; E; F) Progressive decline of CS in diabetic models. C. Normal CS was present in ND mice when measured at 4, 12 and 32 weeks. D. CS in ND+STZ mice decreased moderately between 12 and 32 weeks at SFs above 0.06 c/d. E. Decreased CS was evident at 12 weeks in DD mice and progressed by 32 weeks, particularly at the highest SF tested. F. DD+STZ mice displayed the most dysfunction over time, such that by 32 weeks, they did not respond at the highest SF tested.

Figure 3. Metabolic dysfunction was not improved by daily systemic treatment with MTP-131. Daily MTP-131 treatment is indicated by shading. Dotted lines are traces from Fig. 1, depicting the effect of Veh treatment. A. MTP-131 treatment did not reduce resting fed blood glucose in any of the experimental groups. B. MTP-131 had no effect on glucose clearance at 32 weeks in any experimental group. C. MTP-131 did not mitigate weight gain in the groups fed a DD.

Figure 4. Reversal of visual dysfunction following daily systemic treatment with MTP-131. Daily MTP-131 treatment is indicated by shading. Dotted lines are traces from Fig. 1, depicting the effects of Veh treatment. A. Improvement of SF function was present within 2 weeks of treatment in ND+STZ mice (MTP-131 vs Veh; 0.382

c/d +/- 0.001 (n=7) vs 0.377 c/d +/- 0.006 (n=12)), within 3 weeks in DD mice (MTP-131 vs Veh: 0.342 c/d +/- 0.001 (n=8) vs. 0.347c/d +/- 0.003 (n=7)), and within 1 week in DD+STZ mice (MTP-131 vs Veh: 0.340 c/d +/- 0.001 (n=11) vs 0.313c/d +/- 0.002 (n=6)). Full restoration of function was achieved by 24 weeks in ND+STZ (n=4) and DD+STZ (n=8) mice, and by 31 weeks in DD mice (n=5). ND (MTP-131) did not differ statistically from ND (Veh) at any age (n=6, $p>0.05$). B. Cone- and rod-mediated function was restored by MTP-131 treatment, as measured at 28 weeks of age ($p>0.05$); dotted lines depict the results of Veh-treatment abstracted from Fig. 1. C; D; E; F. MTP-131 restored normal CS in each experimental group by 32 weeks.

Figure 5. Daily administration of MTP-131 in eye drops from 12 weeks reversed visual decline. A; B. 30 mg/ml MTP-131 did not affect resting blood glucose (A; MTP-131 vs Veh, $p>0.05$ vs a $p<0.01$ for two way ANOVA on age, interaction and treatment condition with ND group after 12 weeks) or body weight (B; (A; MTP-131 vs Veh, $p>0.05$ vs a $p<0.001$ for two way ANOVA on age, interaction and treatment condition with ND group). Dotted lines represent control data from ND mice in Fig. 1. C. SF function was restored to control values by 20 weeks, 4 weeks earlier than with systemic treatment ($p>0.05$ Eye Drops (Veh) vs Systemic (Veh); $p<0.001$ for Eye Drops (MTP-131) vs ND from 7-19 weeks of age, $p<0.05$ from 20 weeks of age; Eye Drops (MTP-131) vs Systemic (MTP-131) $p<0.01$ between 17 and 23 weeks of age (Fig. 2A)). D. Dose-dependent effect of MTP-131 eye drop treatment; 1 mg/ml had no effect ($p<0.01$ for 30mg/ml group from 13 weeks of age compared to Veh and 1mg/ml groups; $p<0.01$ for 10mg/ml group from 16 weeks of age compared to Veh and 1mg/ml groups; $p<0.001$ for 30mg/ml group vs 10mg/ml group from 13 to 29 weeks; $p>0.05$ 1mg/ml vs Veh at all points).

Figure 6. Daily administration of MTP-131 in eye drops reversed more severe visual dysfunction present later in the course of disease. A, B) Treatment with MTP-131 in eye drops (30 mg/ml) from 34 weeks (shading) in DD+STZ mice did not change markers of metabolic dysfunction (A. Resting blood glucose @52 weeks- MTP-131: 260 mg/dL +/- 2.64 (n=8) vs Veh: 254 mg/dL +/- 2.11 (n=7), p=0.1363 vs ND: 173 mg/dL +/- 3.06 (n=4)) or body weight (B. @52 weeks- MTP-131: 56.1g +/- 2.5 vs Veh: 56.0g +/- 2.3, p=0.1021 vs ND: 36.5g +/- 3.1). Orange dotted lines represent traces from control ND mice in Fig. 1. Orange squares are measures in age-matched control mice at 52 weeks. C. Reversal of visual decline was evident after 6 weeks of drug treatment, (MTP-131: 0.211 c/d +/- 0.003 vs 0.198 c/d +/- 0.003, $p<0.05$) and recovery to 80% normal (MTP-131: 0.311 c/d +/- 0.003 vs Veh: 0.152 c/d +/- 0.003 vs ND: 0.393 c/d +/- 0.001) was evident by 52 weeks. Dotted orange line depicts the function of ND mice, and teal line is the effect of MTP-131 eye drop treatment, from Fig. 5C.

Translational Impact:

(1) Clinical issue: Current treatments for visual dysfunction in diabetes are focused on managing the symptoms of diabetes, such as hyperglycemia, obesity and retinal edema in the non-proliferative phase, and on improving clarity of the optical axis, or controlling retinal angiogenesis and its consequences in the proliferative stage. These treatments have limited efficacy, and able to slow, but not reverse, visual decline. Our work describes a novel approach to treating diabetic visual dysfunction based on targeting and treating mitochondrial dysfunction with a water-soluble peptide (MTP-131).

(2) Results: We find that progressive decline of spatial visuomotor function emerges in mouse models of Type 1 and Type 2 diabetes early in the course of disease; before typical symptoms of diabetes, such as hyperglycemia and obesity, are present. Both systemic and eye-drop application of MTP-131 early in the course of visual decline, are able to prevent further decline and fully reverse dysfunction without normalizing aberrant glucose clearance, or elevated blood glucose and weight. Equivalent treatment later in disease, after much more severe visual dysfunction is manifest, is also able to substantially restore function.

(3) Implications and future directions: These data indicate that mitochondrial dysfunction, which may be detected with spatial measures of visuomotor function, is an early and treatable pathophysiology of diabetes that is independent of the other symptoms of metabolic dysfunction. They also indicate that improving mitochondrial function can treat the visual dysfunction without remediating glucose dysregulation or obesity. Thus, mitochondrial-based treatment on its own, or in combination with current therapies, may provide a new and more effective approach to treating the visual consequences of diabetes at any stage of disease. Since MTP-131 has an exceptional human safety profile it has the potential to be rapidly translated into clinical trials.

Figure 1

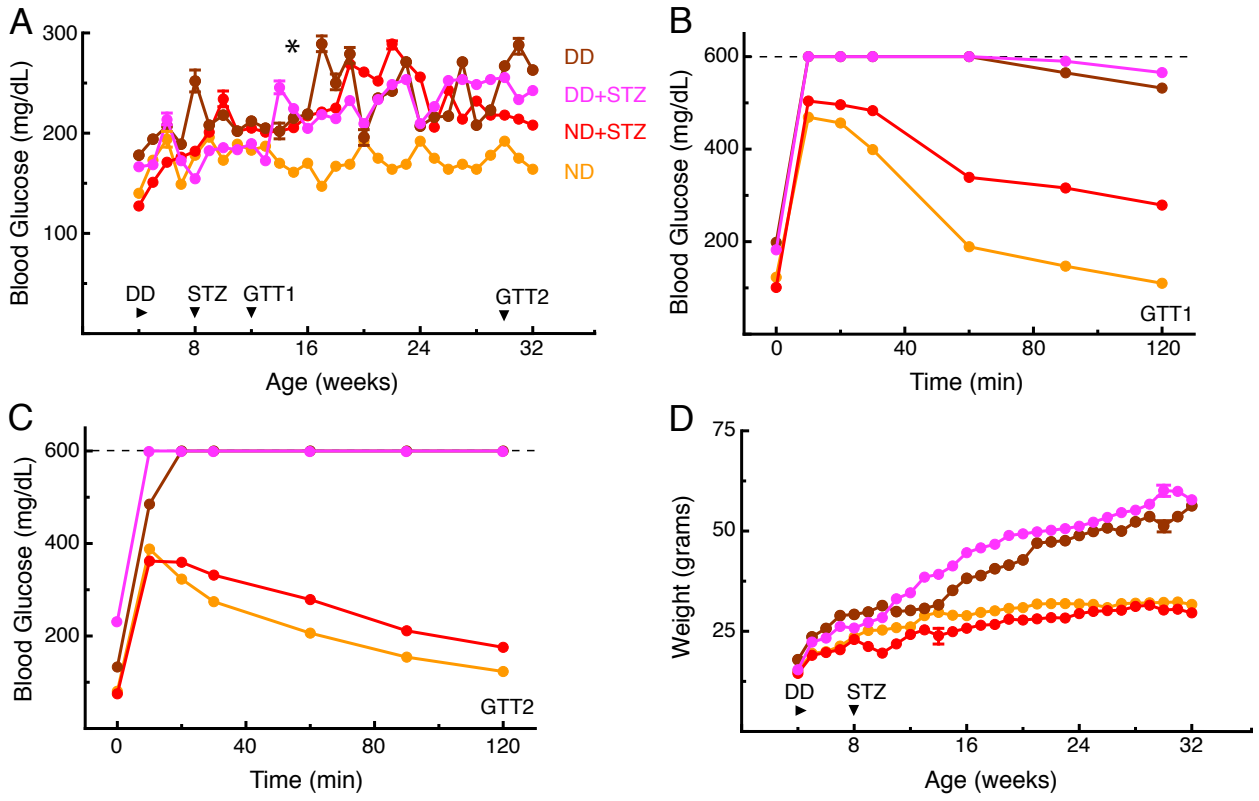
A
300
200
100
Blood Glucose (mg/dL)
*
DD
DD+STZ
ND+STZ
ND
DD
STZ
GTT1
GTT2
8
16
24
32
Age (weeks)
B
600
400
200
Blood Glucose (mg/dL)
GTT1
0
40
80
120
Time (min)
C
600
400
200
Blood Glucose (mg/dL)
GTT2
0
40
80
120
Time (min)
D
75
50
25
Weight (grams)
DD
STZ
8
16
24
32
Age (weeks)

Figure 2

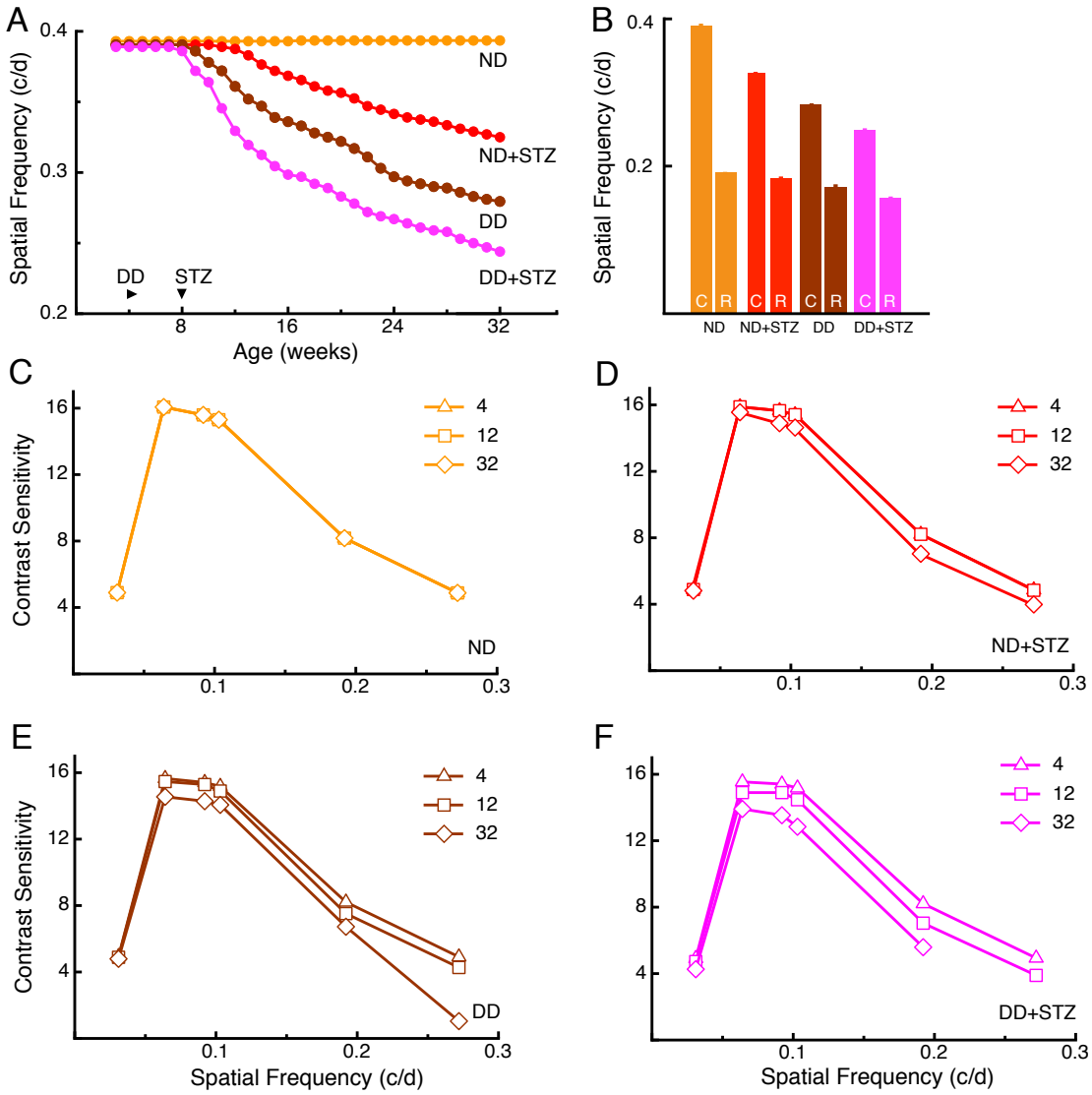
A
Spatial Frequency (c/d)
0.4
0.3
0.2
ND
ND+STZ
DD
DD+STZ
DD
STZ
8
16
24
32
Age (weeks)
B
Spatial Frequency (c/d)
0.4
0.2
C R C R C R C R
ND ND+STZ DD DD+STZ
C
Contrast Sensitivity
16
12
8
4
4
12
32
ND
0.1
0.2
0.3
D
16
12
8
4
4
12
32
ND+STZ
0.1
0.2
0.3
E
Contrast Sensitivity
16
12
8
4
4
12
32
DD
0.1
0.2
0.3
Spatial Frequency (c/d)
F
16
12
8
4
4
12
32
DD+STZ
0.1
0.2
0.3
Spatial Frequency (c/d)

Figure 3

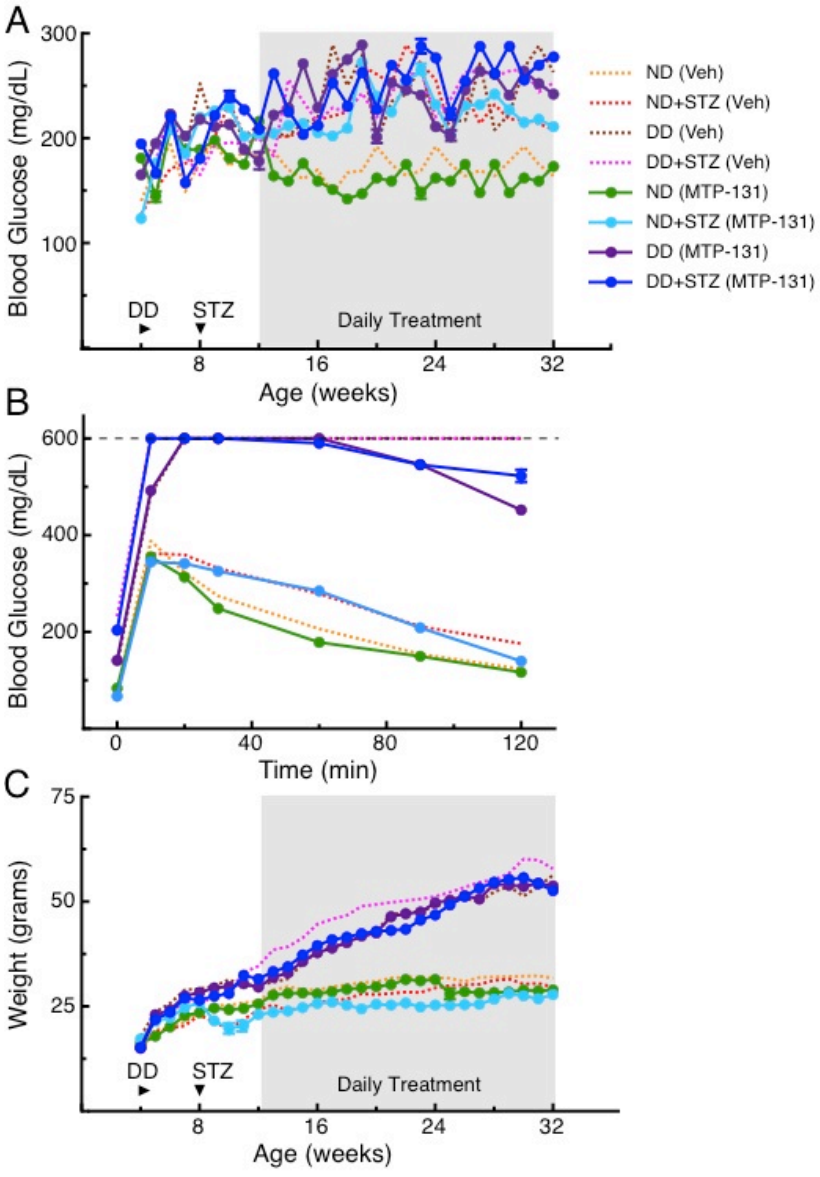
A
300
200
100
Blood Glucose (mg/dL)
DD
STZ
Daily Treatment
8
16
24
32
Age (weeks)
ND (Veh)
ND+STZ (Veh)
DD (Veh)
DD+STZ (Veh)
ND (MTP-131)
ND+STZ (MTP-131)
DD (MTP-131)
DD+STZ (MTP-131)
B
600
400
200
Blood Glucose (mg/dL)
0
40
80
120
Time (min)
C
75
50
25
Weight (grams)
DD
STZ
Daily Treatment
8
16
24
32
Age (weeks)

Figure 4

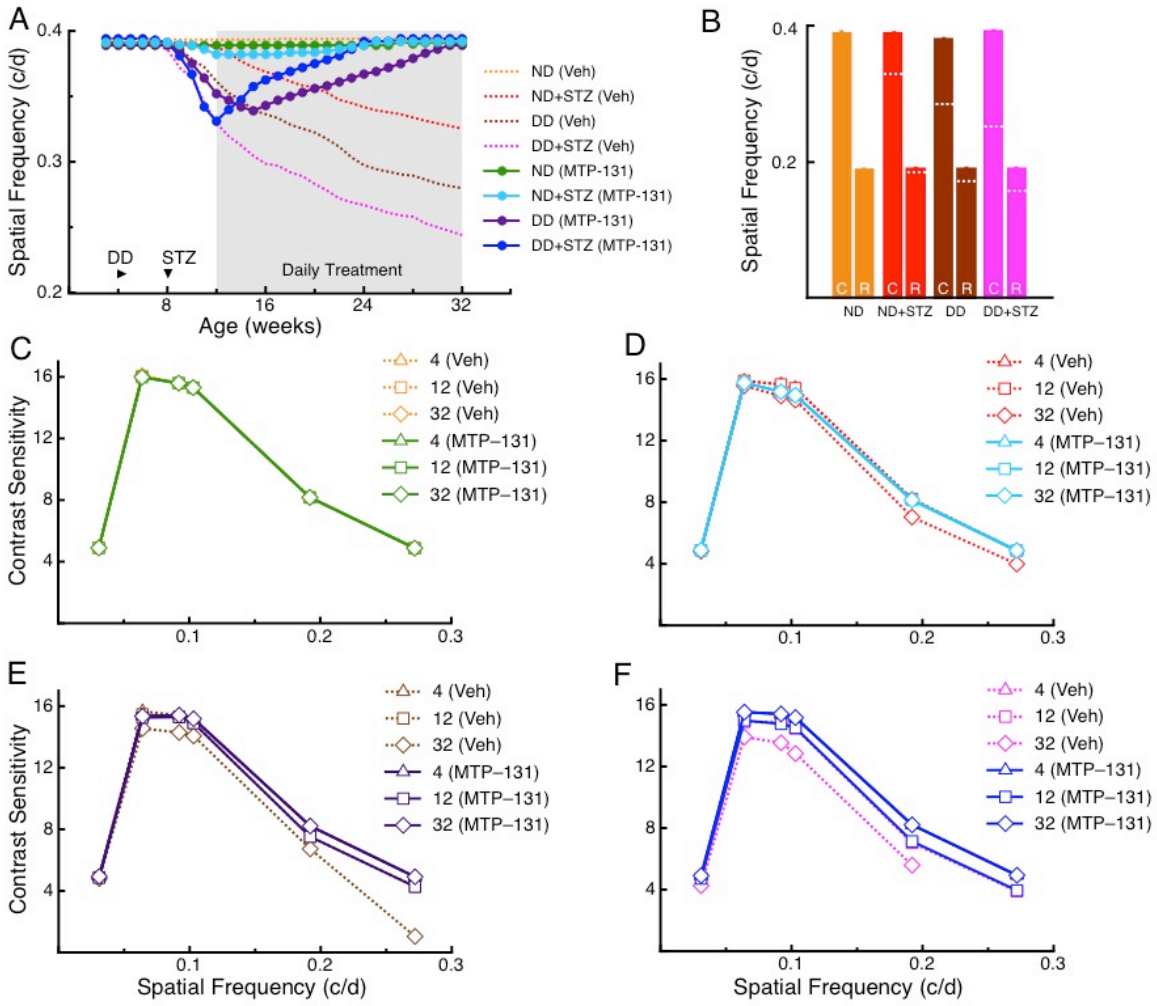
A
Spatial Frequency (c/d)
0.4
0.3
0.2
DD
STZ
Daily Treatment
8
16
24
32
Age (weeks)
ND (Veh)
ND+STZ (Veh)
DD (Veh)
DD+STZ (Veh)
ND (MTP-131)
ND+STZ (MTP-131)
DD (MTP-131)
DD+STZ (MTP-131)
B
Spatial Frequency (c/d)
0.4
0.2
C R C R C R C R
ND ND+STZ DD DD+STZ
C
Contrast Sensitivity
16
12
8
4
0.1
0.2
0.3
4 (Veh)
12 (Veh)
32 (Veh)
4 (MTP–131)
12 (MTP–131)
32 (MTP–131)
D
16
12
8
4
0.1
0.2
0.3
4 (Veh)
12 (Veh)
32 (Veh)
4 (MTP–131)
12 (MTP–131)
32 (MTP–131)
E
Contrast Sensitivity
16
12
8
4
0.1
0.2
0.3
Spatial Frequency (c/d)
4 (Veh)
12 (Veh)
32 (Veh)
4 (MTP–131)
12 (MTP–131)
32 (MTP–131)
F
16
12
8
4
0.1
0.2
0.3
Spatial Frequency (c/d)
4 (Veh)
12 (Veh)
32 (Veh)
4 (MTP–131)
12 (MTP–131)
32 (MTP–131)

Figure 5

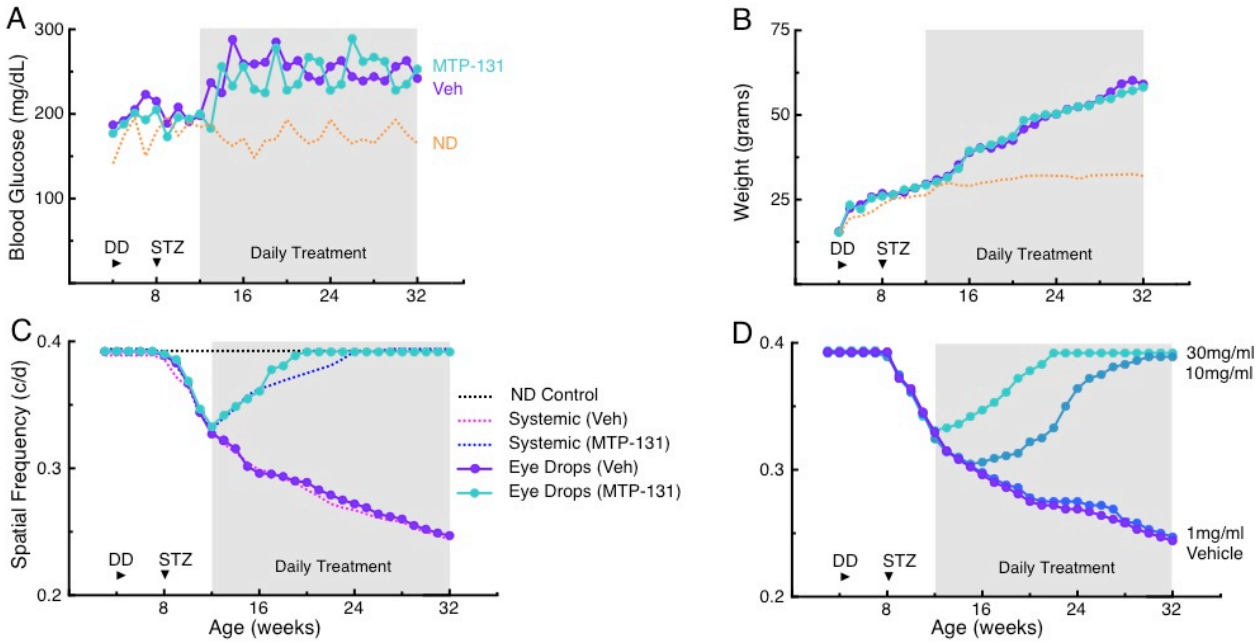
A
Blood Glucose (mg/dL)
300
200
100
MTP-131
Veh
ND
DD
STZ
Daily Treatment
8
16
24
32
B
Weight (grams)
75
50
25
C
Spatial Frequency (c/d)
0.4
0.3
0.2
ND Control
Systemic (Veh)
Systemic (MTP-131)
Eye Drops (Veh)
Eye Drops (MTP-131)
Age (weeks)
D
30mg/ml
10mg/ml
1mg/ml
Vehicle

Figure 6

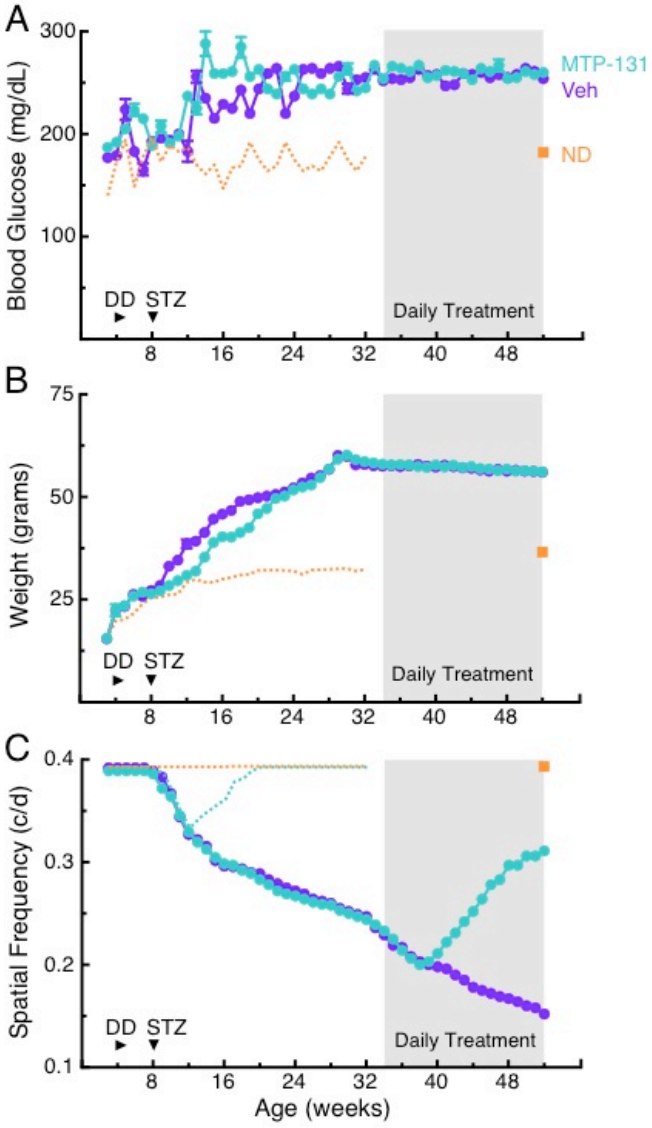
A
300
200
100
Blood Glucose (mg/dL)
MTP-131
Veh
ND
DD
STZ
Daily Treatment
8
16
24
32
40
48
B
75
50
25
Weight (grams)
C
0.4
0.3
0.2
0.1
Spatial Frequency (c/d)
Age (weeks)

CONCLUSION

Almost 100 years have passed since the first treatment for diabetes was developed, yet therapeutic options still fail to both fully prevent disease progression and mitigate end organ dysfunction in hundreds of millions of people worldwide. For decades, research and treatment has focused on the most clinically observable factor: blood glucose levels. This approach has proven unsuccessful for numerous reasons, the first and foremost being that even strict glycemic control fails to prevent the progression of diabetic complications in a large subset of patients (Antonetti, Klein, & Gardner, 2012).

Research focused on hyperglycemia initially described the role of mitochondria in the onset and progression of the disease, yet the role was attributed incorrectly. The temporal relationship discerned by Brownlee is backwards; mitochondrial dysfunction is, first and foremost, a promoter and not a product of diabetic tissue damage. It is true that high glucose concentrations, and high substrate load in general, drive mitochondrial dysfunction (Muoio, 2014). Yet mitochondrial dysfunction is seen in insulin resistant tissues even before the onset of frank hyperglycemia. The reality is the opposite of what Brownlee had proposed: mitochondrial dysfunction originates first and results in a crisis of bioenergetics. Inadequate energy levels create a circumstance where cells cannot carry out vital processes, leading to failure of vision-sustaining tasks (Schütt, Aretz, Auffarth, & Kopitz, 2012). Preventing increases in ROS will not fix a problem of decreased ATP,

and as more recent research has demonstrated, ROS may in fact be decreased in diabetic tissue (Dugan et al., 2013). This view explains why there have been no successful antioxidant therapies despite many promising initial studies in cell culture and animal models – ROS is not the cause, and thus mitigating it does not solve the problem.

Furthermore, the focus on hyperglycemic damage leads to oversight of the complications that may arise from altered insulin signaling. Insulin signaling is tissue specific, so while the focus of most diabetes research is on skeletal muscle, the insulin-sensitive tissues of the eye play a dissimilar role. During the development of diabetes, insulin resistance develops differently in different tissues, requiring a more nuanced understanding of insulin action than a simple model based on the liver, fat or skeletal muscle (Park et al., 2005). In the eye, where constitutive signaling drives the constant uptake of glucose for the metabolically active retina, a decrease in insulin sensitivity spells disaster for the vision-sustaining functions depending upon this substrate supply (Fort et al., 2011). Even with elevated blood glucose levels, the diabetic retina will be starved of glucose, further precipitating the bioenergetic crisis.

Cell culture studies have additionally complicated the field of diabetes research via the Crabtree Effect. When exposed to standard high-glucose media, glycolysis is favored over mitochondrial oxidative phosphorylation, leading to a radically different bioenergetic profile than would occur in living human tissue (Marroquin, Hynes, Dykens, Jamieson, & Will, 2007). Much early research, even investigation of mitochondrial involvement in diabetes was done in such systems, despite a complete failure of the generalizability of this research. Diabetes is a multifaceted, complex

disease of still yet-to-be fully understood origin, which complicates our ability to utilize model systems. Many models fail to accurate recapitulate the origin of the disease, which can lead promising research away from reality. Gender biases (not present in humans) have been demonstrated to complicate mouse model use, as well as off-target STZ toxicity (Robinson, Barathi, Chaurasia, Wong, & Kern, 2012) . Furthermore, while helpful in elucidating certain information, genetic knockout models have a dangerous potential to misinform. Endpoints may look relevant to human manifestations of diabetic complications, yet the processes and underlying causes are so different that findings must be considered with respect to this often-forgotten reality.

Additionally, research on diabetic retinopathy, focused on the human manifestations of the disease, has made the mistake of concentrating on what is most clinically visible. The visualization techniques that make the vascularization of the neuroretina easily observable fail to notice the abnormalities arising in the fundamentally critical choroid of the outer retina. It is this blood supply that feeds 80-90% of the retina's oxygen and is responsible for so many of the processes necessary for vision, yet its less-accessible nature led to a lack of investigation. More recently, research has begun to focus on the choroid and RPE, but targeted treatments are just beginning. Novel visualization techniques for animal models and human patients, especially the development of outer blood-retinal barrier breakdown assays and indocyanine green angiography, will allow for elucidation of early choroidal aberrations in the future, potentially generating earlier diagnoses (Mueller et al., 1999; Witmer & Kiss, 2013; Xu & Le, 2011).

Therapies for diabetic retinopathy have similarly been similarly short sighted. VEGF inhibition, the expensive, complicated and marginally successful current gold standard for proliferative retinopathy fails to mitigate the underlying basis of the disease. VEGF upregulation is driven by hypoxia, and until that condition is mollified its increased production will remain. Here, we present a therapeutic basis for breaking the feed-forward cycle leading to VEGF secretion, abrogating the underlying basis instead of removing one consequent factor. Restoration of adequate bioenergetics allows for the endogenous antioxidant, supportive and vision-producing cellular functions required to maintain proper retinal function. Our proposed therapy will most likely benefit with concomitant pharmacological intervention, but this will require future investigation.

Restoration of the bienergetic capacity of the retina may play a role beyond diabetic retinopathy. Age-related macular degeneration in particular poses as a potential area necessitating further investigation. The disease shares a similar etiology of mitochondrial impairment and diminished bioenergetics (Barot, Gokulgandhi, & Mitra, 2011; Feher et al., 2006; Karunadharma, Nordgaard, Olsen, & Ferrington, 2010). Similar ultrastructural differences are seen in the RPE, as well as early neovascular tufts, albeit to a lesser degree (data unpublished). Our lab and collaborators have recognized similar visual degeneration of spatial frequency threshold, and have compelling preliminary data supporting our therapeutic hypothesis with SS-31.

There is still much work to be done, but the current state of our research has generated some exciting results. Restoration of not just biomarkers for visual function,

but measurable reversal of diabetes-associated visual dysfunction in a mouse model is novel for this field. The focus on preservation of mitochondrial function in order to safeguard adequate bioenergetic capacity shifts the focus from blood glucose control towards what we believe to be more relevant factors: bioenergetic failure, insulin resistance and microvasculopathy. The recognition of visual dysfunction beginning before robust hyperglycemia requires additional research, yet there are other studies documenting onset of visual degeneration earlier than is generally noted (Akimov & Rentería, 2012; Aung, Kim, Olson, Thule, & Pardue, 2013; Hardy, Lipton, Scase, Foster, & Scarpello, 1992; Jackson, Scott, Quillen, Walter, & Gardner, 2012; Kirwin et al., 2011). These factors reframe the contemporary view of diabetic retinopathy as a progressive failure with roots earlier than may be commonly recognized. Treatment of the disease may be possible via bioenergetic restoration, and without a focus on blood glucose control.

The topical formulation of SS-31 ("Ocuvia") represents an additional shift in treatment paradigm in a number of ways. For the doctor and patient, the treatment may represent a lesser cost, greater ease of treatment and reduced risk of complications. The side effect profile of SS-31 in phase 1 trials has been excellent, and could provide a needed reprieve from a first-line treatment consisting of frequent and invasive intravitreal injections. Furthermore, topical SS-31 may provide an excellent form for treatment of diabetic retinopathy in developing and low-income countries, where more complicated distribution and administration of intravitreal injections, let alone the cost of therapy have been prohibitive.

The success or failure of topical SS-31 in humans cannot be guaranteed based solely on our animal research. A phase I/II trial currently ongoing will provide data on the potential of realization and FDA approval in this indication. Results are scheduled for late 2015.

Akimov, N. P., & Rentería, R. C. (2012). Spatial frequency threshold and contrast sensitivity of an optomotor behavior are impaired in the Ins2Akita mouse model of diabetes. *Behav Brain Res*, *226*(2), 601–605. doi:10.1016/j.bbr.2011.09.030.Spatial

Antonetti, D. A., Klein, R., & Gardner, T. W. (2012). Diabetic retinopathy. *The New England Journal of Medicine*, 1227–1239.

Aung, M. H., Kim, M. K., Olson, D. E., Thule, P. M., & Pardue, M. T. (2013). Early visual deficits in streptozotocin-induced diabetic long evans rats. *Investigative Ophthalmology & Visual Science*, *54*(2), 1370–7. doi:10.1167/iovs.12-10927

Barot, M., Gokulgandhi, M. R., & Mitra, A. K. (2011). Mitochondrial Dysfunction in Retinal Diseases. *Current Eye Research*, *36*(July), 1069–1077. doi:10.3109/02713683.2011.607536

Dugan, L. L., You, Y., Ali, S. S., Diamond-stanic, M., Miyamoto, S., Decleves, A., … Sharma, K. (2013). AMPK dysregulation promotes diabetes- related reduction of superoxide and mitochondrial function. *The Journal of Clinical Investigation*, *123*(11). doi:10.1172/JCI66218DS1

Feher, J., Kovacs, I., Artico, M., Cavallotti, C., Papale, A., & Balacco Gabrieli, C. (2006). Mitochondrial alterations of retinal pigment epithelium in age-related macular degeneration. *Neurobiology of Aging*, *27*(7), 983–93. doi:10.1016/j.neurobiolaging.2005.05.012

Fort, P. E., Losiewicz, M. K., Reiter, C. E. N., Singh, R. S. J., Nakamura, M., Abcouwer, S. F., … Gardner, T. W. (2011). Differential roles of hyperglycemia and hypoinsulinemia in diabetes induced retinal cell death: Evidence for retinal insulin resistance. *PLoS ONE*, *6*(10). doi:10.1371/journal.pone.0026498

Hardy, K. J., Lipton, J., Scase, M. O., Foster, D. H., & Scarpello, J. H. (1992). Detection of colour vision abnormalities in uncomplicated type 1 diabetic patients with angiographically normal retinas. *The British Journal of Ophthalmology*, *76*(8), 461–4. Retrieved from http://www.pubmedcentral.nih.gov/articlerender.fcgi?artid=504317&tool=pmcentrez&rendertype=abstract

Jackson, G. R., Scott, I. U., Quillen, D. a, Walter, L. E., & Gardner, T. W. (2012). Inner retinal visual dysfunction is a sensitive marker of non-proliferative diabetic retinopathy. *The British Journal of Ophthalmology*, *96*(5), 699–703. doi:10.1136/bjophthalmol-2011-300467

Karunadharma, P. P., Nordgaard, C. L., Olsen, T. W., & Ferrington, D. a. (2010). Mitochondrial DNA damage as a potential mechanism for age-related macular degeneration. *Investigative Ophthalmology & Visual Science*, *51*(11), 5470–9. doi:10.1167/iovs.10-5429

Kirwin, S. J., Kanaly, S. T., Hansen, C. R., Cairns, B. J., Ren, M., & Edelman, J. L. (2011). Retinal gene expression and visually evoked behavior in diabetic long

evans rats. *Investigative Ophthalmology & Visual Science*, *52*(10), 7654–63. doi:10.1167/iovs.10-6609

Marroquin, L. D., Hynes, J., Dykens, J. a, Jamieson, J. D., & Will, Y. (2007). Circumventing the Crabtree effect: replacing media glucose with galactose increases susceptibility of HepG2 cells to mitochondrial toxicants. *Toxicological Sciences : An Official Journal of the Society of Toxicology*, *97*(2), 539–47. doi:10.1093/toxsci/kfm052

Mueller, A. J., Freeman, W. R., Folberg, R., Bartsch, D. U., Scheider, A., Schaller, U., & Kampik, A. (1999). Evaluation of microvascularization pattern visibility in human choroidal melanomas: Comparison of confocal fluorescein with indocyanine green angiography. *Graefe's Archive for Clinical and Experimental Ophthalmology*, *237*, 448–456. doi:10.1007/s004170050260

Muoio, D. M. (2014). Metabolic Inflexibility: When Mitochondrial Indecision Leads to Metabolic Gridlock. *Cell*, *159*(6), 1253–1262. doi:10.1016/j.cell.2014.11.034

Park, S., Cho, Y., Kim, H., Higashimori, T., Danton, C., Lee, M., … Kim, J. K. (2005). Unraveling the Temporal Pattern of Diet-Induced Insulin in C57BL / 6 Mice. *Diabetes*, *54*(December).

Robinson, R., Barathi, V. a., Chaurasia, S. S., Wong, T. Y., & Kern, T. S. (2012). Update on animal models of diabetic retinopathy: from molecular approaches to

mice and higher mammals. *Disease Models & Mechanisms*, *5*(4), 444–456. doi:10.1242/dmm.009597

Schütt, F., Aretz, S., Auffarth, G. U., & Kopitz, J. (2012). Moderately reduced ATP levels promote oxidative stress and debilitate autophagic and phagocytic capacities in human RPE cells. *Investigative Ophthalmology and Visual Science*, *53*, 5354–5361. doi:10.1167/iovs.12-9845

Witmer, M. T., & Kiss, S. (2013). Wide-field Imaging of the Retina. *Survey of Ophthalmology*, *58*(2), 143–154. doi:10.1016/j.survophthal.2012.07.003

Xu, H. Z., & Le, Y. Z. (2011). Significance of outer blood-retina barrier breakdown in diabetes and ischemia. *Investigative Ophthalmology and Visual Science*, *52*(5), 2160–2164. doi:10.1167/iovs.10-6518

44. Jiang Y, Qi X, Chrenek MA, Gardner C, Dalal N, Boatright JH, Grossniklaus HE, Nickerson JM: Analysis of mouse RPE sheet morphology gives discriminatory categories. Adv Exp Med Biol 2014;801:601-607

45. Xu HZ, Le YZ: Significance of outer blood-retina barrier breakdown in diabetes and ischemia. Invest Ophthalmol Vis Sci 2011;52:2160-2164

46. Liu S, Soong Y, Seshan SV, Szeto HH: Novel cardiolipin therapeutic protects endothelial mitochondria during renal ischemia and mitigates microvascular rarefaction, inflammation, and fibrosis. Am J Physiol Renal Physiol 2014;306:F970-980

47. Li J, Chen X, Xiao W, Ma W, Li T, Huang J, Liu X, Liang X, Tang S, Luo Y: Mitochondria-targeted antioxidant peptide SS31 attenuates high glucose-induced injury on human retinal endothelial cells. Biochem Biophys Res Commun 2011;404:349-356

48. Ruderman NB, Carling D, Prentki M, Cacicedo JM: AMPK, insulin resistance, and the metabolic syndrome. J Clin Invest 2013;123:2764-2772

49. Kubota S, Ozawa Y, Kurihara T, Sasaki M, Yuki K, Miyake S, Noda K, Ishida S, Tsubota K: Roles of AMP-activated protein kinase in diabetes-induced retinal inflammation. Invest Ophthalmol Vis Sci 2011;52:9142-9148

50. Viollet B, Guigas B, Sanz Garcia N, Leclerc J, Foretz M, Andreelli F: Cellular and molecular mechanisms of metformin: an overview. Clin Sci (Lond) 2012;122:253-270